Acute and Chronic Neurotoxicity in Novel Mouse Models of Acute Intoxication with Diverse Chemical Threat Agents

By

JONAS JOHN CALSBEEK
DISSERTATION

Submitted in partial satisfaction of the requirements for the degree of

DOCTOR OF PHILOSOPHY

in

PHARMACOLOGY AND TOXICOLOGY

in the

OFFICE OF GRADUATE STUDIES

of the

UNIVERSITY OF CALIFORNIA

DAVIS

Approved:

Dr. Pamela Lein, Chair

Dr. Gene Gurkoff

Dr. Isaac Pessah

Committee in Charge

2021

Dedication:

For Cait, Jake, and Lily,

and all those who stood in the way.

ABSTRACT

Organophosphate (OP) cholinesterase inhibitors and GABA receptor antagonists represent mechanistically diverse classes of chemicals that can cause seizures and death following acute intoxication at relatively low doses. OPs inhibit acetylcholinesterase (AChE), which results in the over accumulation of acetylcholine (ACh) in the nervous system. Rapid inhibition of > 60-80% of brain AChE triggers seizures that rapidly progress to life-threatening *status epilepticus* (SE). GABA receptor antagonists, exemplified by tetramethylenedisulfotetramine (TETS), induce seizures and death by reducing the inhibitory tone in the nervous system, which results in neuronal hyperexcitability. The standard first-line therapy for the treatment of TETS- or OP-induced SE, high-dose benzodiazepines, are effective at terminating seizure behavior and reducing mortality if administered within minutes after exposure. However, even with timely treatment, benzodiazepines often fail to adequately protect against subsequent brain damage and neurologic deficits. Preclinical rodent models are essential to elucidating the cellular and molecular mechanisms driving acute seizurogenic events and the spatiotemporal progression of brain damage following SE. The major objective of this dissertation was to characterize acute and chronic neurotoxic outcomes in novel mouse models of TETS- and OP-induced SE to gain a better understanding of the pathogenic mechanisms contributing to SE and the consequential neuropathology.

In Chapter 2, *in vivo* imaging is used to compare the spatiotemporal progression of neuropathology after TETS-SE in two different mouse strains commonly used to study chemical-induced SE. The findings in this study demonstrate that the extent of brain damage observed in the mouse brain after TETS-induced SE varies according to strain and the duration of SE. Chapter 3 focuses on the development and characterization of a mouse model of acute

intoxication with diisopropylfluorophosphate (DFP). Specifically, this chapter describes the spatiotemporal progression of AChE inhibition, neuropathology, and behavioral deficits up to 28 days post-exposure. The findings in this chapter demonstrate that this mouse model replicates many of the outcomes observed in rats and humans acutely intoxicated with OPs, suggesting the feasibility of using this model for mechanistic studies and therapeutic screening. The mouse model of acute DFP intoxication was leveraged in Chapter 4 to investigate the role of nicotinic cholinergic receptors (nAChR) in the initiation and propagation of OP-induced SE. The findings described in Chapter 4 identify a role for α4-containing nAChR in the initiation and/or progression of seizures following acute OP intoxication, and support further investigation of nicotinic antagonists as prophylactics for OP-induced SE.

The studies presented in this dissertation support the use of mouse models to investigate the mechanisms contributing to the initiation and consequences of SE caused by chemical threat agents. The findings of this work have important mechanistic and therapeutic implications regarding the pathophysiology and treatment of chemical-induced SE. The observation that genetic background and duration of SE influence the neuropathologic consequences of TETS-SE suggests that humans who do not respond to antiseizure medication after acute TETS intoxication are at increased risk for brain injury, and this susceptibility may vary genetically. The observation that nicotinic receptors play a necessary role in the initiation of OP-induced SE highlights a novel therapeutic target, and supports the strategy of using a nicotinic antagonist as a preventative antidote against OP-induced seizures.

ACKNOWLEDGEMENTS

This dissertation would not have been possible without the guidance and support of many people along the way. I would first like to thank my major professor and mentor, Dr. Pamela Lein, who provided the opportunity and resources for me to be trained in an amazing laboratory. Your insightful feedback taught me to think more critically, communicate more effectively, and ultimately brought my work to a higher level.

To my committee members, Drs. Gene Gurkoff and Isaac Pessah: thank you for asking tough questions and providing your guidance and feedback along the way. Your expertise helped to shape my research project and challenged me to consider new perspectives.

I would also like to acknowledge my lab manager and project scientist, Donald Bruun and Cris Grodzki, for their constant mentoring and support. It would not be possible to reach this point in my education without your help and guidance, and I am forever grateful for the conversations and friendship that helped me survive graduate school and my time in the lab. I will genuinely miss working with you both.

To my friends in the Lein lab, thank you for all your support and for being my lunch buddies. To Michelle Guignet and Kelley Patten, thank you for being there for me unconditionally, even in the darkest of times. I will always cherish the memories of surviving this process with you both, and I look forward to reuniting in the future for hiking trips and rock-climbing adventures. To Eduardo González, thank you for always being my procedure room buddy and for helping me understand academic culture when I arrived to the lab. I wouldn't have been able to finish this project during the pandemic without your assistance.

To Caitlin, Jacob, Liliana, and Brenda: thank you for tolerating the overwhelming stress and anxiety, and for being my safe harbor to keep me afloat. I am eternally grateful for the constant support you provided so that I could focus on my education. To Cait, thank you for being there for me in the best and worst moments, and for loving me despite my faults. None of this work would mean anything without the love and support that I receive from you. To Jake and Lily, I can't thank you enough for sacrificing play time while I worked late, and for providing the motivation to persevere even when I felt overwhelmed. To my brother Andrew, I can't express how much it has meant to stay close to you and share memories traveling together. I will always look forward to vacation time with you and hope we can live closer to each other someday.

I would also like to thank the late Christopher Hitchens for challenging my worldview when I was wandering and for inspiring me to strive for a well-examined life. Your written and verbal critiques of the role of religion in human culture were instrumental in my desire to pursue higher education. To Andy Riley, thank you for providing comic relief with bunny cartoons to keep me laughing on days when I needed it.

Table of Contents

Chapter 1

Introduction

Abbreviations

ACh = acetylcholine

AChE = acetylcholinesterase

AlloP = allopregnanolone

CNS = central nervous system

DPE = days post-exposure

$GABA_AR$ = $GABA_A$ receptor

GFAP = glial fibrillary acidic protein

IBA1 = ionized calcium binding adaptor molecule 1

nAChR = nicotinic cholinergic receptor

OP = organophosphate

PAM = positive allosteric modulator

SE = *status epilepticus*

TETS = tetramethylenedisulfotetramine

Introduction

Acute intoxication with proconvulsant chemicals is a clear and present danger in many parts of the world, as demonstrated by the continued occurrence of accidental or intentional poisoning with organophosphate (OP) cholinesterase inhibitors and pesticides or $GABA_A$ receptor antagonists (Figure 1). Acute exposure to high doses of these chemical classes can trigger seizures that quickly progress to life-threatening *status epilepticus* (SE; Figueiredo, Apland et al. 2018, Lauková, Velíšková et al. 2020). This high level of toxicity coupled with the ready availability of these chemicals is the motivation for the United States Department of Homeland Security to classify them as credible chemical threat agents (Watson, Opresko et al. 2015, Shakarjian, Laukova et al. 2016, Richardson, Fitsanakis et al. 2019). Human survivors and preclinical rodent models of acute intoxication with proconvulsant chemicals demonstrate long-term neurological consequences, such as electroencephalographic abnormalities, including spontaneous recurrent seizures, and cognitive deficits (Okumura, Hisaoka et al. 2005, Chen 2012, Jett, Sibrizzi et al. 2020, Lauková, Velíšková et al. 2020). The current first-line therapy for seizures induced by these chemicals is early treatment with benzodiazepines to terminate SE and thereby increase survival and decrease the brain injury that underlies chronic neurologic consequences (Eddleston, Buckley et al. 2008). However, there are numerous limitations such as refractoriness and serious adverse effects on respiration and blood pressure associated with benzodiazepines in this clinical setting, particularly when administered at the high doses required for treating chemical induced-SE or when administered at delayed times post-exposure (Forster, Gardaz et al. 1980, Kitajima, Kanbayashi et al. 2004, Masson 2011, Bruun, Cao et al. 2015). Additionally, humans and rodents that do respond favorably to benzodiazepines can still demonstrate long-term cognitive or behavioral consequences despite the termination of SE

(McDonough, Zoeffel et al. 1999, Shih 2000). Therefore, there is a clear need to identify better therapies to improve outcomes for survivors of SE induced by chemical threat agents.

$GABA_AR$ antagonists as proconvulsants

The $GABA_AR$ antagonist tetramethylenedisulfotetramine (2,6-dithia-1,3,5,7-tetraazadamantane,2,2,6,6-tetraoxide; TETS) is considered a credible chemical threat agent (Velisek 2005, Shakarjian, Velíšková et al. 2012, Zolkowska, Banks et al. 2012). TETS gained popularity as a highly effective rodenticide for reforestation efforts in the United States in the 1950s (Croddy 2004), but was eventually banned in 1984 due to an extremely low LD_{50} of 100 µg/kg or 7-10 mg total in humans and its persistence in the environment (Guan, Liu et al. 1993, reviewed in Whitlow, Belson et al. 2005). By the early 2000's, TETS production was banned worldwide, but due to high consumer demand for effective and cheap rodenticides, TETS is still widely available on the black market in Asia (reviewed in Patocka, Franca et al. 2018). A large number of mass poisonings have occurred in China and elsewhere, and it is likely that tens of thousands of people have been poisoned with TETS, many deliberately (Wu and Sun 2004, Li, Gan et al. 2012). TETS exposure is typically via ingestion and does not always result in convulsions (reviewed in Zhang, Su et al. 2011). Less severe symptoms include nausea, dizziness, or headache, including pulmonary edema, congestion, dark fluid in the heart, calcium depositions in the kidney, and fatty liver (Zhou, Liu et al. 1998). Brainstem hemorrhage as well as edema and congestion of brain tissue have also been found in patients poisoned with TETS (reviewed in Whitlow, Belson et al. 2005).

TETS is a potent noncompetitive reversible antagonist of the $GABA_AR$, which leads to hyperexcitability by disrupting chloride regulation in neurons (Figure 2). TETS preferentially inhibits $GABA_AR$ comprised of α2/β3 or α6/β3 subunits, with the highest activity at the α2β3γ2 subunit conformation (Pressly, Nguyen et al. 2018). The reduction of inhibitory tone as a result of $GABA_AR$ inhibition causes increased excitation in the central nervous system (CNS), which can lead to convulsions, seizures, SE, and/or death (Lu, Wang et al. 2008, Cao, Hammock et al. 2012, Shakarjian, Velíšková et al. 2012). TETS persists in the body for days after exposure (Ning, He et al. 1997, reviewed in Patocka, Franca et al. 2018, Pressly, Vasylieva et al. 2020). While the toxicokinetic explanation for this long biological half-life remains to be elucidated, survivors of TETS poisoning can experience electrographic abnormalities that can persist for more than a year post-exposure (Liu and Zhang 2004, Lu, Wang et al. 2008), emphasizing the need for more research on treatment strategies for TETS exposure.

Several antiseizure drugs are used clinically to treat TETS-induced seizures. As TETS specifically targets the $GABA_AR$, positive allosteric modulators (PAMs) for this receptor class, which include benzodiazepines and barbiturates, are the most widely used medications used to terminate seizures in TETS-intoxicated individuals. Diazepam, a PAM that targets synaptic α1/γ2 prominent $GABA_AR$ (Sigel and Ernst 2018), is highly effective at terminating seizures in TETS-intoxicated humans (Bai, Zhang et al. 2005) and preclinical rodent models (reviewed in Pessah, Rogawski et al. 2016). Sodium phenobarbital (Voss, Haskell et al. 1961, Guo and Zhang 2007), allopregnanolone (AlloP) (Bruun, Cao et al. 2015, Zolkowska, Wu et al. 2018), and propofol (Guo and Zhang 2007) also terminate seizures and increase survival in both humans and rodents intoxicated with TETS. AlloP is of significant interest due to its activity at both synaptic $GABA_AR$ (phasic inhibition) and extrasynaptic $GABA_AR$ (tonic inhibition) as compared to

benzodiazepines, which only target the synaptic $GABA_AR$ that are internalized during prolonged seizure activity (Olsen 1981, Mohler, Fritschy et al. 2002). AlloP also increases the open channel duration of $GABA_AR$ (Akk, Bracamontes et al. 2004, Akk, Covey et al. 2010) as opposed to benzodiazepines, which increase channel opening frequency (Bianchi, Botzolakis et al. 2009, Bianchi 2010). Thus, AlloP has some advantages over benzodiazepines that may prove beneficial for terminating seizures and providing neuroprotection by preventing reoccurring seizures.

A major challenge in identifying more effective medical countermeasures for acute TETS intoxication has been the lack of preclinical models that recapitulate the acute and chronic neurotoxic effects observed in humans acutely poisoned with TETS. While the current standard of care for TETS poisoning (high-dose benzodiazepines) is sufficient to protect against death after exposure, human survivors can still experience long-term cognitive deficits and electroencephalographic abnormalities (Croddy 2004, Whitlow, Belson et al. 2005, Deng, Li et al. 2012). Whether these neurological consequences are due to the toxicodynamic effects of TETS, or a direct result of TETS-induced seizure activity remains unclear. Previous rodent models developed to study the consequences of acute TETS intoxication have been limited by a lack of prolonged seizures or SE (Shakarjian, Veliskova et al. 2012, Zolkowska, Banks et al. 2012, Rice, Rauscher et al. 2017). To address this limitation, we recently developed a mouse model of TETS-induced SE that produces continuous seizures beginning within minutes after TETS injection and lasting between 60-90 min post-TETS (Pessah, Rogawski et al. 2016, Zolkowska, Wu et al. 2018). While the new TETS SE model better recapitulates the acute seizure activity observed in TETS-intoxicated humans, there has been little investigation of its long-term neurologic effects.

Organophosphates

Organophosphates (OPs) are a class of synthetic, neurotoxic compounds that include warfare agents (e.g., sarin, soman) and pesticides (e.g., diisopropylfluorophosphate [DFP], parathion) that can cause convulsions, status epilepticus (SE), and death following acute intoxication. OPs exert these effects by prolonged inhibition of acetylcholinesterase (AChE; Figure 4), a protease that regulates cholinergic signaling in the body by hydrolyzing synaptic acetylcholine (ACh; Pope and Brimijoin 2018). Inhibition of AChE by OPs can cause an excessive buildup of ACh at nicotinic and muscarinic ACh receptors (AChRs) in the peripheral and central nervous systems, resulting in a toxidrome known as a cholinergic crisis with symptoms of increased salivation, lacrimation, urination, and diarrhea (SLUD; Adeyinka and Kondamudi 2018). Individuals who survive acute OP exposure often experience significant morbidity, including persistent neuropathology, cognitive impairments, and electroencephalographic abnormalities (Pereira, Aracava et al. 2014, Figueiredo, Apland et al. 2018, Jett, Sibrizzi et al. 2020).

The toxic properties of OPs were discovered in the 1930's, when German chemist Gerhard Schrader and his graduate student accidentally exposed themselves to OPs in the laboratory (Petroianu 2010). This exposure caused respiratory difficulty, altered consciousness, and impaired vision; effects later defined as symptoms of the cholinergic crisis. The published description of these acute symptoms of exposure led a German chemical company to pursue the development of OP chemicals as insecticides. For this reason, the German military took interest in the effects of OP chemicals as weapons and hired a scientist in the 1940's to develop the first OP nerve agents for use against humans (Ganesan, Raza et al. 2010). These newer nerve agents were different from insecticides in their toxic and physical properties, which are directly related

to their chemical structure (Figure 3). OP compounds are generally defined by a structure of $O=P(OR)_3$, with variation in R-groups giving rise to differences in physical properties and neurotoxic profiles (Can 2014, Mukherjee and Gupta 2020). Nerve agents tend to have high volatility and they exist as a vapor at room temperature, which leads to low persistence in the environment after deployment (Figueiredo, Apland et al. 2018). Pesticides typically remain in liquid form at room temperature with low volatility, and often need to be metabolized in the body to become toxic. Despite these differences in physical properties, both OP nerve agents and pesticides inhibit AChE, causing disease or death in insects and mammals.

During World War II, the OP nerve agents sarin, soman, and tabun were produced and stockpiled by the Nazis, but were fortunately not deployed on the battlefield (Munro 1994). In the 1980's, tabun and sarin were used in attacks during the Iran-Iraq war by the Iraqi army against Iranians, killing thousands (Haines and Fox 2014). In 1995, sarin was used by domestic terrorists in attacks on Tokyo subway lines, killing or injuring thousands of innocent people (Okumura, Hisaoka et al. 2005). More recent examples of human OP exposure include the use of sarin gas against civilians in Syria in 2017 (UN 2020, HRW 2021), the assassination of a North Korean official in 2017 with a VX nerve agent (OPCW 2018), and assassination attempts using novichok nerve agent in the United Kingdom in 2018 (Chai, Hayes et al. 2018, Haley 2018) and in Russia in 2020 (Masterson 2020, OPCW 2020). While these unfortunate incidents illustrate the acute toxicity of nerve agents, deliberate and accidental exposures to OP pesticides harm significantly more individuals. Indeed, OP pesticides are some of the most commonly used chemicals in suicide attempts in developing nations due to their low cost and prevalence (Kar 2006). Homicidal, suicidal, and accidental poisonings with OP pesticides have been documented for many years and remain the cause of hundreds of thousands of global deaths annually (Mew,

Padmanathan et al. 2017, Eddleston 2019). In addition to suicide, long-term exposure to OP pesticides in agricultural settings has been implicated in adverse health effects seen in workers who were exposed for days to months (Muñoz-Quezada, Lucero et al. 2016). These compounds cause toxicity through the same mechanism as nerve agents, raising great concern about their prevalence and lack of regulation. For these reasons, the Department of Homeland Security lists OPs as credible chemical threat agents (Watson, Opresko et al. 2015).

One key difference between OP nerve agents and pesticides is whether they "age". This term describes the chemical process in which binding of the OP to AChE becomes irreversible, thereby inhibiting AChE function permanently (Sirin, Zhou et al. 2012). This process typically begins with phosphorylation of the active serine site of AChE by the OP, followed by a dealkylation of the OP, causing AChE to become refractory to oxime therapy (Quinn, Topczewski et al. 2017). Most OP nerve agents complete the aging process in minutes to hours after exposure, while most OP pesticides "age" over many hours, or sometimes not at all (Dunn and Sidell 1989). The cause of death from acute OP intoxication is often suffocation from a combination of effects in the peripheral and central nervous system that control respiration (Robb and Baker 2017).

Understanding when to administer a medical countermeasure can be extremely challenging. The current medical countermeasures for the treatment of acute OP intoxication include the rapid intramuscular administration of a muscarinic cholinergic antagonist (e.g., atropine) and oxime (e.g., pralidoxime) to reactivate AChE, and a $GABA_A$ receptor PAM (e.g., the benzodiazepines diazepam or midazolam) to terminate seizures (Eddleston, Buckley et al. 2008). However, these therapies are only effective if administered within minutes and do not provide protection against the long-term neurological consequences observed in survivors

(McDonough, Zoeffel et al. 1999, Shih 2000, Masson 2011). Additionally, benzodiazepines are only transiently effective at blocking OP-induced seizure activity due to the downregulation of their target, synaptic $GABA_A$ receptors during SE (Kuruba, Wu et al. 2018). For these reasons, there is an urgent need for more effective medical countermeasures against acute OP intoxication, as failure to stop seizures quickly can result in significant brain damage. However, the development of new therapeutic strategies has been stymied by the lack of understanding of the pathogenic mechanisms underlying the acute seizure response, and the long-term neurologic sequelae.

Preclinical rodent models have been developed to assess the acute and chronic toxicity of acute OP intoxication and can be used to test novel therapies for antiseizure and/or neuroprotective efficacy (Pereira, Aracava et al. 2014, Pessah, Rogawski et al. 2016). These models provide a reliable platform for screening therapeutics for acute exposure to OP chemicals because they mimic consequences seen in humans acutely intoxicated with OPs (Pereira, Aracava et al. 2014, Pessah, Rogawski et al. 2016). Rodent models reliably reproduce several characteristics of human epilepsy, accurately reflecting the timeline of epileptogenesis and patterns of seizure of progression (Kandratavicius, Balista et al. 2014). Importantly, rodent models also generate the variability in epilepsy severity seen in human patients, more faithfully reflecting clinical cases (Becker 2018, Fallah and Eubanks 2020). Moreover, a number of anti-seizure drugs have been developed in rodent models before progressing to use in humans (Löscher 2011). This predictive quality points to the relevance of animal models of acute OP intoxication and suggests that these approaches are suitable for the development of improved countermeasures. Recently, our lab developed a rat model of DFP-induced SE that recapitulates key features of acute OP intoxication in humans (Pessah, Rogawski et al. 2016, Guignet, Dhakal

et al. 2020). After DFP is administered subcutaneously, seizures begin within 10 minutes and persist for at least 4 hours. Robust neuropathology is apparent in the brain tissue of DFP-intoxicated rats within hours of exposure and can persist for up to 60 days post-exposure (DPE). Specifically, a spatiotemporal pattern of severe neurodegeneration occurs and long-term neuroinflammatory responses like reactive astrogliosis and microglial activation are also observed (Guignet, Dhakal et al. 2020). These neuropathologic responses precede and are comorbid with long-term behavioral deficits and electroencephalographic abnormalities like spontaneous recurrent seizures (SRS), commonly referred to as acquired epilepsy. Despite significant research effort to discover an antidote for OP intoxication, current therapies in preclinical models are limited in their ability to prevent acute or chronic neurological effects, in part because the mechanisms underlying these effects are not fully understood.

Mechanistic role of cholinergic receptors in OP intoxication

The cholinergic crisis caused by OP intoxication is initiated by the effects of excessive ACh signaling via muscarinic cholinergic receptors (mAChRs) and nicotinic cholinergic receptors (nAChRs; Adeyinka and Kondamudi 2018), and OPs have also been shown to cause direct pathological effects in both types of receptors (Bakry, El-Rashidy et al. 1988). Hyperstimulation of mAChRs is thought to be the primary cause for symptoms like salivation, lacrimation, urination, diarrhea, gastrointestinal discomfort, emesis, or miosis (SLUDGEM; Adeyinka and Kondamudi 2018), which is why current strategies to dampen cholinergic tone for OP intoxication focus exclusively on muscarinic receptor antagonism (Sheridan, Smith et al. 2005). The mechanistic role of mAChRs has also been validated by preclinical models of OP intoxication using pharmacologic antagonism of mAChRs to prevent some of the long-term

consequences of acute OP exposure with caramiphen or scopolamine after atropine rescue (Figueiredo, Aroniadou-Anderjaska et al. 2011, Jackson, Ardinger et al. 2019). While this strategy can improve survival and long-term outcomes, nAChRs remain active in the brain during OP-SE (Smythies and Golomb 2004) and consequently are a potential mechanism for seizure and SE initiation.

While existing anticholinergic therapies for OP intoxication target muscarinic receptors, questions have been raised in the literature about the absence of therapies targeting nAChRs (Smythies and Golomb 2004, Sheridan, Smith et al. 2005). When activated, these ionotropic receptors can allow the influx of cations like sodium or calcium into a cell, thereby contributing to depolarization, hyperexcitability, and the cascade of OP-induced neuropathology (Pidoplichko, Prager et al. 2013, Pankratov and Lalo 2014, Prager, Pidoplichko et al. 2014). This description is consistent with preclinical literature using nAChR antagonists after OP exposure to assess their role in OP-induced consequences. The nAChR antagonist MB327 (33.8 mg/kg) has been shown to significantly improve survival in guinea pigs following high-dose (525 µg/kg) soman intoxication when given at 1 min post-soman (Price, Whitmore et al. 2018), suggesting these receptors have a mechanistic role in soman-induced lethality. In support of this, the use of the nAChR antagonist 4R-cembranoid (6 mg/kg) 24 h post-DFP intoxication (9 mg/kg) significantly reduced neurodegeneration and reactive astrogliosis in the hippocampus at 2 DPE (Ferchmin, Andino et al. 2014). However, these studies only evaluated neuropathology in the days following OP intoxication, and did not investigate the role of nAChRs in the initiation or maintenance of acute SE. Therefore, it is of great interest to determine the potential role of nAChRs in the pathophysiology of OP-induced SE to gain a better understanding of their contribution to acute intoxication.

The nAChR is a pentameric, ionotropic receptor that allows the influx of cations including sodium or calcium into the postsynaptic cell when activated (Davis and de Fiebre 2006). In the CNS, the α4β2 and α7 are the predominant nAChR subtypes that are expressed (Davis and de Fiebre 2006). The α4β2 nAChR is a heteropentamer consisting of a combination of α4 and β2 subunits, and the agonist binding site for ACh is located at the extracellular α4 and β2 interface. This subtype is known to be involved with epilepsy, as some patients have displayed missense mutations in the transcript for the α4 subunit (Steinlein, Mulley et al. 1995), and transgenic mice with hypersensitive α4 receptors display higher sensitivity to agonist-induced seizures (Fonck, Nashmi et al. 2003). The α7 nAChR is a homopentamer consisting exclusively of α7 subunits (Davis and de Fiebre 2006), and the ACh binding site is found between each interface of the extracellular subunits, allowing five active domains for binding ACh (Davis and de Fiebre 2006). When activated, these receptors can influence synaptic remodeling and neurotransmitter release (Orr-Urtreger, Goldner et al. 1997). The α4 and α7 nAChR subunits have been implicated in cognitive dysfunction, brain matter loss, and neuroinflammation that are seen in neurodegenerative diseases such as Alzheimer's Disease and Parkinson's (Lloyd and Williams 2000). Collectively, these observations suggest that the α4 and/or α7 nicotinic receptor subtypes may be required for the induction and maintenance of DFP-induced hyperexcitability, and that these receptors could be viable targets for prophylactic therapy before exposure to OPs.

Dissertation Overview

This dissertation addresses critical data gaps in the understanding of SE induced by chemical threat agents. Specifically, I focused on evaluating the neurologic consequences of SE

using two mechanistically diverse mouse models of SE induced by chemical threat agents. TETS-SE mice were used for *in vivo* imaging in the days after acute TETS intoxication and DFP-SE mice were used for investigation of pathogenic mechanisms contributing to OP intoxication. First, neuropathologic responses have not yet been characterized in the TETS SE mouse model. In Chapter 2, neuropathology in a mouse model of acute TETS-induced SE is characterized using longitudinal MR and PET imaging to describe the spatiotemporal profile of brain damage over the first 14 days post-intoxication. Second, while there are several rat models of DFP-induced SE exhibiting long-term neurological deficits, there is a lack of long-term data in existing mouse models of DFP-SE. The development of a C57BL/6J mouse model in this context would establish long-term consequences in this strain of mice and provide a platform to leverage C57BL/6J knockout mice for mechanistic studies of OP intoxication. Therefore, in Chapter 3, long-term neuropathology and behavioral deficits are established in a mouse model of DFP-induced SE using histological, biochemical, and behavioral approaches. Third, the role of nicotinic cholinergic receptors in OP intoxication is not well understood and gaining more knowledge about the role of these receptors in the cholinergic crisis and initiation of SE can assist in prophylactic strategies for exposure to OPs. By leveraging a mouse model of DFP-SE, pharmacologic and genetic approaches could be used to illuminate which nicotinic receptor subtypes are most vulnerable to the initiation of SE. In Chapter 4, nicotinic receptors are investigated for their role in DFP-induced SE using nicotinic antagonists or knockout mice lacking nicotinic receptors in the newly generated DFP mouse model of SE. In summary, this thesis expands the utility of mouse models for studying brain damage following SE induced by chemical threat agents and identifies a mechanistic role for nicotinic receptors in the pathophysiology of OP-SE. These findings enhance the current understanding of pathological

mechanisms of OPs and can help to identify novel therapies to improve medical countermeasures against intoxication.

Figure 1.

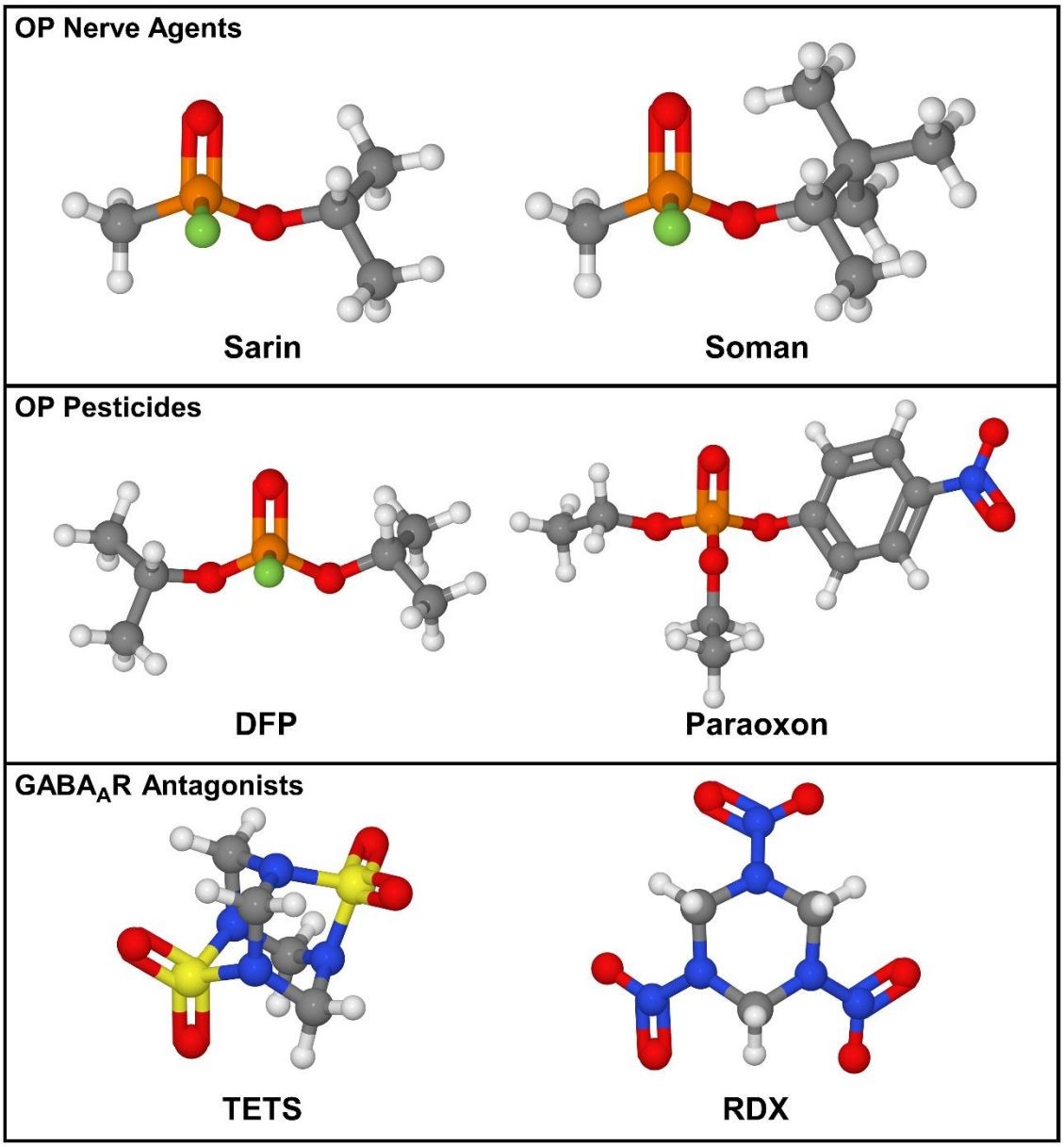
OP Nerve Agents
Sarin
Soman
OP Pesticides
DFP
Paraoxon
GABA$_A$R Antagonists
TETS
RDX

Figure 1. Illustration of the 3-dimensional chemical structures of organophosphate (OP) nerve agents (sarin and soman), OP pesticides (diisopropylfluorophosphate (DFP) and paraoxon), and $GABA_A$ receptor antagonists [tetramethylenedisulfotetramine (TETS) and RDX].

Figure 2.

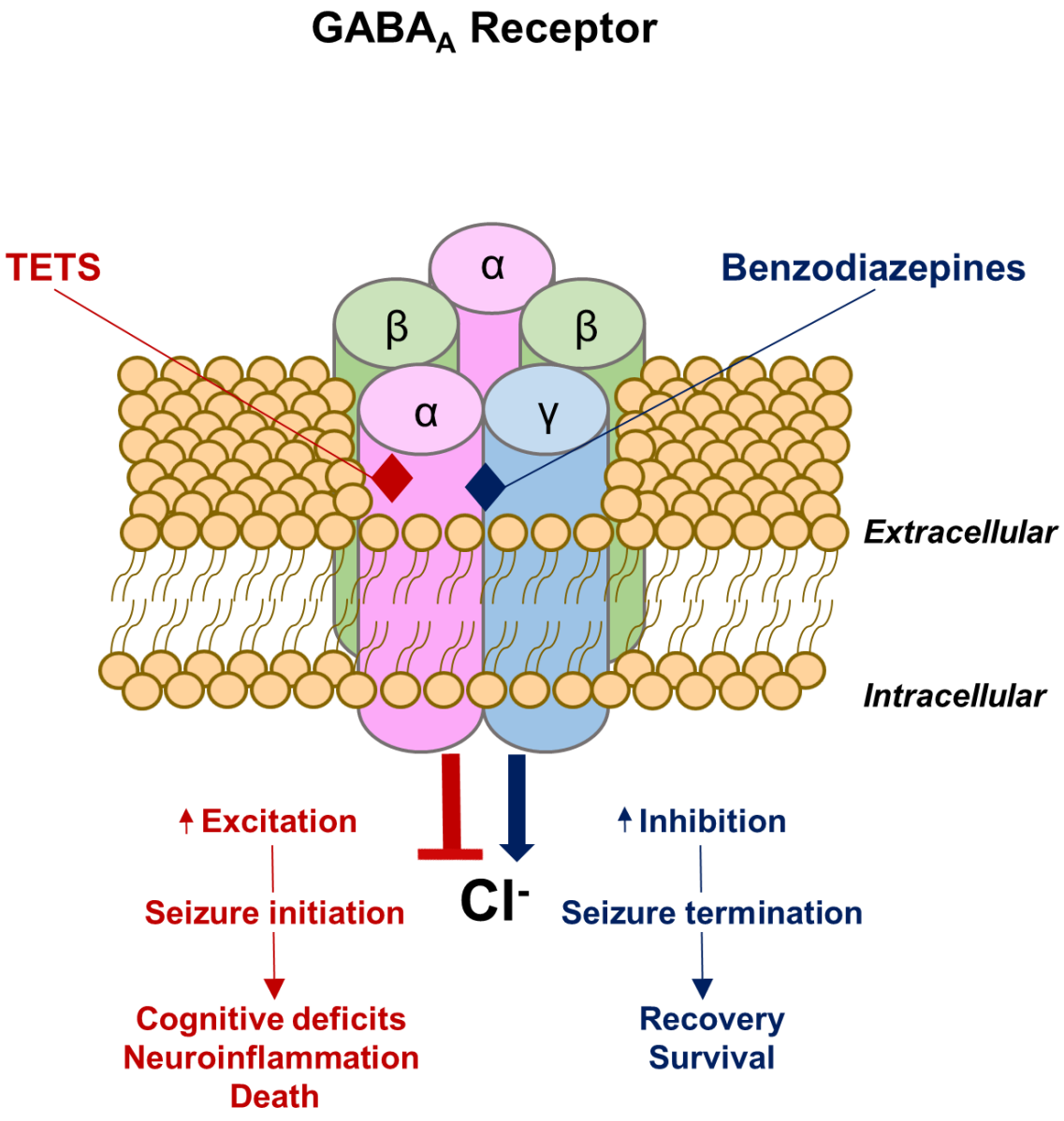
GABA$_A$ Receptor
TETS
Benzodiazepines
α
β
β
α
γ
Extracellular
Intracellular
Excitation
Inhibition
Cl$^-$
Seizure initiation
Seizure termination
Cognitive deficits
Neuroinflammation
Death
Recovery
Survival

Figure 2. Diagram illustrating $GABA_A$ receptor subunits with binding domains for TETS (red diamond) and benzodiazepines (blue diamond), and the potential downstream effects related to seizures.

Figure 3.

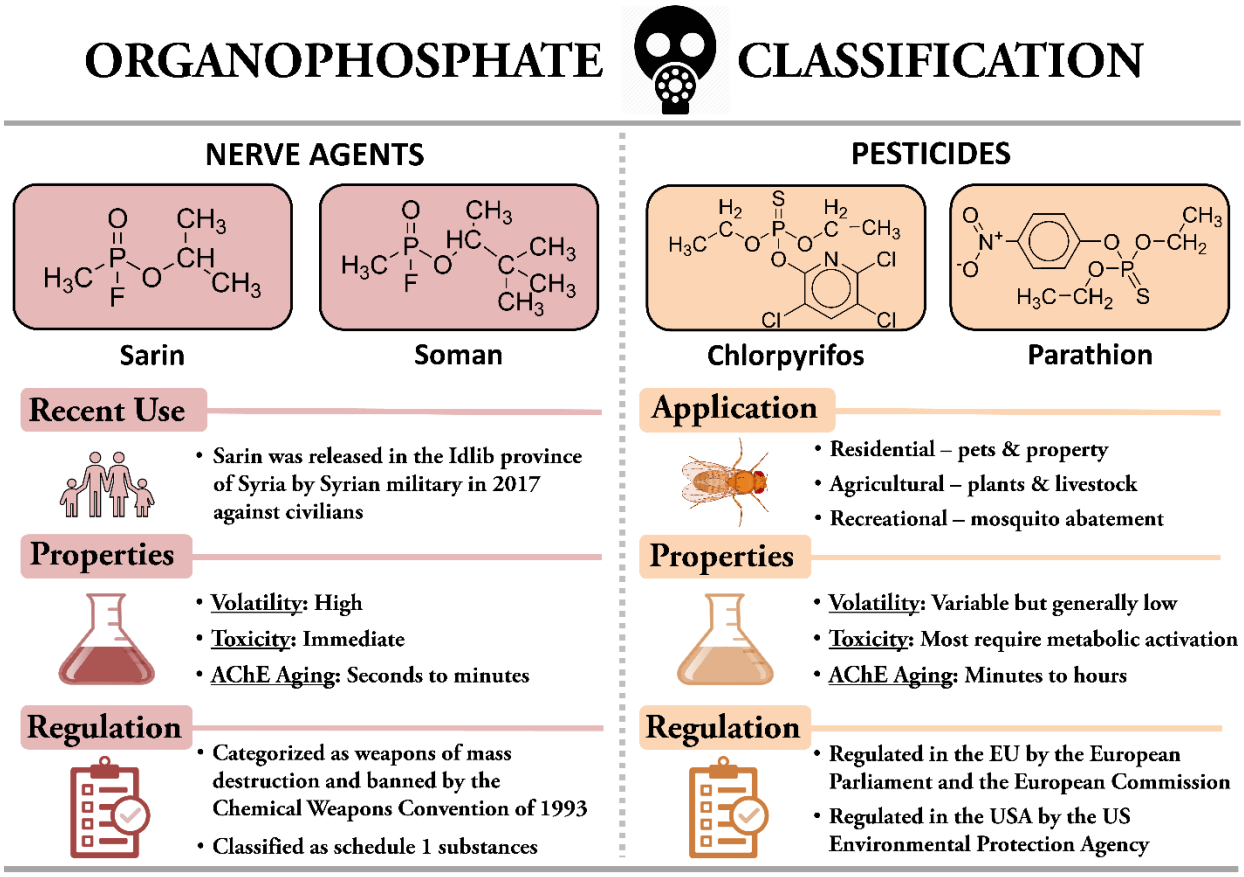
ORGANOPHOSPHATE CLASSIFICATION
NERVE AGENTS
PESTICIDES
Sarin
Soman
Chlorpyrifos
Parathion
Recent Use
• Sarin was released in the Idlib province of Syria by Syrian military in 2017 against civilians
Properties
• Volatility: High
• Toxicity: Immediate
• AChE Aging: Seconds to minutes
Regulation
• Categorized as weapons of mass destruction and banned by the Chemical Weapons Convention of 1993
• Classified as schedule 1 substances
Application
• Residential – pets & property
• Agricultural – plants & livestock
• Recreational – mosquito abatement
Properties
• Volatility: Variable but generally low
• Toxicity: Most require metabolic activation
• AChE Aging: Minutes to hours
Regulation
• Regulated in the EU by the European Parliament and the European Commission
• Regulated in the USA by the US Environmental Protection Agency

Figure 3. Illustrated comparison of the recent use, chemical characteristics, and government regulation of organophosphate nerve agents and pesticides.

Figure 4.

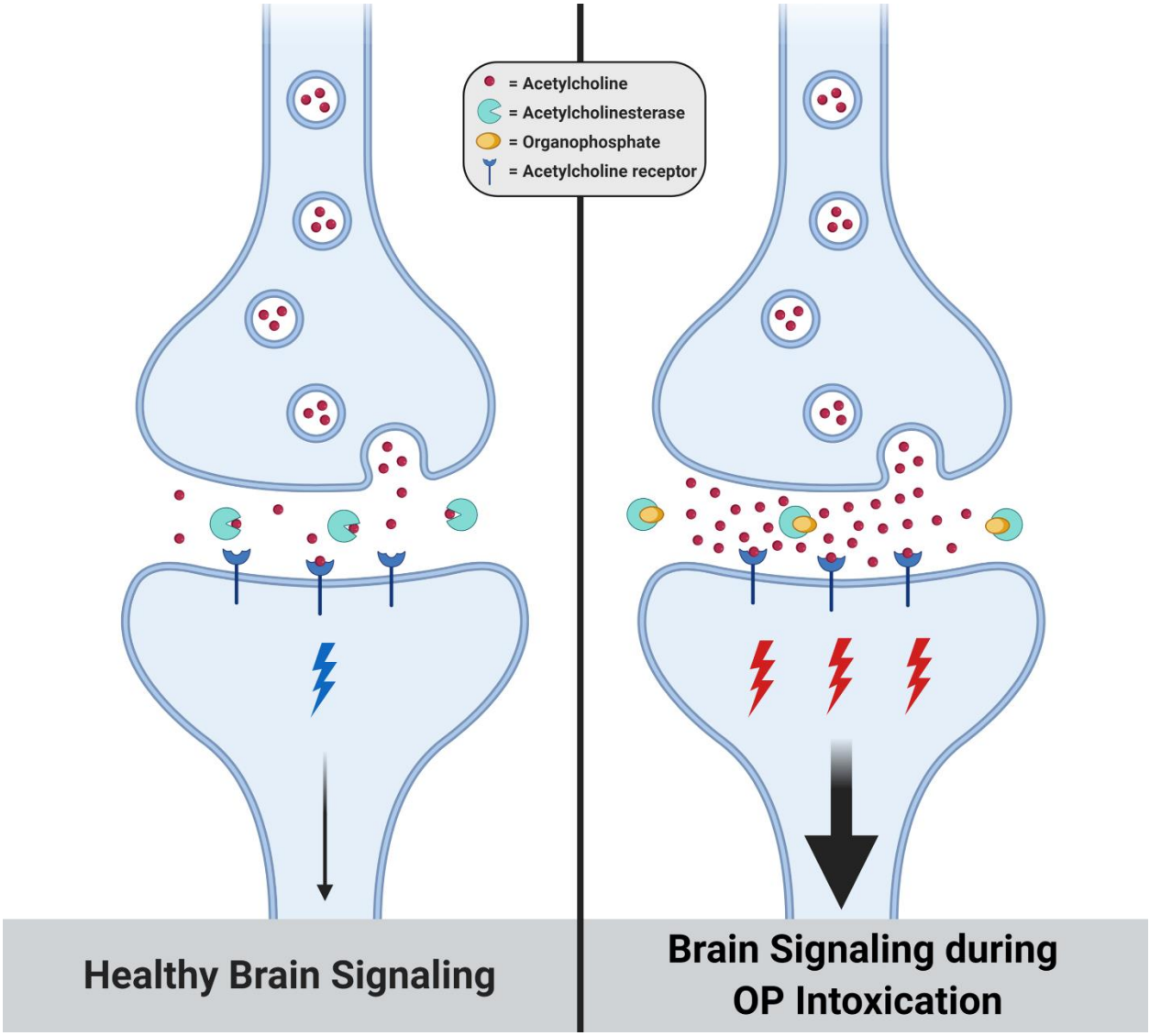
= Acetylcholine
= Acetylcholinesterase
= Organophosphate
= Acetylcholine receptor
Healthy Brain Signaling
Brain Signaling during OP Intoxication

Figure 4. Illustration of neurotransmission at a cholinergic synapse in healthy conditions (left) compared to the cholinergic crisis after intoxication with cholinesterase inhibitors (right). Acetylcholinesterase is an enzyme that regulates cholinergic neurotransmission through the breakdown of acetylcholine at the cholinergic synapse. Therefore, the inhibition of acetylcholinesterase by organophosphates can lead to the excessive accumulation of acetylcholine, which can cause the cholinergic crisis. Created with BioRender.com.

References

Adeyinka, A. and N. P. Kondamudi (2018). "Cholinergic crisis."

Akk, G., J. R. Bracamontes, D. F. Covey, A. Evers, T. Dao and J. H. Steinbach (2004). "Neuroactive steroids have multiple actions to potentiate GABAA receptors." J Physiol **558**(Pt 1): 59-74.

Akk, G., D. F. Covey, A. S. Evers, S. Mennerick, C. F. Zorumski and J. H. Steinbach (2010). "Kinetic and structural determinants for GABA-A receptor potentiation by neuroactive steroids." Curr Neuropharmacol **8**(1): 18-25.

Bai, H., S. L. Zhang, H. S. Zhang, J. T. Ji, P. B. Ma, H. S. Wang, Y. W. Bai, X. R. Zhou, M. B. Ding, X. R. Lu and C. Y. Sun (2005). "[Evaluation of therapeutic project on acute tetramethylene disulphotetramine poisoning and effect on intelligence in children]." Zhonghua Yu Fang Yi Xue Za Zhi **39**(2): 95-98.

Bakry, N. M., A. H. El-Rashidy, A. T. Eldefrawi and M. E. Eldefrawi (1988). "Direct actions of organophosphate anticholinesterases on nicotinic and muscarinic acetylcholine receptors." Journal of biochemical toxicology **3**(4): 235-259.

Becker, A. (2018). "Animal models of acquired epilepsy: insights into mechanisms of human epileptogenesis." Neuropathology and applied neurobiology **44**(1): 112-129.

Bianchi, M. T. (2010). "Context dependent benzodiazepine modulation of GABA(A) receptor opening frequency." Curr Neuropharmacol **8**(1): 10-17.

Bianchi, M. T., E. J. Botzolakis, A. H. Lagrange and R. L. Macdonald (2009). "Benzodiazepine modulation of GABA(A) receptor opening frequency depends on activation context: a patch clamp and simulation study." Epilepsy Res **85**(2-3): 212-220.

Bruun, D. A., Z. Cao, B. Inceoglu, S. T. Vito, A. T. Austin, S. Hulsizer, B. D. Hammock, D. J. Tancredi, M. A. Rogawski, I. N. Pessah and P. J. Lein (2015). "Combined treatment with diazepam and allopregnanolone reverses tetramethylenedisulfotetramine (TETS)-induced calcium dysregulation in cultured neurons and protects TETS-intoxicated mice against lethal seizures." Neuropharmacology **95**: 332-342.

Can, A. (2014). "Quantitative structure–toxicity relationship (QSTR) studies on the organophosphate insecticides." Toxicology letters **230**(3): 434-443.

Cao, Z., B. D. Hammock, M. McCoy, M. A. Rogawski, P. J. Lein and I. N. Pessah (2012). "Tetramethylenedisulfotetramine alters Ca^{2+} dynamics in cultured hippocampal neurons: mitigation by NMDA receptor blockade and GABA(A) receptor-positive modulation." Toxicological sciences : an official journal of the Society of Toxicology **130**(2): 362-372.

Chai, P. R., B. D. Hayes, T. B. Erickson and E. W. Boyer (2018). "Novichok agents: a historical, current, and toxicological perspective." Toxicology communications **2**(1): 45-48.

Chen, Y. (2012). "Organophosphate-induced brain damage: mechanisms, neuropsychiatric and neurological consequences, and potential therapeutic strategies." Neurotoxicology **33**(3): 391-400.

Croddy, E. (2004). "Rat poison and food security in the People's Republic of China: focus on tetramethylene disulfotetramine (tetramine)." Arch Toxicol **78**(1): 1-6.

Croddy, E. (2004). "Rat poison and food security in the People's Republic of China: focus on tetramethylene disulfotetramine (tetramine)." Archives of toxicology **78**(1): 1-6.

Davis, T. J. and C. M. de Fiebre (2006). "Alcohol's actions on neuronal nicotinic acetylcholine receptors." Alcohol Res Health **29**(3): 179-185.

Deng, X., G. Li, R. Mei and S. Sun (2012). "Long term effects of tetramine poisoning: an observational study." Clin Toxicol (Phila) **50**(3): 172-175.

Dunn, M. A. and F. R. Sidell (1989). "Progress in medical defense against nerve agents." Jama **262**(5): 649-652.

Eddleston, M. (2019). "Novel clinical toxicology and pharmacology of organophosphorus insecticide self-poisoning." Annual review of pharmacology and toxicology **59**: 341-360.

Eddleston, M., N. A. Buckley, P. Eyer and A. H. Dawson (2008). "Management of acute organophosphorus pesticide poisoning." The Lancet **371**(9612): 597-607.

Fallah, M. S. and J. H. Eubanks (2020). "Seizures in mouse models of rare neurodevelopmental disorders." Neuroscience **445**: 50-68.

Ferchmin, P. A., M. Andino, R. Reyes Salaman, J. Alves, J. Velez-Roman, B. Cuadrado, M. Carrasco, W. Torres-Rivera, A. Segarra, A. H. Martins, J. E. Lee and V. A. Eterovic (2014). "4R-cembranoid protects against diisopropylfluorophosphate-mediated neurodegeneration." Neurotoxicology **44**: 80-90.

Figueiredo, T. H., J. P. Apland, M. F. Braga and A. M. Marini (2018). "Acute and long-term consequences of exposure to organophosphate nerve agents in humans." Epilepsia **59**: 92-99.

Figueiredo, T. H., V. Aroniadou-Anderjaska, F. Qashu, J. P. Apland, V. Pidoplichko, D. Stevens, T. M. Ferrara and M. F. M. Braga (2011). "Neuroprotective efficacy of caramiphen against soman and mechanisms of its action." British Journal of Pharmacology **164**(5): 1495-1505.

Fonck, C., R. Nashmi, P. Deshpande, M. I. Damaj, M. J. Marks, A. Riedel, J. Schwarz, A. C. Collins, C. Labarca and H. A. Lester (2003). "Increased sensitivity to agonist-induced seizures, straub tail, and hippocampal theta rhythm in knock-in mice carrying hypersensitive alpha 4 nicotinic receptors." J Neurosci **23**(7): 2582-2590.

Forster, A., J. P. Gardaz, P. M. Suter and M. Gemperle (1980). "Respiratory depression by midazolam and diazepam." Anesthesiology **53**(6): 494-497.

Ganesan, K., S. Raza and R. Vijayaraghavan (2010). "Chemical warfare agents." Journal of pharmacy and bioallied sciences **2**(3): 166.

Guan, F. Y., Y. T. Liu, Y. Luo, X. Y. Hu, F. Liu, Q. Y. Li and Z. W. Kang (1993). "GC/MS identification of tetramine in samples from human alimentary intoxication and evaluation of artificial carbonic kidneys for the treatment of the victims." J Anal Toxicol **17**(4): 199-201.

Guignet, M., K. Dhakal, B. M. Flannery, B. A. Hobson, D. Zolkowska, A. Dhir, D. A. Bruun, S. Li, A. Wahab, D. J. Harvey, J. L. Silverman, M. A. Rogawski and P. J. Lein (2020). "Persistent behavior deficits, neuroinflammation, and oxidative stress in a rat model of acute organophosphate intoxication." Neurobiol Dis **133**: 104431.

Guo, J. X. and H. L. Zhang (2007). "[A reflection on successful treatment of severe tetramine intoxication in 9 cases]." Zhongguo Wei Zhong Bing Ji Jiu Yi Xue **19**(5): 310.

Haines, D. D. and S. C. Fox (2014). "Acute and long-term impact of chemical weapons: lessons from the Iran-Iraq war." Forensic Sci Rev **26**(2): 97-114.

Haley, N. (2018). "Remarks at an Emergency UN Security Council Briefing on Chemical Weapons Use by Russia in the United Kingdom." United States Mission to the United Nations.

HRW. (2021). "The Syrian Government's Widespread and Systematic Use of Chemical Weapons." from https://www.hrw.org/report/2017/05/01/death-chemicals/syrian-governments-widespread-and-systematic-use-chemical-weapons.

Jackson, C., C. Ardinger, K. M. Winter, J. H. McDonough and H. S. McCarren (2019). "Validating a model of benzodiazepine refractory nerve agent-induced status epilepticus by evaluating the anticonvulsant and neuroprotective effects of scopolamine, memantine, and phenobarbital." J Pharmacol Toxicol Methods **97**: 1-12.

Jett, D. A., C. A. Sibrizzi, R. B. Blain, P. A. Hartman, P. J. Lein, K. W. Taylor and A. A. Rooney (2020). "A national toxicology program systematic review of the evidence for long-term effects after acute exposure to sarin nerve agent." Crit Rev Toxicol **50**(6): 474-490.

Kandratavicius, L., P. A. Balista, C. Lopes-Aguiar, R. N. Ruggiero, E. H. Umeoka, N. Garcia-Cairasco, L. S. Bueno Jr and J. P. Leite (2014). "Animal models of epilepsy: use and limitations." Neuropsychiatric disease and treatment.

Kar, N. (2006). "Lethality of suicidal organophosphorus poisoning in an Indian population: exploring preventability." Annals of general psychiatry **5**(1): 1-5.

Kitajima, T., T. Kanbayashi, Y. Saito, Y. Takahashi, Y. Ogawa, T. Sugiyama, Y. Kaneko, R. Aizawa and T. Shimizu (2004). "Diazepam reduces both arterial blood pressure and muscle sympathetic nerve activity in human." Neurosci Lett **355**(1-2): 77-80.

Kuruba, R., X. Wu and D. S. Reddy (2018). "Benzodiazepine-refractory status epilepticus, neuroinflammation, and interneuron neurodegeneration after acute organophosphate

intoxication." Biochimica et Biophysica Acta (BBA)-Molecular Basis of Disease **1864**(9): 2845-2858.

Lauková, M., J. Velíšková, L. Velíšek and M. P. Shakarjian (2020). "Tetramethylenedisulfotetramine neurotoxicity: What have we learned in the past 70 years?" Neurobiology of disease **133**: 104491.

Li, J. M., J. Gan, T. F. Zeng, J. W. Sander and D. Zhou (2012). "Tetramethylenedisulfotetramine intoxication presenting with de novo Status Epilepticus: a case series." Neurotoxicology **33**(2): 207-211.

Liu, X. and J. Zhang (2004). "EEG analysis in 12 patients with tetramine poisoning [in Chinese]. ." Shi Yong Yi Ji Za Zhi **11**(12b): 2660-2661.

Lloyd, G. K. and M. Williams (2000). "Neuronal nicotinic acetylcholine receptors as novel drug targets." J Pharmacol Exp Ther **292**(2): 461-467.

Löscher, W. (2011). "Critical review of current animal models of seizures and epilepsy used in the discovery and development of new antiepileptic drugs." Seizure **20**(5): 359-368.

Lu, Y., X. Wang, Y. Yan, Z. Xiao and U. Stephani (2008). "Nongenetic Cause of Epileptic Seizures in 2 Otherwise Healthy Chinese Families: Tetramine-Case Presentation and Literature Survey." Clinical Neuropharmacology **31**(1): 57-61.

Masson, P. (2011). "Evolution of and perspectives on therapeutic approaches to nerve agent poisoning." Toxicology letters **206**(1): 5-13.

Masterson, J. (2020). "OPCW to Investigate Navalny Poisoning." Arms Control Today **50**(8): 28-29.

McDonough, J. H., L. D. Zoeffel, J. McMonagle, T. L. Copeland, C. D. Smith and T.-M. Shih (1999). "Anticonvulsant treatment of nerve agent seizures: anticholinergics versus diazepam in soman-intoxicated guinea pigs." Epilepsy Research **38**(1): 1-14.

Mew, E. J., P. Padmanathan, F. Konradsen, M. Eddleston, S.-S. Chang, M. R. Phillips and D. Gunnell (2017). "The global burden of fatal self-poisoning with pesticides 2006-15: systematic review." Journal of affective disorders **219**: 93-104.

Mohler, H., J. M. Fritschy and U. Rudolph (2002). "A new benzodiazepine pharmacology." J Pharmacol Exp Ther **300**(1): 2-8.

Mukherjee, S. and R. D. Gupta (2020). "Organophosphorus nerve agents: types, toxicity, and treatments." Journal of toxicology **2020**.

Muñoz-Quezada, M. T., B. A. Lucero, V. P. Iglesias, M. P. Muñoz, C. A. Cornejo, E. Achu, B. Baumert, A. Hanchey, C. Concha and A. M. Brito (2016). "Chronic exposure to organophosphate (OP) pesticides and neuropsychological functioning in farm workers: a review." International journal of occupational and environmental health **22**(1): 68-79.

Munro, N. (1994). "Toxicity of the organophosphate chemical warfare agents GA, GB, and VX: implications for public protection." Environmental health perspectives **102**(1): 18-37.

Ning, P., Q. He, F. Yu, Z. Feng, P. Deng and T. Jia (1997). "Fifty two cases of acute tetramine poisoning." Chin. J. Ind. Hyg. Occup. Dis **15**: 108-109.

Okumura, T., T. Hisaoka, T. Naito, H. Isonuma, S. Okumura, K. Miura, H. Maekawa, S. Ishimatsu, N. Takasu and K. Suzuki (2005). "Acute and chronic effects of sarin exposure from the Tokyo subway incident." Environmental toxicology and pharmacology **19**(3): 447-450.

Okumura, T., T. Hisaoka, A. Yamada, T. Naito, H. Isonuma, S. Okumura, K. Miura, M. Sakurada, H. Maekawa and S. Ishimatsu (2005). "The Tokyo subway sarin attack—lessons learned." Toxicology and applied pharmacology **207**(2): 471-476.

Olsen, R. W. (1981). "The GABA postsynaptic membrane receptor-ionophore complex. Site of action of convulsant and anticonvulsant drugs." Mol Cell Biochem **39**: 261-279.

OPCW (2018). Statement by h.e. ambassador Ahmad Nazri Yusof permanent representative of malaysia to the OPCW at the eighty-seventh session of the executive council

OPCW. (2020). "OPCW Issues Report on Technical Assistance Requested by Germany; Alexei Navalny." from https://www.opcw.org/media-centre/news/2020/10/opcw-issues-report-technical-assistance-requested-germany.

Orr-Urtreger, A., F. M. Goldner, M. Saeki, I. Lorenzo, L. Goldberg, M. De Biasi, J. A. Dani, J. W. Patrick and A. L. Beaudet (1997). "Mice deficient in the alpha7 neuronal nicotinic acetylcholine receptor lack alpha-bungarotoxin binding sites and hippocampal fast nicotinic currents." J Neurosci **17**(23): 9165-9171.

Pankratov, Y. and U. Lalo (2014). "Calcium permeability of ligand-gated Ca2+ channels." Eur J Pharmacol **739**: 60-73.

Patocka, J., T. C. C. Franca, Q. Wu and K. Kuca (2018). "Tetramethylenedisulfotetramine: A Health Risk Compound and a Potential Chemical Warfare Agent." Toxics **6**(3).

Pereira, E. F., Y. Aracava, L. J. DeTolla, E. J. Beecham, G. W. Basinger, E. J. Wakayama and E. X. Albuquerque (2014). "Animal models that best reproduce the clinical manifestations of human intoxication with organophosphorus compounds." Journal of Pharmacology and Experimental Therapeutics **350**(2): 313-321.

Pessah, I. N., M. A. Rogawski, D. J. Tancredi, H. Wulff, D. Zolkowska, D. A. Bruun, B. D. Hammock and P. J. Lein (2016). "Models to identify treatments for the acute and persistent effects of seizure-inducing chemical threat agents." Ann N Y Acad Sci **1378**(1): 124-136.

Pessah, I. N., M. A. Rogawski, D. J. Tancredi, H. Wulff, D. Zolkowska, D. A. Bruun, B. D. Hammock and P. J. Lein (2016). "Models to identify treatments for the acute and persistent effects of seizure-inducing chemical threat agents." Annals of the New York Academy of Sciences **1378**(1): 124.

Petroianu, G. (2010). "Toxicity of phosphor esters: Willy Lange (1900–1976) and Gerda von Krueger (1907–after 1970)." Die Pharmazie-An International Journal of Pharmaceutical Sciences **65**(10): 776-780.

Pidoplichko, V. I., E. M. Prager, V. Aroniadou-Anderjaska and M. F. Braga (2013). "alpha7-Containing nicotinic acetylcholine receptors on interneurons of the basolateral amygdala and their role in the regulation of the network excitability." J Neurophysiol **110**(10): 2358-2369.

Pope, C. N. and S. Brimijoin (2018). "Cholinesterases and the fine line between poison and remedy." Biochemical pharmacology **153**: 205-216.

Prager, E. M., V. I. Pidoplichko, V. Aroniadou-Anderjaska, J. P. Apland and M. F. Braga (2014). "Pathophysiological mechanisms underlying increased anxiety after soman exposure: reduced GABAergic inhibition in the basolateral amygdala." Neurotoxicology **44**: 335-343.

Pressly, B., H. M. Nguyen and H. Wulff (2018). "GABA(A) receptor subtype selectivity of the proconvulsant rodenticide TETS." Archives of toxicology **92**(2): 833-844.

Pressly, B., N. Vasylieva, B. Barnych, V. Singh, L. Singh, D. A. Bruun, S. H. Hwang, Y.-J. Chen, J. C. Fettinger and S. Johnnides (2020). "Comparison of the toxicokinetics of the convulsants picrotoxinin and tetramethylenedisulfotetramine (TETS) in mice." Archives of toxicology **94**(6): 1995-2007.

Price, M. E., C. L. Whitmore, J. E. H. Tattersall, A. C. Green and H. Rice (2018). "Efficacy of the antinicotinic compound MB327 against soman poisoning – Importance of experimental end point." Toxicology Letters **293**: 167-171.

Quinn, D. M., J. Topczewski, N. Yasapala and A. Lodge (2017). "Why is aged acetylcholinesterase so difficult to reactivate?" Molecules **22**(9): 1464.

Rice, N. C., N. A. Rauscher, J. L. Langston and T. M. Myers (2017). "Behavioral intoxication following voluntary oral ingestion of tetramethylenedisulfotetramine: Dose-dependent onset, severity, survival, and recovery." Neurotoxicology **63**: 21-32.

Richardson, J. R., V. Fitsanakis, R. H. Westerink and A. G. Kanthasamy (2019). "Neurotoxicity of pesticides." Acta neuropathologica **138**(3): 343-362.

Robb, E. L. and M. B. Baker (2017). "Organophosphate toxicity."

Shakarjian, M. P., M. Laukova, J. Veliskova, P. K. Stanton, D. E. Heck and L. Velisek (2016). "Tetramethylenedisulfotetramine: pest control gone awry." Ann N Y Acad Sci **1378**(1): 68-79.

Shakarjian, M. P., J. Veliskova, P. K. Stanton and L. Velisek (2012). "Differential antagonism of tetramethylenedisulfotetramine-induced seizures by agents acting at NMDA and GABA(A) receptors." Toxicol Appl Pharmacol **265**(1): 113-121.

Shakarjian, M. P., J. Velíšková, P. K. Stanton and L. Velíšek (2012). "Differential antagonism of tetramethylenedisulfotetramine-induced seizures by agents acting at NMDA and GABA(A) receptors." Toxicology and applied pharmacology **265**(1): 113-121.

Sheridan, R. D., A. P. Smith, S. R. Turner and J. E. Tattersall (2005). "Nicotinic antagonists in the treatment of nerve agent intoxication." Journal of the Royal Society of Medicine **98**(3): 114-115.

Shih, T. (2000). "Anticonvulsant treatment of nerve agent seizures: anticholinergics vs diazepam in soman-intoxicated guinea pigs." Epilepsy Res **38**: 114National.

Sigel, E. and M. Ernst (2018). "The Benzodiazepine Binding Sites of GABAA Receptors." Trends Pharmacol Sci **39**(7): 659-671.

Sirin, G. S., Y. Zhou, L. Lior-Hoffmann, S. Wang and Y. Zhang (2012). "Aging mechanism of soman inhibited acetylcholinesterase." The Journal of Physical Chemistry B **116**(40): 12199-12207.

Smythies, J. and B. Golomb (2004). "Nerve gas antidotes." J R Soc Med **97**(1): 32.

Steinlein, O. K., J. C. Mulley, P. Propping, R. H. Wallace, H. A. Phillips, G. R. Sutherland, I. E. Scheffer and S. F. Berkovic (1995). "A missense mutation in the neuronal nicotinic acetylcholine receptor α4 subunit is associated with autosomal dominant nocturnal frontal lobe epilepsy." Nature genetics **11**(2): 201-203.

UN. (2020). "Independent International Commission of Inquiry on the Syrian Arab Republic." Retrieved March 14, 2021, from https://www.ohchr.org/EN/HRBodies/HRC/Pages/NewsDetail.aspx?NewsID=21481&LangID=E.

Velisek, L. (2005). Models of chemically-induced acute seizures. Models of Seizures and Epilepsy. A. Pitkanen, P. A. Schwartzkroin and S. L. Moshe. Waltham, MA, Academic Press**:** 127-152.

Voss, E., A. R. Haskell and L. Gartenberg (1961). "Reduction of tetramine toxicity by sedatives and anticonvulsants." J Pharm Sci **50**: 858-860.

Watson, A., D. Opresko, R. A. Young, V. Hauschild, J. King and K. Bakshi (2015). Organophosphate nerve agents. Handbook of toxicology of chemical warfare agents, Elsevier**:** 87-109.

Whitlow, K. S., M. Belson, F. Barrueto, L. Nelson and A. K. Henderson (2005). "Tetramethylenedisulfotetramine: old agent and new terror." Ann Emerg Med **45**(6): 609-613.

Wu, Y. Q. and C. Y. Sun (2004). "Poison control services in China." Toxicology **198**(1-3): 279-284.

Zhang, Y., M. Su and D. P. Tian (2011). "Tetramine poisoning: A case report and review of the literature." Forensic Sci Int **204**(1-3): e24-27.

Zhou, Y., L. Liu and L. Tang (1998). "[An autopsy analysis on 5 cases of poisoning death with tetramethylenedisulfotertramine]." Fa Yi Xue Za Zhi **14**(4): 214-215, 217, 252.

Zolkowska, D., C. N. Banks, A. Dhir, B. Inceoglu, J. R. Sanborn, M. R. McCoy, D. A. Bruun, B. D. Hammock, P. J. Lein and M. A. Rogawski (2012). "Characterization of Seizures Induced by Acute and Repeated Exposure to Tetramethylenedisulfotetramine." The Journal of Pharmacology and Experimental Therapeutics **341**(2): 435-446.

Zolkowska, D., C. N. Banks, A. Dhir, B. Inceoglu, J. R. Sanborn, M. R. McCoy, D. A. Bruun, B. D. Hammock, P. J. Lein and M. A. Rogawski (2012). "Characterization of seizures induced by acute and repeated exposure to tetramethylenedisulfotetramine." J Pharmacol Exp Ther **341**(2): 435-446.

Zolkowska, D., C. Y. Wu and M. A. Rogawski (2018). "Intramuscular allopregnanolone and ganaxolone in a mouse model of treatment-resistant status epilepticus." Epilepsia.

Chapter 2

Strain and seizure duration influence the extent of brain injury in mice after tetramethylenedisulfotetramine-induced *status epilepticus*

Jonas J. Calsbeek[1]*, Eduardo A. González[1]*, Casey A. Boosalis[1], Dorota Zolkowska[2], Donald A. Bruun[1], Douglas J. Rowland[3], Naomi H. Saito[4], Danielle J. Harvey[4], Abhijit J. Chaudhari[3], Michael A. Rogawski[2], Joel R. Garbow[5], Pamela J. Lein[1]

[1]Department of Molecular Biosciences, University of California, Davis, School of Veterinary Medicine, Davis, CA 95616, USA (jcalsbeek@ucdavis.edu, azgonzalez@ucdavis.edu, caboosalis@ucdavis.edu, dabruun@ucdavis.edu, pjlein@ucdavis.edu); [2]Department of Neurology, University of California, Davis, School of Medicine, Davis, CA 95616, USA (dzolkowska@ucdavis.edu, rogawski@ucdavis.edu); [3]Center for Molecular and Genomic Imaging, University of California, Davis, College of Engineering, Davis, CA 95616, USA (djrowland@ucdavis.edu; ajchaudhari@ucdavis.edu); [4]Department of Public Health Sciences, University of California, Davis, School of Medicine, Davis, CA 95616, USA (djharvey@ucdavis.edu, nhsaito@ucdavis.edu); [5]Biomedical Magnetic Resonance Laboratory, Mallinckrodt Institute of Radiology, Washington University in St. Louis, School of Medicine, St. Louis, MO 63110, USA (garbow@wustl.edu).

*These authors contributed equally to this manuscript.

Abstract:

Acute intoxication with tetramethylenedisulfotetramine (TETS) can trigger *status epilepticus* (SE) in humans. Survivors often exhibit long-term neurological effects, including electrographic abnormalities and cognitive deficits, but the pathogenic mechanisms linking acute toxic effects of TETS to chronic outcomes are not known. Here, we use advanced *in vivo* imaging techniques to longitudinally monitor the neuropathological consequences of TETS-induced SE in two different mouse strains. Adult male NIH Swiss and C57BL/6J mice were injected with riluzole (10 mg/kg, i.p.), followed 10 min later by an acute dose of TETS (0.2-0.3 mg/kg, i.p.) or an equal volume of vehicle (10% DMSO in 0.9% sterile saline). Seizure behavior began within minutes of TETS exposure and rapidly progressed to SE that was interrupted after 40 min by administration of midazolam (1.8 mg/kg, i.m.). The brains of vehicle and TETS-exposed mice were imaged using *in vivo* magnetic resonance (MR) and translocator protein (TSPO) positron emission tomography (PET) at 1, 3, 7, and 14 days post-exposure to monitor brain injury and neuroinflammation, respectively. When the brain scans of TETS mice were compared to those of vehicle controls, subtle and transient neuropathology was observed in both mouse strains, but more extensive and persistent TETS-induced neuropathology was observed in C57BL/6J mice. In addition, one NIH Swiss TETS mouse that did not respond to the rescue therapy, but remained in SE for more than 2 h, displayed robust neuropathology as determined by *in vivo* imaging and confirmed by FluoroJade C staining and IBA-1 immunohistochemistry as readouts of neurodegeneration and neuroinflammation, respectively. The findings in this study demonstrate that the extent of injury observed in the mouse brain after TETS-induced SE varies according to strain and the duration of SE. These observations suggest that humans who do not respond to

antiseizure medication after acute TETS intoxication are at increased risk for brain injury, justifying efforts to identify more effective medical countermeasures against TETS.

Keywords*:* MRI, neurodegeneration, neuroinflammation, PET, tetramine

Abbreviations

ADC = apparent diffusion coefficient

DWI = diffusion-weighted imaging

MDZ = midazolam

MRI = magnetic resonance imaging

PAM = positive allosteric modulator

PET = positron emission tomography

SE = *status epilepticus*

SUV = standardized uptake value

T2W = T_2-weighted

TETS = tetramethylenedisulfotetramine

TSPO = translocator protein

VEH = vehicle

Introduction

Tetramethylenedisulfotetramine (TETS) is a globally banned rodenticide listed by the United States Department of Homeland Security as a potential chemical threat agent (Shakarjian et al., 2016). Despite being a highly effective rodenticide, worldwide production of TETS was banned in 1984 because of its extremely low LD_{50} of 100 µg/kg, which is approximately 7-10 mg in a 70 kg human, and because of its persistence in the environment (Guan et al., 1993; reviewed in Whitlow et al., 2005). Nevertheless, because of high consumer demand for effective rodenticides, and because of the low-cost and ease of synthesizing TETS, this rodenticide remains widely available on the black market in Asian countries (reviewed in Patocka et al., 2018). Accidental and intentional poisonings are not uncommon in Asia, and typically occur through ingestion since TETS is tasteless and odorless (reviewed in Zhang et al., 2011). Ensuing symptoms are dose-dependent and include nausea, dizziness, headache, pulmonary edema, organ congestion, calcium depositions in the kidney, fatty liver, and seizures that can progress to *status epilepticus* (SE) (Zhou et al., 1998). Acute intoxication with high doses can be fatal within a few hours (Barrueto et al., 2003). Brainstem hemorrhage as well as edema and congestion of brain tissue have been observed in patients who survived acute poisoning with TETS (reviewed in Whitlow et al., 2005).

The mechanism by which TETS triggers seizures involves $GABA_A$ receptor ($GABA_AR$) antagonism (Pressly et al., 2021; Pressly et al., 2018; Shakarjian et al., 2016).The current standard of care for terminating TETS-induced seizure activity is treatment with $GABA_AR$ positive allosteric modulators, typically, high dose benzodiazepines (Whitlow et al., 2005). While this treatment is sufficient to prevent death, it does not protect against the long-term electrographic abnormalities, including recurrent seizures, and cognitive deficits observed in

survivors (Croddy, 2004; Deng et al., 2012; Whitlow et al., 2005). It remains unclear whether these neurological deficits are the result of excitotoxicity downstream of prolonged seizure activity or the consequence of seizure-independent toxicodynamic actions of TETS. This uncertainty reflects the paucity of clinical or preclinical data regarding the pathogenic mechanisms that underlie the long-term consequences of TETS-induced SE. To address this data gap, rodent models of TETS-induced seizures have been developed to study the consequences of acute TETS exposure (Rice et al., 2017; Shakarjian et al., 2012; Zolkowska et al., 2012). However, in these early models of TETS-induced seizures, animals did not develop SE. For example, in the NIH Swiss mouse, during the first 18-20 min post-TETS exposure, mice experienced 2 bursts of clonic seizure activity of several minutes in duration followed by a tonic-clonic seizure of several minutes duration that often resulted in death (Pessah et al., 2016; Zolkowska et al., 2012). Administration of high dose benzodiazepine or combined low dose benzodiazepine and neurosteroid prior to the onset of the tonic-clonic seizures rescued animals from death (Bruun et al., 2015; Vito et al., 2014). In these TETS models, neurodegeneration was not detected by FluoroJade C staining at 1, 2, 3, and 7 days post-exposure, but there was a transient neuroinflammatory response, evident as increased IBA-1 and GFAP immunoreactivity in the cortex and hippocampus during the first 1-3 days post-exposure (Bruun et al., 2015; Zolkowska et al., 2012). These animals did not exhibit changes in cognition, anxiety, or depression (Flannery et al., 2015). The failure of these models to recapitulate the chronic effects observed in humans who survive acute TETS intoxication was attributed to the fact that mice did not develop SE using these dosing paradigms.

We recently developed a mouse model of TETS-induced SE in which animals are injected with riluzole 10 min prior to TETS to prevent tonic-clonic seizures (Pessah et al., 2016;

Zolkowska et al., 2018). In this model, TETS-intoxicated animals experienced continuous seizures that began within minutes of TETS injection and continued until the animal died, usually within 60-90 min post-exposure. Treatment with a benzodiazepine or neurosteroid at 40-60 min post-exposure rescued most animals exposed to TETS using this modified dosing paradigm. Here, we leveraged this novel mouse model to determine whether TETS-induced SE is associated with robust and persistent neurodegeneration and neuroinflammation as has been documented in preclinical models of organophosphate-induced SE (reviewed by Andrew and Lein, 2021; Naughton and Terry, 2018; Tsai and Lein, 2021). Additionally, while preclinical models of TETS-induced seizures have primarily used NIH Swiss or C57BL/6 mice, no direct comparison has been made to address strain differences in chronic responses to acute TETS intoxication. The overall goal of this study was to use *in vivo* imaging techniques to quantify the spatiotemporal patterns of neuropathology after TETS-induced SE and to determine whether these patterns varied between two mouse strains commonly used to study seizure disorders. Specifically, we used magnetic resonance imaging (MRI) and positron emission tomography (PET), which we have previously validated as methods to monitor spatiotemporal profiles of brain damage in preclinical models of chemical-induced SE (Hobson et al., 2019; Hobson et al., 2017). We utilized three-dimensional, T_2-weighted (T2W) anatomic MR images of the brain collected longitudinally to track the spatiotemporal changes in brain or ventricle volume, and diffusion-weighted imaging (DWI) to document changes in regional tissue water diffusion that distinguish healthy versus pathologic tissue (Hobson et al., 2017). For PET we employed a radiolabeled ligand of the translocator protein (TSPO), which has been shown to be a biomarker of neuroinflammation in clinical and preclinical studies (Guilarte, 2019).

Materials and Methods

Animals

All studies involving animals were designed to minimize pain and suffering and were conducted in accordance with protocols approved by the University of California, Davis, Institutional Animal Care and Use Committee. All animals were housed in facilities accredited by AAALAC International. Adult male C57BL/6J mice (8-10 weeks old; 22-33g) and NIH Swiss mice (8-10 weeks old; 22-33g) were maintained on a 12:12 light:dark cycle in a temperature and humidity-controlled vivarium (22 ± 2 ºC; 40-50% humidity). Mice were singly housed in standard plastic cages, provided standard mouse chow (LabDiet, #5058) and tap water *ad libitum*, and allowed to acclimate for at least 7 days prior to experimentation.

Drugs and Dosing Paradigm

Riluzole was purchased from Oakwood Products (West Columbia, SC, USA) and recrystallized to increase purity (>98%). TETS was synthesized and its purity (>99%) determined as previously described (Zhao et al., 2014). Pharmaceutical grade midazolam (MDZ; 5 mg/mL MDZ in 0.8% sodium chloride, 0.01% edetate disodium, 1% benzyl alcohol) was purchased from Hospira (Lake Forest, IL, USA). Mice were injected with riluzole (10 mg/kg, i.p.; Figure 1) 10 min prior to injection with TETS (0.2-0.3 mg/kg, i.p.), a dosing paradigm previously shown to induce SE in mice (Pessah et al., 2016; Zolkowska et al., 2018). Pilot studies were conducted to identify a dose of TETS that caused SE with similar onset and severity in NIH Swiss (0.2 mg/kg, i.p.) and C57BL/6J (0.3 mg/kg, i.p.) in order to compare potential strain differences in vulnerability to neuropathology caused by SE. Animals were administered MDZ (1.8 mg/kg, i.m.) 40 min post-TETS to terminate seizure behavior. Vehicle animals were

similarly treated with riluzole and MDZ but injected with vehicle (10% DMSO in 0.9% sterile saline) in place of TETS. Animals looking weak or ill following dosing were placed on heating pads and injected with 1 mL dextrose (10%, s.c.) as needed.

In Vivo Imaging and Analysis

Magnetic resonance imaging (MRI)

MRI scans were performed at the Center for Molecular and Genomic Imaging (CMGI) at the University of California, Davis, using a Bruker Biospec 70/30 (7T) preclinical MR scanner (Bruker BioSpin MRI; Ettlingen, Germany). Whole brain anatomical T2W and diffusion-weighted MRI data were collected from mice at 1, 3, 7, and 14 days after TETS exposure, similar to what has been previously described (Hobson et al., 2017). MRI was performed using a 116 mm internal diameter B-GA12S gradient (450 mT/m, 4500 T/m/s), a 72 mm internal diameter linear transmit coil, and a four-channel mouse brain surface coil for signal reception. Mice were continuously anesthetized with isoflurane (1-3%), which was adjusted to maintain a respiration rate of 70-90 breaths per min and were secured to a stereotactic restraint to prevent motion with warm air used to maintain body temperature (37 ºC) during image acquisition. T2W rapid acquisition with repeated echoes (RARE) images were acquired for ~12 min using the following parameters: repetition time (TR) = 6100 ms; effective echo time (TE) = 60 ms; RARE factor = 8; averages = 8; field of view (FOV) = 15x15 mm^2 (120x120 data matrix); 44 slices with 0.25 mm thickness. Diffusion Tensor Imaging (DTI) scans were acquired immediately after T2W acquisition for up to 1 h using the following parameters: TR = 5500 ms; TE = 30 ms; FOV = 17.5x15 mm^2 (140x120 data matrix); 13 slices with 0.5mm thickness; averages = 4. Paravision

5.1 software (Bruker BioSpin MRI) was used for image acquisition, reconstruction, and the generation of parametric apparent diffusion coefficient (ADC) maps.

Positron emission topography (PET)

PET imaging was performed using a radiolabeled ligand ([^{18}F]PBR111) that targets TSPO 18 kDa, a validated marker of neuroinflammation (Ottoy et al., 2018; Van Camp et al., 2010). Automated synthesis of [^{18}F]PBR111 was performed as previously described (Bourdier et al., 2012). PET scans were performed at the CMGI at the University of California, Davis, using a Siemens Inveon DPET small animal scanner (Siemens Corporation; Munich, Germany) or a microPET Focus 120 (Siemens Corporation), as previously described (Hobson et al., 2019). For repeated measures in the same animal at different times post-exposure, animals were scanned on the same PET scanner. Mice were continuously anesthetized with isoflurane (1-3%), which was adjusted to maintain a respiration rate of 70-90 breaths per min during acquisition. Mice were secured in a stereotactic restraint to minimize motion during PET scans, and whole brain scans were acquired at 1, 3, 7, and 14 days post-exposure. Immediately following the beginning of data acquisition, a bolus of [^{18}F]PBR111 (avg activity = 39.6 $\pm$ 2.2 MBq; in 200 µL saline) was injected via tail-vein, and PET scan acquisition duration was ~60 min.

Image Analysis

Image processing and analysis were performed using PMOD v.3.9 (PMOD Technologies; Zurich, Switzerland). A mouse brain digital atlas (Mirrione et al., 2007) was used to isolate individual brain regions in three dimensions for each subject and was manually adjusted for regional accuracy and registered to the T2W and diffusion MR scans. ADC values were

extracted, initially calculated in a voxel-by-voxel basis and averaged for each brain region of interest. The standard deviation of the ADC ('ADC SD') between voxels in each brain region was also calculated and provided a useful metric for quantifying neurodegeneration (Hobson et al., 2017). PET scans were registered to the T2W reference image to extract the standardized uptake value (SUV) of the radiolabeled tracer for each brain region. The SUV averaged over each brain region ('Average SUV') served as a measure of neuroinflammation.

Histology

At 7 days post-TETS exposure, a subset of mice imaged in this study was anesthetized with 4-5% isoflurane in medical-grade oxygen, perfused with ~25 mL of 4% (w/v) paraformaldehyde (PFA; Sigma; St. Louis, MO, USA) in phosphate-buffered saline (PBS; 3.6 mM Na_2HPO_4, 1.4 mM NaH_2PO_4, 150 mM NaCl; pH 7.2) using a Peri-Star Pro peristaltic pump (5 mL/min). Brains were removed, and the freshly perfused whole brains were immediately placed into 20 mL glass scintillation vials containing 10 mL of 4% (w/v) PFA in PBS (pH 7.2). After 24 h, whole brains were transferred into 30% (w/v) sucrose (Fisher; Houston, TX, USA) in PBS (3.6 mM Na_2HPO_4, 1.4 mM NaH_2PO_4, 150 mM NaCl; pH 7.2) for an additional 48 h or until the tissue sank completely to the bottom of the vial. Fixed whole brains were serially sectioned into 2 mm thick coronal slices using a mouse brain matrix (Zivic Instruments, #5325; Pittsburgh, PA, USA) and embedded by flash freezing in optimal cutting temperature medium (OCT; Fisher HealthCare; Waltham, MA, USA). Blocked brain sections were stored at -80º C until cryosectioned using a Microm HM550 cryostat (Thermo Fisher Scientific, Waltham, MA, USA) into 10 µm thick slices on Superfrost plus microscope slides (Fisher HealthCare). Slides were stored at -80º C prior to staining or immunohistochemistry.

FluoroJade C (FJC) staining

Neurodegeneration was assessed using FJC (AG325, MilliporeSigma; Burlington, MA, USA) staining. Brain slices were thawed on ice, then incubated in 0.06% (w/v) $KMnO_4$ (Sigma) in distilled H_2O (dH_2O) for 10 min, rinsed 3x in dH_2O, and incubated in 0.00015%, w/v FJC and 0.5 µg/mL DAPI (Invitrogen; Carlsbad, CA, USA) in 0.1% acetic acid (Acros Organics; Geel, Belgium) in dH_20 for 10 min in the dark. Slides were then dipped in xylene (X5SK-4, Assay grade; Thermo Fisher Scientific) for 1 min, mounted in Permount (Thermo Fisher Scientific), coverslipped, and imaged at 20X magnification on a high content ImageXpress imaging system (Molecular Devices; Sunnyvale, CA, USA). Neurodegeneration of the cortex and hippocampus was evaluated by counting neurons positively labeled with FJC (per mm^2) at 7 days post-exposure, as described previously (Zolkowska et al., 2012).

Immunohistochemical analyses of neuroinflammation

Neuroinflammation was assessed by quantifying ionized calcium binding adaptor molecule 1 (IBA-1) immunoreactivity, a biomarker of microglia (Ito et al., 1998), as previously described (Guignet et al., 2020). Briefly, brain slices were incubated in blocking buffer (PBS containing 10% normal goat serum (v/v; Vector Laboratories, Burlingame, CA, USA), 1% bovine serum albumin (w/v; Sigma), and 0.03% Triton (v/v; ThermoFisher Scientific) for 1 h at room temperature to prevent nonspecific binding of the primary antibody. Brain slices were then incubated in primary rabbit anti-IBA-1 antibody (1:1000 in blocking buffer; RRID:AB_839504, Wako Laboratory Chemicals; Richmond, VA, USA) overnight at 4 ºC. At the end of incubation, brain slices were washed 3x for 5 min with PBS and then incubated in secondary antibody solution (Goat anti-rabbit IgG AlexaFluor 568 diluted 1:500 in PBS containing 0.03% Triton

(v/v); RRID:AB_10563566, Life Technologies; Carlsbad, CA, USA) for 1 h at room temperature in the dark. Slides were then mounted in ProlongGold anti-fade reagent with DAPI (Thermo Fisher Scientific), coverslipped, and imaged on a high content ImageXpress imaging system at 20X magnification. Neuroinflammation in the cortex and hippocampus of all animals was evaluated by measuring the percent area of brain tissue positively labeled with IBA-1 at 7 days post-exposure, as described previously (Zolkowska et al., 2012).

Statistical Analyses

Primary outcomes from the *in vivo* imaging studies included regional measures of the ADC SD and average SUV. Regions of interest (ROIs) included the amygdala, hippocampus, piriform cortex, somatosensory cortex, striatum, and thalamus. The ADC, ADC SD, and average SUV were available for all ROIs in all animals. Measures from the right and left hemisphere were averaged for the amygdala, hippocampus, piriform cortex, and striatum. Data were available for two strains of mice (C57BL/6J, NIH Swiss), for two treatment groups (TETS, vehicle), and at various days post-exposure (1, 3, 7, 14). Days post-exposure was treated as a categorical variable to allow for comparisons between experimental groups by day. Due to the repeated measures across brain regions and days post-exposure, mixed effects regression models were used to assess differences between TETS and vehicle. Both the average SUV and the ADC SD were transformed using the natural log prior to analysis to meet assumptions of the model including normality and constant variance. All models considered days post-exposure, brain region, treatment group and their interactions, and included an animal-specific random effect. Akaike Information Criterion was used for model selection. Contrasts specifically comparing experimental groups overall, by treatment or by day, were constructed and used to test for

differences between TETS and vehicle. Benjamini-Hochberg False Discovery Rate (FDR) was used to control for multiple comparisons across all contrasts within a model (Benjamini and Hochberg, 1995). Primary analyses were conducted separately for each mouse strain, although secondary analyses directly assessed differences between strains, by including strain and related interactions in the models. All analyses were performed in SAS (version 9.4, SAS Institute, Inc.; Cary, NC, USA), and graphics were created in R (version 3.6.3, R Core Team, Vienna, Austria).

Results

Diffusion-Weighted MRI

Exposure effects were not dependent on brain region, so regions were collapsed for both strains of mice (Figure 2). The ADC SD was significantly higher in C57BL/6J TETS animals than vehicle (VEH) animals on days 3 ($p<0.001$), 7 ($p<0.001$), and 14 ($p<0.05$) post-exposure, but there was no difference on day 1 ($p=0.8$). For the NIH Swiss mice, there were no significant differences in the ADC SD between TETS and VEH animals on any day that survived the FDR correction. Individual data points used to generate this figure can be found in the supplemental material (Tables S1 and S2).

TSPO PET Imaging

There were no significant differences in the average SUV between C57BL/6J TETS and VEH mice in any brain region on day 1 post exposure (Figure 3). However, on days 3 and 7 post-exposure, the average SUV was significantly higher in TETS than VEH animals across all brain regions ($p<.02$) except the thalamus. On day 14 post-exposure, average SUV remained

significantly higher in TETS than VEH animals in the piriform cortex only (Geometric mean ratio (GMR) =1.1, 95% CI: (1.05, 1.25), p=.003). In NIH Swiss mice, brain regions were collapsed because exposure effects were not region dependent. Average SUV was significantly higher in TETS animals than VEH animals on day 3 only (GMR: 1.1, 95% CI: (1.04, 1.23), p=.003). Individual data points used to generate this figure can be found in the supplemental material (Table S3).

Strain Comparison

Exposure effects were not significantly different between mouse strains for any outcome. In C57BL/6J mice, the exposure effect was 13% lower than that in NIH Swiss mice on day 1 (90% CI: 0.63, 1.21), 4.6% higher on day 3 (90% CI: 0.94, 1.16), 11% higher on day 7 (90% CI: 0.97, 1.27) and 3.8% lower on day 14 (90% CI: 0.81, 1.14). Similarly, the effect measured by ADC SD was 2.6% higher in C57BL/6J mice than NIH Swiss mice (90% CI: 0.89, 1.19).

Seizure Duration Predicts Neuropathology

During the course of this study, we observed one NIH Swiss mouse acutely intoxicated with TETS that continued to seize after MDZ treatment, and thus experienced SE >120 min. This mouse survived for 7 days post-exposure. Histological analysis of the brain from this animal revealed abundant FJC labeling in the outer cortex and in the CA1 and CA3 regions of the hippocampus, demonstrating severe neurodegeneration. In contrast, no FJC-labeled cells were observed in the cortex or hippocampus of any of the other NIH Swiss mice 7 days after exposure to VEH or TETS with SE terminated at 40 min by midazolam (Figure 4A). Quantitative analysis confirmed this observation with VEH, TETS SE 40 min, and TETS SE >120 animals showing 5,

67, and 1237 FJC-positive cells per square millimeter in the cortex and 0, 9, and 735 FJC-positive cells in the hippocampus, respectively (Figure 4B). The TETS animal who experienced SE >120 min also had significantly increased IBA-1 immunoreactivity in the outer cortex and in the CA1 and CA3 regions of the hippocampus compared to VEH and TETS animals with SE for 40 min, suggesting an elevated neuroinflammatory response in the animal with SE >120 min (Figure 4A). This finding was confirmed by quantitative analysis of the percent area of regional IBA-1 staining: VEH, TETS SE 40 min, and TETS SE >120 animals showed areas of 3.7, 6.7, and 34.4% IBA-1 immunoreactivity in the cortex and 3.5, 3.3, and 33.8% IBA-1 immunoreactivity in the hippocampus, respectively (Figure 4B).

T2W MRI revealed regions of hyperintensity in the cortex and hippocampus of the TETS animal with SE >120 min compared to VEH and TETS animals with SE of 40 min, suggesting tissue degeneration with increased duration of SE. A parametric map of ADC showed visibly lower levels of intensity in the outer cortex and hippocampus of the TETS SE >120 min animal as well (Figure 4A). ADC SD values in the VEH, TETS SE 40 min, and TETS SE >120 min animals were 0.08, 0.08, and 0.12 in the cortex and 0.07, 0.06, and 0.11 in the hippocampus, respectively (Figure 4B). The TSPO PET images show noticeably higher levels of radiotracer uptake in the cortex and hippocampus regions of the TETS animal with SE >120 min compared to the VEH and TETS animal with SE of 40 min (Figure 4A). Average SUV values of the VEH, TETS SE 40 min, and TETS SE >120 min animals were 0.57, 0.68, and 0.77 in the cortex and 0.37, 0.41, and 0.64 in the hippocampus, respectively (Figure 4B).

Discussion

The goal of this study was to use *in vivo* imaging to longitudinally monitor neuropathology in a novel mouse model of TETS-induced SE (Pessah et al., 2016; Zolkowska et

al., 2018), and to compare quantitative outcomes between two mouse strains, NIH Swiss and C57BL/6J, that are commonly used to investigate seizure disorders. Our major findings were: (1) Mice that experienced ~40 min of TETS-induced SE exhibited delayed and transient neuropathology. (2) While statistically significant differences in imaging metrics between strains were not observed, TETS-induced brain injury as indicated by significantly increased ADC SD from diffusion-weighed MRI was observed only in C57BL/6J mice. TETS-induced neuroinflammation measured as increased average SUV in TSPO PET was observed at 3 and 7 days post-exposure in the C57BL/6J mice but only at 3 days post-exposure in the NIH Swiss mouse. (3) In a rare TETS-intoxicated NIH Swiss mouse that survived SE for at least 120 min in duration, both *in vivo* imaging and histologic assessments documented significant neurodegeneration and a more robust neuroinflammatory response at 7 days post-exposure compared to NIH Swiss mice with TETS-induced SE of ~40 min.

Previous studies have demonstrated that acute intoxication with TETS can trigger dose-dependent seizures and death in NIH Swiss (Zolkowska et al., 2012) and C57BL/6 (Shakarjian et al., 2015; Shakarjian et al., 2012) mice, but these exposures did not cause SE. Histologic and behavioral analyses of brains from NIH Swiss mice that experienced TETS-induced clonic seizures, but were rescued from death by benzodiazepine treatment at 20 min post-TETS exposure prior to the onset of tonic-clonic seizures, identified markedly increased expression of GFAP and IBA-1 at 1 to 3 days post-exposure in cortex and hippocampus, but no neurodegeneration or behavioral deficits (Bruun et al., 2015; Flannery et al., 2015; Vito et al., 2014). The mild neurological profile associated with these TETS exposures was attributed to the fact that these animals did not develop SE. Recently, we found that pretreatment with riluzole to prevent tonic hindlimb extension caused mice acutely intoxicated with TETS to transition from

clonic-tonic seizures to prolonged SE that developed within minutes after exposures and persisted until animals died, typically 60-90 min post-exposure (Pessah et al., 2016; Zolkowska et al., 2018). In this model of TETS-induced SE, mice were rescued from death by administration of midazolam at 40 min post-TETS injection (Pessah et al., 2016; Zolkowska et al., 2018).

Preclinical studies have demonstrated that 20-40 min of SE triggered by organophosphates (OPs) and other chemical convulsants, such as pilocarpine and kainic acid causes significant neuroinflammation and neurodegeneration in multiple brain regions that persists for days to months [reviewed by (de Araujo Furtado et al., 2012; Guignet and Lein, 2019)]. Thus, we hypothesized that animals that survived TETS-induced SE for ~40 min would show extensive and persistent brain injury detectable by MRI and TSPO PET as previously reported for a rat model of OP-induced SE (Hobson et al., 2019; Hobson et al., 2017). Compared to our earlier histologic evaluation of neurodegeneration in TETS-intoxicated NIH Swiss mice that did not develop SE, in which no neurodegeneration was observed by FluoroJade B staining in any brain region from 4 h to 7 days post-exposure (Zolkowska et al., 2012), the NIH Swiss mouse model of TETS SE appeared to have greater brain damage as evidenced by a significantly increased ADC SD from diffusion-weighted MRI at 3 days post-exposure. While a direct comparison between these two models is not possible because of the different methods used to assess brain damage, our previous studies in a rat model of OP-induced SE has demonstrated a strong positive correlation between the ADC SD and FJC labeling (Hobson et al., 2017). In contrast, both the earlier TETS seizure and the novel TETS SE NIH Swiss models exhibited increased neuroinflammation at 3 days post-exposure, although again, different methods (GFAP and IBA-1 immunohistochemistry vs. TSPO PET) were used. However, the magnitude and

persistence of brain injury detected by diffusion-weighted MRI and TSPO PET in the TETS SE mouse model was notably less severe compared to that reported in OP SE rat models (Hobson et al., 2019; Hobson et al., 2017). The reason(s) for these differences in neuropathology between TETS and OP models are not known but may include differences in species, the nature of electrographic changes during SE (Calsbeek et al., 2018), seizure-independent toxicodynamics (e.g., acetylcholinesterase inhibition by OPs vs. $GABA_A$ receptor inhibition by TETS), or more effective termination by midazolam of SE triggered by TETS (Zolkowska, unpublished data) vs. OPs (Supasai et al., 2020; Wu et al., 2018). Collectively, however, these observations suggest that chemical-induced SE is not necessarily associated with extensive brain damage.

However, consistent with what has been shown in preclinical models of OP-induced SE (Baille et al., 2005; McDonough et al., 1995; Siso et al., 2017), we observed that the duration of TETS-induced SE was directly correlated with the extent of neuropathology. While administration of midazolam at 40 min post-TETS injection terminated seizure in almost all mice in our study, one NIH Swiss mouse continued to seize for $\geq$80 min after treatment with midazolam. Analyses of brain damage at 7 days post-exposure by *in vivo* imaging and histology (FJC staining to detect neurodegeneration and IBA-1 immunohistochemistry to detect neuroinflammation) revealed greater neuropathology in the NIH Swiss mouse that experienced SE for $\geq$120 min than was observed in an NIH Swiss mouse that responded to midazolam and thus experienced SE for ~40 min. A major limitation of this observation is that we only had one animal in the group with SE $\geq$120 min, therefore, no statistically significant conclusions can be drawn. However, the magnitude of the differences in the severity of neuropathology between the animals with 40 min vs. 120 min of SE suggests that the correlation between seizure duration and neuropathology following TETS-induced SE is likely real.

In mice, seizure response and behavioral outcomes following seizures have been shown to be influenced by genetic background (Copping et al., 2019), therefore, another key question addressed in this study was whether the neuropathologic consequences of TETS-induced SE differed between NIH Swiss and C57BL/6J mice, the two strains previously used to investigate TETS-induced seizures (Shakarjian et al., 2015; Shakarjian et al., 2012; Zolkowska et al., 2012). Despite the lack of statistically significant differences in direct comparison of *in vivo* imaging metrics between strains, the presence and time course of brain damage measured by MR and PET imaging varied by strain. Exposure effects between VEH and TETS NIH Swiss mice were significantly different only for PET imaging and only on day 3 post-exposure, whereas TETS-intoxicated C57BL/6J were found to be significantly different from VEH as determined by MR and PET imaging at days 3 and 7 post-exposure, suggesting genetic background may influence the neuropathologic consequences of TEST-induced SE. However, the dose of TETS was increased in C57BL/6J mice (0.3 mg/kg TETS) relative to NIH Swiss mice (0.2 mg/kg TETS), therefore, it is possible that the more persistent damage observed in the C57BL/6J mouse is due to dose-dependent, seizure-independent toxicodynamic effects of TETS. Nonetheless, these different doses were used in order to produce SE with similar time-to-onset, duration, and severity between the two strains, suggesting the possibility of variable neuropathologic responses in a diverse human population after comparable seizure activity triggered by acute TETS intoxication.

In conclusion, TETS-induced SE of ~40 min in duration caused a delayed and subtle, transient neuropathology, the spatiotemporal profile and magnitude of which varied between strains. In contrast, TETS-induced SE of ~120 min was associated with much more severe neuropathology. This suggests that the therapeutic window for effectively mitigating the

neurological consequences of acute TETS intoxication may be longer than it is for other chemical convulsants, such as OPs. Collectively, these data suggest that the extent and persistence of neuropathologic changes following TETS-induced SE is likely influenced by genetic factors and by the duration of SE. Therefore, TETS-intoxicated patients who either do not respond to standard of care medical countermeasures or receive such medications at significantly delayed times post-exposure, are at increased risk for more extensive and severe neuropathology.

Acknowledgements

The authors thank Suzette Smiley-Jewell for assistance in manuscript preparation and Dr. Andrew Katsifis for donating the precursor for synthesizing the PET radiotracer used in this study. This work was supported by the CounterACT Program, National Institutes of Health Office of the Director and the National Institute of Neurological Disorders and Stroke [U54 NS079202 to P.J.L.]. J.J.C. was supported by a predoctoral fellowship from the UC Davis School of Veterinary Medicine; E.A.G. was supported by predoctoral fellowships from the National Institute of Neurological Disorders and Stroke [grant number F31 NS110522] and the National Institutes of Health Initiative for Maximizing Student Development [grant number R25 GM5676520]. D.J.R. was supported by the Chan Zuckerberg Initiative DAF, an advised fund of Silicon Valley Community Foundation [2019-198156 to D.J.R.]. This project used core facilities supported by the UC Davis MIND Institute Intellectual and Developmental Disabilities Research Center (Eunice Kennedy Shriver National Institute of Child Health and Human Development grant U54 HD079125). The sponsors were not involved in the study design, in the collection, analysis, or interpretation of data, in the writing of the report, or in the decision to submit the paper for publication.

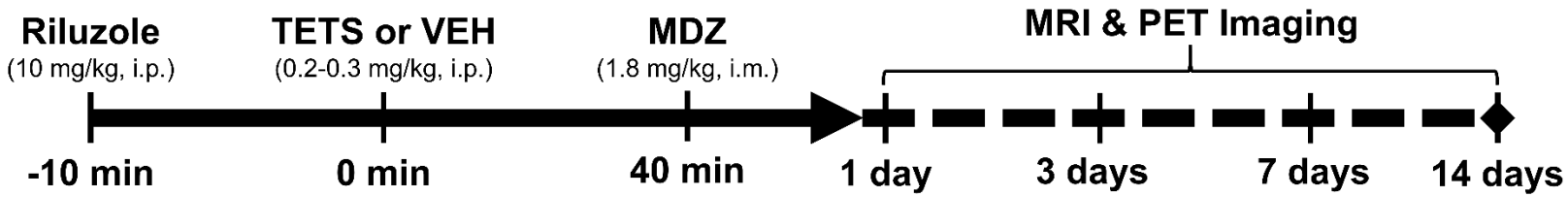

Strain	Group	1 day		3 days		7 days		14 days
NIH Swiss	VEH	n=3	→	n=3	→	n=3	→	n=3
	TETS	n=10	→	n=10	→	n=7	→	n=3
C57BL/6J	VEH	n=3	→	n=3	→	n=3	→	n=3
	TETS	n=8	→	n=8	→	n=8	→	n=3

Sample sizes by strain and exposure group for repeated imaging measures within subjects.

Figure 1. Dosing paradigm and imaging schedule. Adult mice were pretreated with riluzole 10 min prior to the administration of vehicle or tetramethylenedisulfotetramine (TETS). NIH Swiss mice were injected with TETS (0.2 mg/kg) or VEH, and C57BL/6J were injected with TETS (0.3 mg/kg) or VEH. 40 min later, a rescue dose of midazolam (MDZ) was administered to stop seizure behavior. Brains of TETS-intoxicated and vehicle control mice were imaged using MRI and PET at 1, 3, 7, and 14 days post exposure. Sample sizes for each strain and exposure group are shown in the table to indicate repeated imaging time points within subjects for mice in this study.

C57BL/6

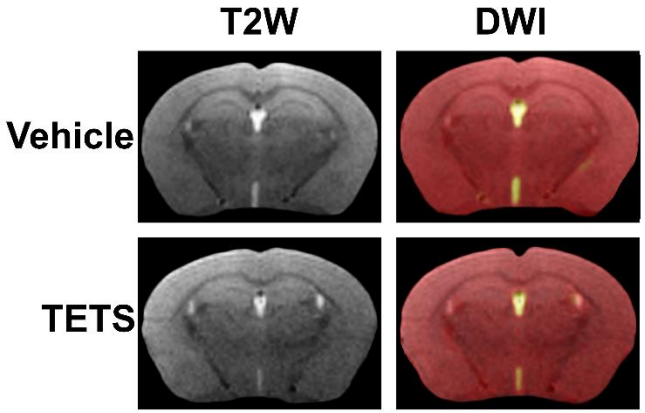

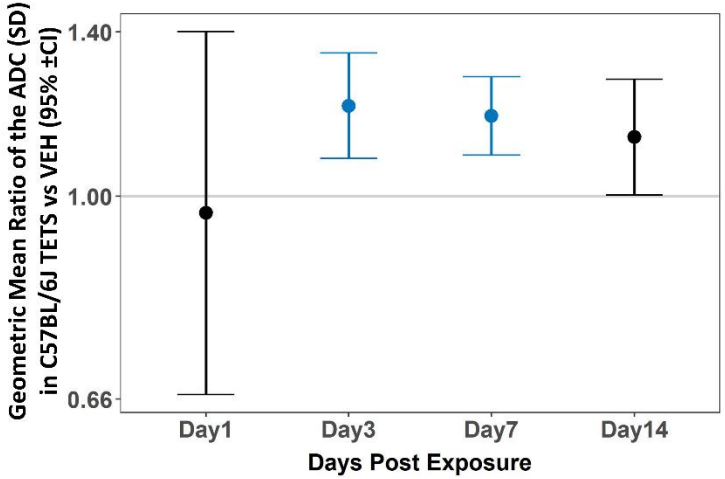

NIH Swiss

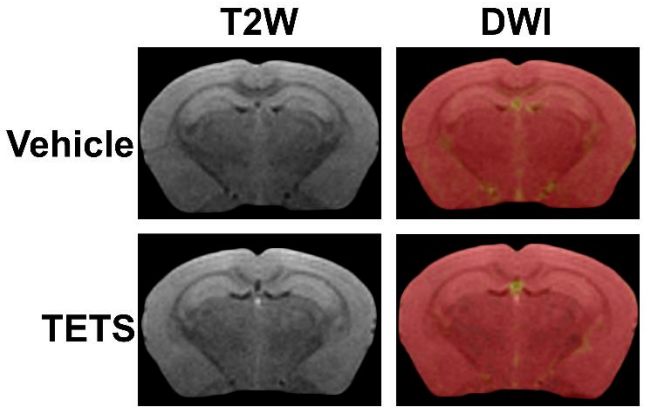

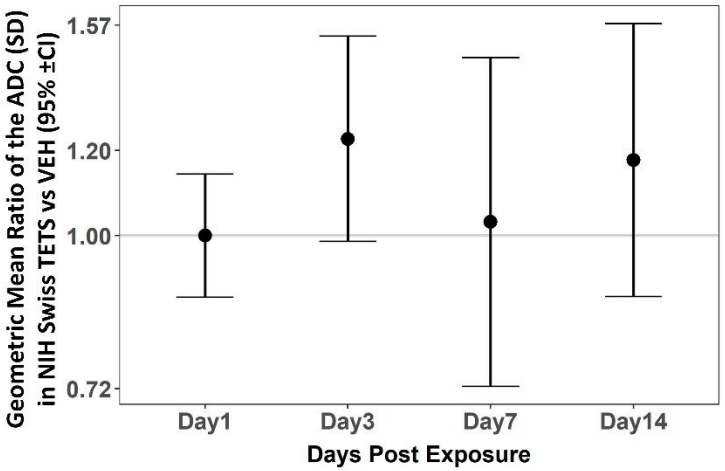

Figure 2. Acute TETS intoxication-induced neuropathology, as detected by diffusion-weighted imaging (DWI). Representative anatomical (T2W, left column) and parametric maps (DWI, right column) of vehicle (VEH) and TETS-intoxicated C57BL/6J and NIH Swiss mice. Geometric mean ratio (dot) of the standard deviation (SD) of the apparent diffusion coefficient (ADC SD) average for TETS vs. VEH mice with 95% confidence intervals (bars). Confidence intervals that do not include 1 (gray line) indicate a significant difference between TETS and VEH (identified in turquoise). All VEH groups had n=3 for each time point. Sample sizes for TETS time points: Day 1: n=8-9; Day 3: n=8-9; Day 7: n=7-8; Day 14: n=3. Individual data points used to generate this figure can be found in the supplemental material (Tables S1 and S2).

C57BL/6

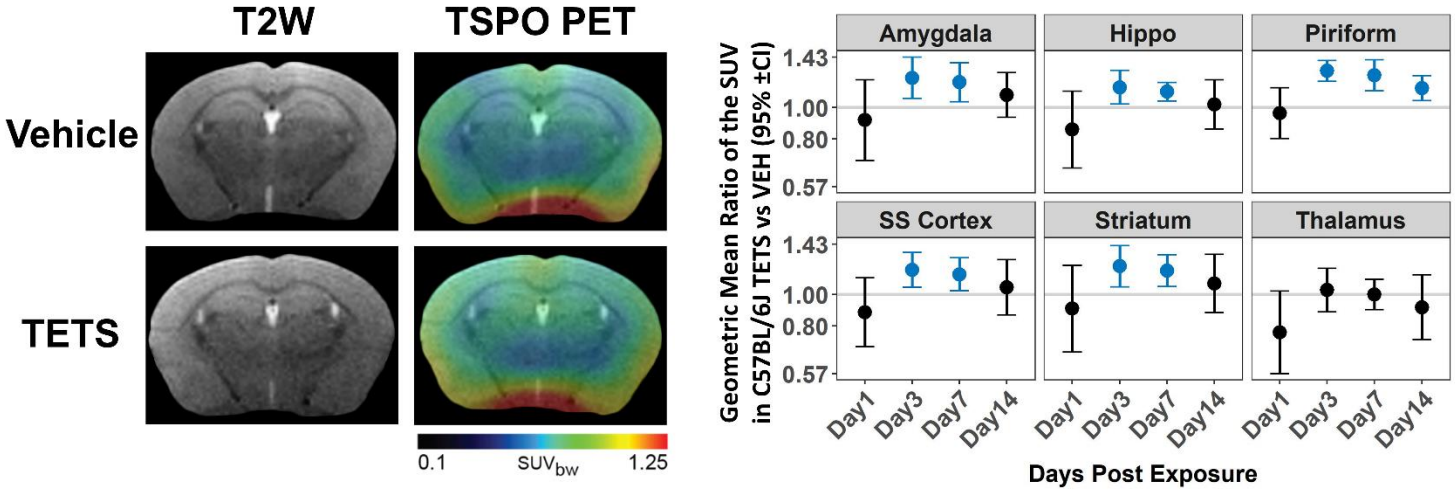

NIH Swiss

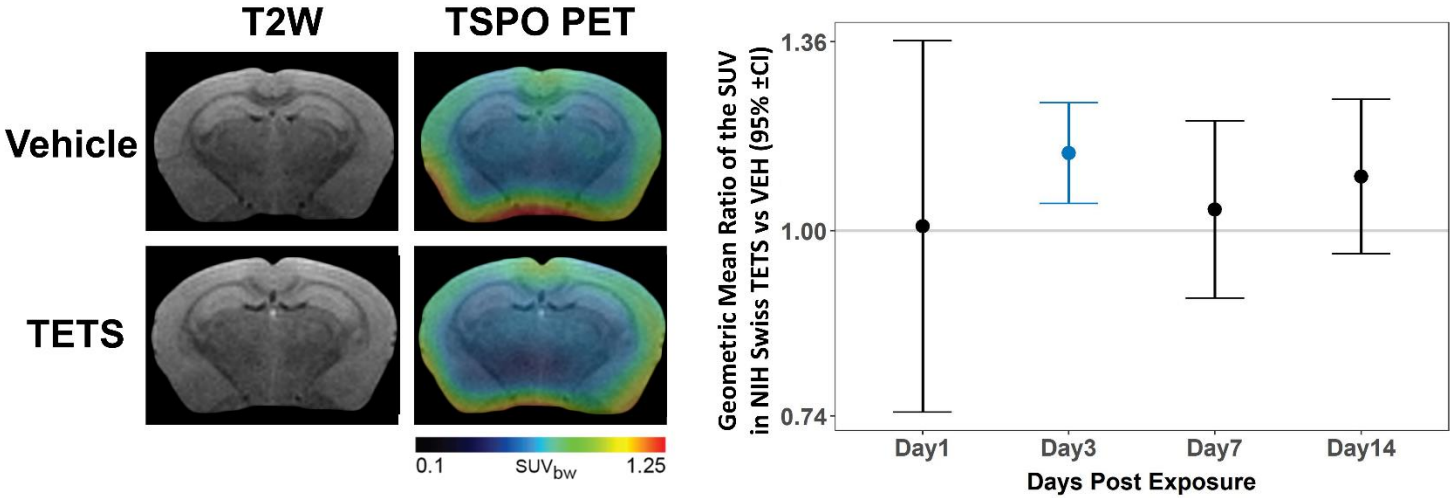

Figure 3. Acute TETS intoxication-induced neuroinflammation, as detected by TSPO PET imaging. Representative anatomical (T2W, left column) and parametric maps (TSPO PET, right column) of vehicle (VEH) and TETS-intoxicated C57BL/6J and NIH Swiss mice. Geometric mean ratio (dot) of the TSPO standard uptake value (SUV) for TETS vs. VEH mice with 95% confidence intervals (bars). Confidence intervals that do not include 1 (gray line) indicate a significant difference between TETS and VEH (identified in turquoise). All VEH groups had n=3 for each time point. Sample sizes for TETS time points: Day 1: n=8-9; Day 3: n=8-9; Day 7: n=7-8; Day 14: n=3. Individual data points used to generate this figure can be found in the supplemental material (Table S3).

A.

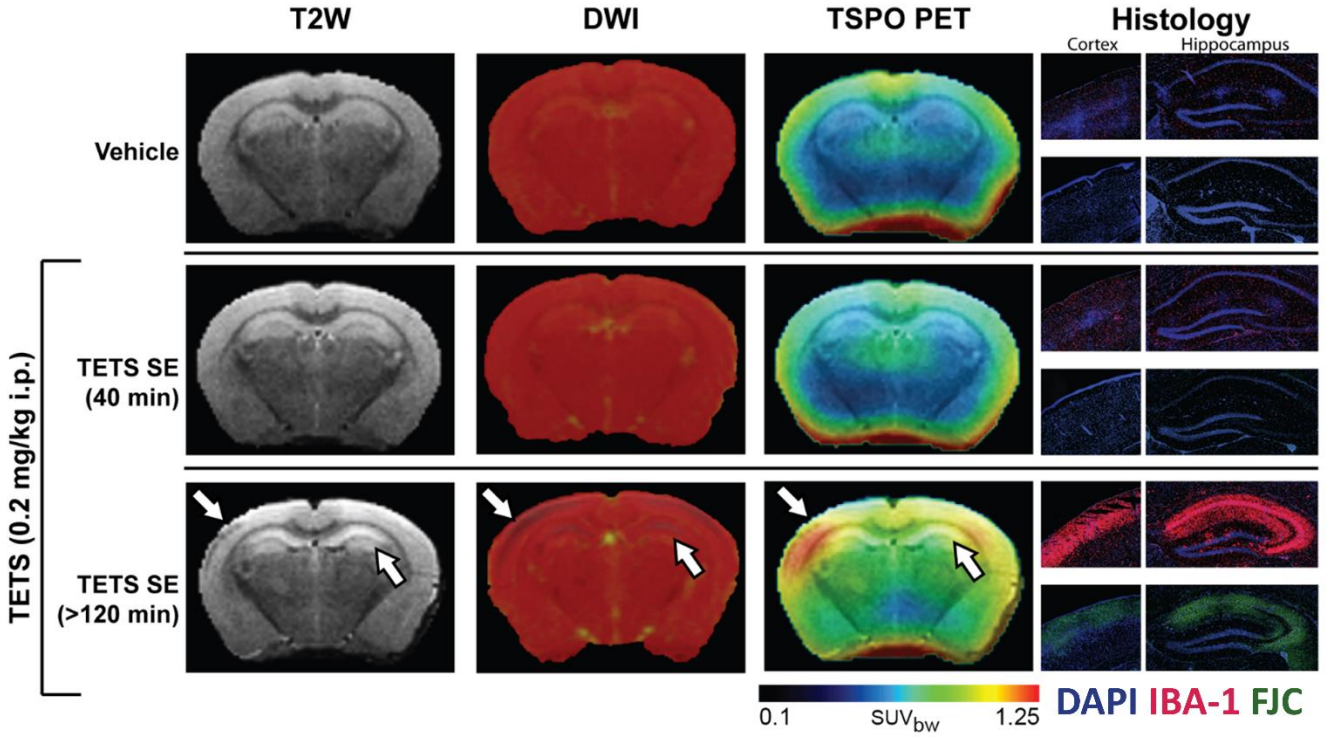

B.

	ADC (SD)		Average SUV		% Area IBA-1		FJC+ Cells/mm²	
	Cortex	Hippo	Cortex	Hippo	Cortex	Hippo	Cortex	Hippo
Vehicle	0.08	0.07	0.57	0.37	3.7	3.5	5	0
TETS SE (40 min)	0.08	0.06	0.68	0.41	6.7	3.3	67	9
TETS SE (>120 min)	0.12	0.11	0.77	0.64	34.4	33.8	1237	735

Figure 4. Seizure duration correlates with severity of neuropathology at 7 days post-exposure in NIH Swiss mice acutely intoxicated with TETS. (A) Representative anatomical T2W MRI (first column), diffusion-weighted MRI (second column), TSPO PET (third column), and histology (last columns) images from VEH mouse (top row), TETS-intoxicated mouse that experienced SE for 40 min (middle row), and TETS-intoxicated mouse that exhibited SE >120 min (bottom row). The middle row shows a TETS animal that responded normally to rescue by midazolam at 40 min after seizure initiation (40 min seizure), whereas the bottom row is of a TETS animal that continued to seize after midazolam treatment yet survived (>120 min seizure). Arrows point to regions of hypointensity (T2W & DWI) and high radiotracer uptake (TSPO PET), indicating neurodegeneration and neuroinflammation, respectively. IBA-1 (red) identifies microglia; FJC (green), degenerating neurons; DAPI (blue), nuclei. (B) Quantitative data table reporting regional ADC SD, average PET SUV, % area IBA1-positive, and FJC-positive cells/mm^2 from the vehicle (n=1), TETS SE (40 min; n=1), and prolonged TETS SE (>120 min; n=1) mice.

References

Andrew, P.M., Lein, P.J., 2021. Neuroinflammation as a Therapeutic Target for Mitigating the Long-Term Consequences of Acute Organophosphate Intoxication. Frontiers in Pharmacology 12, 1184.

Baille, V., Clarke, P.G., Brochier, G., Dorandeu, F., Verna, J.M., Four, E., Lallement, G., Carpentier, P., 2005. Soman-induced convulsions: the neuropathology revisited. Toxicology 215(1-2), 1-24.

Barrueto, F., Jr., Furdyna, P.M., Hoffman, R.S., Hoffman, R.J., Nelson, L.S., 2003. Status epilepticus from an illegally imported Chinese rodenticide: "tetramine". Journal of toxicology. Clinical toxicology 41(7), 991-994.

Benjamini, Y., Hochberg, Y., 1995. Controlling the False Discovery Rate: A Practical and Powerful Approach to Multiple Testing. Journal of the Royal Statistical Society. Series B (Methodological) 57(1), 289-300.

Bourdier, T., Pham, T.Q., Henderson, D., Jackson, T., Lam, P., Izard, M., Katsifis, A., 2012. Automated radiosynthesis of [18F]PBR111 and [18F]PBR102 using the Tracerlab FXFN and Tracerlab MXFDG module for imaging the peripheral benzodiazepine receptor with PET. Appl Radiat Isot 70(1), 176-183.

Bruun, D.A., Cao, Z., Inceoglu, B., Vito, S.T., Austin, A.T., Hulsizer, S., Hammock, B.D., Tancredi, D.J., Rogawski, M.A., Pessah, I.N., Lein, P.J., 2015. Combined treatment with diazepam and allopregnanolone reverses tetramethylenedisulfotetramine (TETS)-induced calcium dysregulation in cultured neurons and protects TETS-intoxicated mice against lethal seizures. Neuropharmacology 95, 332-342.

Calsbeek, J., Gonzalez, E., Boosalis, C., Zolkowska, D., Rogawski, M., Lein, P., 2018. Neuroinflammatory Responses in a Mouse Model of Tetramethylenedisulfotetramine-Induced Status Epilepticus. The FASEB Journal 32, lb645-lb645.

Copping, N.A., Adhikari, A., Petkova, S.P., Silverman, J.L., 2019. Genetic backgrounds have unique seizure response profiles and behavioral outcomes following convulsant administration. Epilepsy Behav 101(Pt A), 106547.

Croddy, E., 2004. Rat poison and food security in the People's Republic of China: focus on tetramethylene disulfotetramine (tetramine). Arch Toxicol 78(1), 1-6.

de Araujo Furtado, M., Rossetti, F., Chanda, S., Yourick, D., 2012. Exposure to nerve agents: from status epilepticus to neuroinflammation, brain damage, neurogenesis and epilepsy. Neurotoxicology 33(6), 1476-1490.

Deng, X., Li, G., Mei, R., Sun, S., 2012. Long term effects of tetramine poisoning: an observational study. Clin Toxicol (Phila) 50(3), 172-175.

Flannery, B.M., Silverman, J.L., Bruun, D.A., Puhger, K.R., McCoy, M.R., Hammock, B.D., Crawley, J.N., Lein, P.J., 2015. Behavioral assessment of NIH Swiss mice acutely intoxicated with tetramethylenedisulfotetramine. Neurotoxicol Teratol 47, 36-45.

Guan, F.Y., Liu, Y.T., Luo, Y., Hu, X.Y., Liu, F., Li, Q.Y., Kang, Z.W., 1993. GC/MS identification of tetramine in samples from human alimentary intoxication and evaluation of artificial carbonic kidneys for the treatment of the victims. J Anal Toxicol 17(4), 199-201.

Guignet, M., Dhakal, K., Flannery, B.M., Hobson, B.A., Zolkowska, D., Dhir, A., Bruun, D.A., Li, S., Wahab, A., Harvey, D.J., Silverman, J.L., Rogawski, M.A., Lein, P.J., 2020. Persistent behavior deficits, neuroinflammation, and oxidative stress in a rat model of acute organophosphate intoxication. Neurobiol Dis 133, 104431.

Guignet, M., Lein, P.J., 2019. Organophosphates, in: Aschner, M., Costa, L.G. (Eds.), Advances in Neurotoxicology: Role of Inflammation in Environmental Neurotoxicity. Academic Press, Cambridge, MA, pp. 35-79.

Guilarte, T.R., 2019. TSPO in diverse CNS pathologies and psychiatric disease: A critical review and a way forward. Pharmacology & therapeutics 194, 44-58.

Hobson, B.A., Rowland, D.J., Siso, S., Guignet, M.A., Harmany, Z.T., Bandara, S.B., Saito, N., Harvey, D.J., Bruun, D.A., Garbow, J.R., Chaudhari, A.J., Lein, P.J., 2019. TSPO PET Using [18F]PBR111 Reveals Persistent Neuroinflammation Following Acute Diisopropylfluorophosphate Intoxication in the Rat. Toxicol Sci 170(2), 330-344.

Hobson, B.A., Siso, S., Rowland, D.J., Harvey, D.J., Bruun, D.A., Garbow, J.R., Lein, P.J., 2017. From the Cover: MagneticResonance Imaging Reveals Progressive Brain Injury in Rats Acutely Intoxicated With Diisopropylfluorophosphate. Toxicol Sci 157(2), 342-353.

Ito, D., Imai, Y., Ohsawa, K., Nakajima, K., Fukuuchi, Y., Kohsaka, S., 1998. Microglia-specific localisation of a novel calcium binding protein, Iba1. Molecular brain research 57(1), 1-9.

McDonough, J.H., Jr., Dochterman, L.W., Smith, C.D., Shih, T.M., 1995. Protection against nerve agent-induced neuropathology, but not cardiac pathology, is associated with the anticonvulsant action of drug treatment. Neurotoxicology 16(1), 123-132.

Mirrione, M.M., Schiffer, W.K., Fowler, J.S., Alexoff, D.L., Dewey, S.L., Tsirka, S.E., 2007. A novel approach for imaging brain-behaviour relationships in mice reveals unexpected metabolic patterns during seizures in the absence of tissue plasminogen activator. NeuroImage 38(1), 34-42.

Naughton, S.X., Terry, A.V., Jr., 2018. Neurotoxicity in acute and repeated organophosphate exposure. Toxicology 408, 101-112.

Ottoy, J., De Picker, L., Verhaeghe, J., Deleye, S., Wyffels, L., Kosten, L., Sabbe, B., Coppens, V., Timmers, M., Van Nueten, L., Ceyssens, S., Stroobants, S., Morrens, M., Staelens, S., 2018. [(18)F]PBR111 PET Imaging in Healthy Controls and Schizophrenia: Test - Retest

Reproducibility and Quantification of Neuroinflammation. Journal of nuclear medicine : official publication, Society of Nuclear Medicine.

Patocka, J., Franca, T.C.C., Wu, Q., Kuca, K., 2018. Tetramethylenedisulfotetramine: A Health Risk Compound and a Potential Chemical Warfare Agent. Toxics 6(3).

Pessah, I.N., Rogawski, M.A., Tancredi, D.J., Wulff, H., Zolkowska, D., Bruun, D.A., Hammock, B.D., Lein, P.J., 2016. Models to identify treatments for the acute and persistent effects of seizure-inducing chemical threat agents. Annals of the New York Academy of Sciences 1378(1), 124-136.

Pressly, B., Lee, R.D., Barnych, B., Hammock, B.D., Wulff, H., 2021. Identification of the Functional Binding Site for the Convulsant Tetramethylenedisulfotetramine in the Pore of the alpha 2 beta 3 gamma 2 GABAA Receptor. Mol Pharmacol 99(1), 78-91.

Pressly, B., Nguyen, H.M., Wulff, H., 2018. GABAA receptor subtype selectivity of the proconvulsant rodenticide TETS. Arch Toxicol 92(2), 833-844.

Rice, N.C., Rauscher, N.A., Langston, J.L., Myers, T.M., 2017. Behavioral intoxication following voluntary oral ingestion of tetramethylenedisulfotetramine: Dose-dependent onset, severity, survival, and recovery. Neurotoxicology 63, 21-32.

Shakarjian, M.P., Ali, M.S., Veliskova, J., Stanton, P.K., Heck, D.E., Velisek, L., 2015. Combined diazepam and MK-801 therapy provides synergistic protection from tetramethylenedisulfotetramine-induced tonic-clonic seizures and lethality in mice. Neurotoxicology 48, 100-108.

Shakarjian, M.P., Laukova, M., Veliskova, J., Stanton, P.K., Heck, D.E., Velisek, L., 2016. Tetramethylenedisulfotetramine: pest control gone awry. Annals of the New York Academy of Sciences 1378(1), 68-79.

Shakarjian, M.P., Veliskova, J., Stanton, P.K., Velisek, L., 2012. Differential antagonism of tetramethylenedisulfotetramine-induced seizures by agents acting at NMDA and GABA(A) receptors. Toxicol Appl Pharmacol 265(1), 113-121.

Siso, S., Hobson, B.A., Harvey, D.J., Bruun, D.A., Rowland, D.J., Garbow, J.R., Lein, P.J., 2017. Editor's Highlight: Spatiotemporal Progression and Remission of Lesions in the Rat Brain Following Acute Intoxication With Diisopropylfluorophosphate. Toxicol Sci 157(2), 330-341.

Supasai, S., Gonzalez, E.A., Rowland, D.J., Hobson, B., Bruun, D.A., Guignet, M.A., Soares, S., Singh, V., Wulff, H., Saito, N., Harvey, D.J., Lein, P.J., 2020. Acute administration of diazepam or midazolam minimally alters long-term neuropathological effects in the rat brain following acute intoxication with diisopropylfluorophosphate. Eur J Pharmacol 886, 173538.

Tsai, Y.-H., Lein, P.J., 2021. Mechanisms of Organophosphate Neurotoxicity. Current Opinion in Toxicology.

Van Camp, N., Boisgard, R., Kuhnast, B., Thézé, B., Viel, T., Grégoire, M.-C., Chauveau, F., Boutin, H., Katsifis, A., Dollé, F., 2010. In vivo imaging of neuroinflammation: a comparative study between [18 F] PBR111,[11 C] CLINME and [11 C] PK11195 in an acute rodent model. European journal of nuclear medicine and molecular imaging 37(5), 962-972.

Vito, S.T., Austin, A.T., Banks, C.N., Inceoglu, B., Bruun, D.A., Zolkowska, D., Tancredi, D.J., Rogawski, M.A., Hammock, B.D., Lein, P.J., 2014. Post-exposure administration of diazepam combined with soluble epoxide hydrolase inhibition stops seizures and modulates neuroinflammation in a murine model of acute TETS intoxication. Toxicol Appl Pharmacol 281(2), 185-194.

Whitlow, K.S., Belson, M., Barrueto, F., Nelson, L., Henderson, A.K., 2005. Tetramethylenedisulfotetramine: old agent and new terror. Annals of emergency medicine 45(6), 609-613.

Wu, X., Kuruba, R., Reddy, D.S., 2018. Midazolam-Resistant Seizures and Brain Injury after Acute Intoxication of Diisopropylfluorophosphate, an Organophosphate Pesticide and Surrogate for Nerve Agents. J Pharmacol Exp Ther 367(2), 302-321.

Zhang, Y., Su, M., Tian, D.P., 2011. Tetramine poisoning: A case report and review of the literature. Forensic Sci Int 204(1-3), e24-27.

Zhao, C., Hwang, S.H., Buchholz, B.A., Carpenter, T.S., Lightstone, F., Yang, J., Hammock, B.D., Casida, J.E., 2014. GABAA receptor target of tetramethylenedisulfotetramine. Proceedings of the National Academy of Sciences of the United States of America 111(23), 8607-8612.

Zhou, Y., Liu, L., Tang, L., 1998. [An autopsy analysis on 5 cases of poisoning death with tetramethylenedisulfotertramine]. Fa Yi Xue Za Zhi 14(4), 214-215, 217, 252.

Zolkowska, D., Banks, C.N., Dhir, A., Inceoglu, B., Sanborn, J.R., McCoy, M.R., Bruun, D.A., Hammock, B.D., Lein, P.J., Rogawski, M.A., 2012. Characterization of Seizures Induced by Acute and Repeated Exposure to Tetramethylenedisulfotetramine. The Journal of Pharmacology and Experimental Therapeutics 341(2), 435-446.

Zolkowska, D., Wu, C.Y., Rogawski, M.A., 2018. Intramuscular allopregnanolone and ganaxolone in a mouse model of treatment-resistant status epilepticus. Epilepsia.

Chapter 3

Persistent neuropathology and behavioral deficits in a mouse model of *status epilepticus* induced by acute intoxication with diisopropylfluorophosphate

Jonas J. Calsbeek[1], Eduardo A. González[1], Donald A. Bruun[1], Michelle A. Guignet[1], Nycole A. Copping[3,4], Mallory E. Dawson[1], Alexandria J. Yu[1], Jeremy A. MacMahon[1], Naomi H. Saito[2] Danielle J. Harvey[2], Jill L. Silverman[3, 4], Pamela J. Lein[1, 4]

[1]Department of Molecular Biosciences, University of California, Davis, School of Veterinary Medicine, Davis, CA 95616, USA (jcalsbeek@ucdavis.edu, azgonzalez@ucdavis.edu, dabruun@ucdavis.edu, mguignet@ucdavis.edu, medawson@ucdavis.edu, aljyu@ucdavis.edu, jamacmahon@ucdavis.edu, pjlein@ucdavis.edu); [2]Department of Public Health Sciences, University of California, Davis, School of Medicine, Davis, CA 95616, USA (nhsaito@ucdavis.edu, djharvey@ucdavis.edu); [3]Department of Psychiatry and Behavioral Sciences, School of Medicine, University of California, Davis, Sacramento, CA 95817, USA (nacopping@ucdavis.edu, jsilverman@ucdavis.edu); [4]MIND Institute, School of Medicine, University of California, Davis, Sacramento, CA 95817, USA.

Abstract:

Organophosphate (OP) nerve agents and pesticides are a class of neurotoxic compounds that can cause *status epilepticus* (SE), and death following acute high-dose exposures. While the standard of care for acute OP intoxication (atropine, oxime, and high dose benzodiazepine) can prevent mortality, survivors of OP poisoning often experience long-term brain damage and cognitive deficits. Preclinical studies of acute OP intoxication have primarily used rat models to identify candidate medical countermeasures. However, the mouse offers the advantage of readily available knockout strains for mechanistic studies of acute and chronic consequences of OP-induced SE. Therefore, the main objective of this study was to determine whether a mouse model of acute diisopropylfluorophosphate (DFP) intoxication would produce acute and chronic neurotoxicity similar to that observed in rat models and humans following acute OP intoxication. Adult male C57Bl/6J mice injected with DFP (9.5 mg/kg, s.c.) followed 1 min later with atropine sulfate (0.1 mg/kg, i.m.) and 2-pralidoxime (25 mg/kg, i.m.) developed behavioral and electrographic signs of SE within minutes that continued for at least 4 h. Acetylcholinesterase inhibition persisted for at least 3 d in the blood and 14 d in the brain of DFP mice relative to vehicle (VEH) controls. Immunohistochemical analyses revealed significant neurodegeneration and neuroinflammation in multiple brain regions at 1, 7, and 28 d post-exposure in the brains of DFP mice relative to VEH controls. Deficits in locomotor and home-cage behavior were observed in DFP mice at 28 d post-exposure. These findings demonstrate that this mouse model replicates many of the outcomes observed in rats and humans acutely intoxicated with OPs, suggesting the feasibility of using this model for mechanistic studies and therapeutic screening.

Keywords: acetylcholinesterase, neurodegeneration, neuroinflammation, organophosphate, seizures

Abbreviations

AChE = acetylcholinesterase

DFP = diisopropylfluorophosphate

DPE = days post-exposure

FJC = FluoroJade-C

GFAP = glial fibrillary acidic protein

IBA1 = ionized calcium binding adaptor molecule 1

OP = Organophosphate

SE = *status epilepticus*

SLUD = salivation, lacrimation, urination, defecation

SRS = spontaneous recurrent seizures

VEH = vehicle

Introduction

Organophosphates (OPs) were first synthesized in the 1930s as insecticides and later discovered to kill insects via inhibition of acetylcholinesterase (AChE). AChE is conserved across species, so this discovery led to the subsequent development of OPs as G-series nerve agents (e.g. sarin, soman, tabun), V-series nerve agents (e.g. VX), and Novichok agents (Adeyinka, Muco et al. 2020). While OPs were developed as chemical weapons during World War II (Munro 1994), they were not deployed then, but were used in later conflicts such as the Iran-Iraq War and Syrian Civil War (UN 2020, HRW 2021). They have also been used in high profile assassinations and assassination attempts: VX agent was used to murder Kim Jong-nam in 2017 (OPCW 2018) and Novichok agent was deployed in the attempted assassinations of Sergei and Yulia Skripal in the U.K. in 2018 (Chai, Hayes et al. 2018, Haley 2018) and Alexei Navalny in Russia in 2020 (OPCW 2020). Consequences of acute OP intoxication in these cases included the loss of consciousness, seizures, and/or death (Figueiredo, Apland et al. 2018, Jett and Spriggs 2020) due to the excessive accumulation of acetylcholine in cholinergic synapses throughout the peripheral and central nervous systems (Eddleston, Buckley et al. 2008, Hulse, Davies et al. 2014). Moreover, each year, OP insecticides are responsible for an estimated 250,000 cases of suicide in developing nations (Eddleston, Buckley et al. 2008). Thus, there is a strong interest in developing effective medical countermeasures for OP poisoning.

The current standard of care for acute OP intoxication includes the use of a muscarinic antagonist (e.g., atropine) to prevent the binding of acetylcholine (ACh) to muscarinic receptors, an oxime (e.g., 2-pralidoxime) to reactivate AChE, and a benzodiazepine (typically diazepam or midazolam) to increase GABAergic signaling in the nervous system (Eddleston, Buckley et al.

2008). When injected within minutes of OP exposure, benzodiazepines can reduce seizure behavior and prevent death, but when their administration is delayed, they do not effectively protect against neuropathology or behavioral deficits (McDonough, Zoeffel et al. 1999, Shih 2000, Masson 2011). Preclinical studies have identified potentially more effective strategies for terminating acute OP-induced *status epilepticus* (SE) (Lumley, Miller et al. 2019, Aroniadou-Anderjaska, Figueiredo et al. 2020, Guignet, Dhakal et al. 2020, Marrero-Rosado, de Araujo Furtado et al. 2020), but there has been comparatively little progress made in identifying novel neuroprotective therapies. The latter reflects the challenge of identifying pathogenic mechanisms of chronic neurotoxicity following acute OP intoxication, which involves multiple cell types and neural circuits, as well as logistical challenges of preclinical models in which long-term survival rates can be low.

Preclinical rat models of SE induced by OPs, including diisopropylfluorophosphate (DFP), have demonstrated persistent neuropathology and/or behavioral deficits (Deshpande, Carter et al. 2010, Flannery, Bruun et al. 2016, Pouliot, Bealer et al. 2016, Hobson, Rowland et al. 2019, Guignet, Dhakal et al. 2020) that recapitulate long-term effects observed in human survivors of acute OP poisoning (Jett, Sibrizzi et al. 2020). However, a mouse model of OP-induced SE would be desirable because of the availability of transgenic strains that could be leveraged to investigate pathogenic mechanisms underlying the chronic neurotoxicity of acute OP intoxication. OP-induced SE has been studied in mice (see Table 1), but these studies (Dhote, Peinnequin et al. 2007, Collombet, Pierard et al. 2008, Coubard, Beracochea et al. 2008, Dhote, Carpentier et al. 2012, Golderman, Shavit-Stein et al. 2019, Enderlin, Igert et al. 2020, McCarren, Eisen et al. 2020, Maupu, Enderlin et al. 2021) have not rigorously measured the

spatiotemporal progression of neuropathology at delayed times post-exposure or evaluated long-term behavioral effects. The main objective of this study was to develop a mouse model of OP-induced SE that will facilitate characterization of chronic neurotoxic effects with the long-term goal of using this model to investigate pathogenic mechanisms and evaluate novel therapeutics. Here, we evaluate adult male C57BL/6J mice as a model of acute DFP intoxication and determine whether it exhibits chronic neuropathology and long-term behavioral deficits comparable to those observed in rat models of OP-induced SE.

Materials and Methods

Animals

All studies involving animals conformed to the ARRIVE guidelines. Studies were designed to minimize pain and suffering and were conducted in accordance with protocols approved by the University of California, Davis Institutional Animal Care and Use Committee. Animals were housed in facilities accredited by the Association for Assessment and Accreditation of Laboratory Animal Care International. Adult male C57BL/6 mice (8-10 weeks old; 22-33g; Jackson Laboratory, Sacramento, CA, USA) were maintained on a 12:12 hour light:dark cycle in a temperature and humidity-controlled vivarium (22 ± 2º C; 40-50% humidity). Mice were housed in standard plastic cages, provided chow (LabDiet, #5058) and tap water *ad libitum*, and allowed to acclimate for at least 7 d prior to experimentation. All animals used in this study were randomly assigned to experimental groups using a random number generator. Animals were group-housed (4 mice per cage) until dosed with DFP, after which animals were singly housed with additional environmental enrichment until euthanized.

Drugs and Dosing Paradigm

DFP was purchased from Sigma-Aldrich (St. Louis, MO, USA) and confirmed to be ~90±7% pure using previously published NMR methods (Gao, Naughton et al. 2016), and stored at -80ºC. DFP was prepared in sterile, ice-cold phosphate-buffered saline (PBS; 3.6 mM Na_2HPO_4, 1.4 mM NaH_2PO_4, 150 mM NaCl, pH 7.2) immediately before injection. Mice were injected with a single 100 µL dose of DFP (9.5-12.7 mg/kg, s.c.; Sigma-Aldrich) followed 1 min later by a single injection of atropine sulfate (AS; 0.1 mg/kg, i.m.; Sigma-Aldrich) and 2-pralidoxime (2-PAM; 25 mg/kg, i.m.; Sigma-Aldrich) to prevent peripheral toxicity (Figure 3.1). This dosing paradigm was determined in preliminary experiments testing a range of DFP or AS doses to produce continuous seizures in DFP-exposed mice (Supplemental material, Figure S1). Certificates of analysis provided by the manufacturers confirmed the purity of AS (>97%, lot #BCBM6966V) and 2-PAM (>99%, lot #MKCG3184). Animals in the VEH group were injected with an equivalent volume (100 µL) of sterile PBS, s.c. followed 1 min later by AS (0.1 mg/kg, i.m.) and 2-PAM (25 mg/kg, i.m.). Animals were continuously monitored for seizure behavior for 4 h after injection with DFP or VEH using a modified behavioral seizure scoring scale (Figure 3.2A). At the end of the 4 h exposure period, animals were injected subcutaneously with 1 mL of 5% dextrose in sterile saline (Baxter Healthcare Co., Deerfield, IL, USA) to replace fluids lost as a result of cholinergic crisis, returned to their home cages, and given soft, moist chow daily until they resumed normal consumption of solid food and water (typically within 7 days). Body weights were measured daily after dosing with DFP, and any animal appearing weak or ill in the days following dosing with DFP were injected with 1 mL of 5% dextrose in sterile saline per day as needed.

EEG recording

A subset of mice used in this study were implanted with wireless EEG telemetry devices from Data Sciences International (HD-X02; DSI, St. Paul, MN, USA). Surgical implantation of electrodes for EEG recordings was performed in accordance with the UC Davis Rodent Survivable Surgery course. Adult mice were anesthetized using continuous isoflurane inhalation (4-5% for induction, 1-3% for maintenance). The head was shaved with a hair clipper and then cleaned alternately with betadine and alcohol repeated 3 times. Next, the animal was positioned in a stereotaxic frame with mouse-sized ear bars and an appropriately sized inhalation mask. A water-heated pad was put between the animal's body and the base of the stereotaxic frame to prevent hypothermia. Sterile ophthalmic ointment (Altalube; McKesson Brand, #Q187-08) was applied to the eyes to prevent dryness. Once the appropriate depth of anesthesia was confirmed using the foot pinch reflex, an approximately 0.7 inch long incision was made on the scalp along the midline from eye level to the neck level. The skin was retracted to the sides with hemostats. The periosteum was carefully scraped away from the skull to expose the bone. During the surgery, sterile saline was regularly applied to keep the surgical area hydrated. A head mount with up to 4 cortical screws, with 3 anchor crews in the skull, was implanted according to the Data Sciences International (DSI) manual. A mini drill was used to create small holes in the skull where electrodes were placed according to stereotaxic coordinates. For optimal EEG alignment, the front edge of the implant was placed 3.0 – 3.5 mm anterior of bregma. The tip of the implanted electrodes was located near the cortex relative to bregma using the stereotaxic coordinate system. The head mount was fixed on the skull using standard dental acrylic cement (Lang Dental Manufacturing Co Inc., Wheeling, IL, USA). The skin incision was closed with sutures, and dental cement was used to complete the skull cap. After surgery, the animals were

allowed to recover for at least 7 d before experimentation, and only healthy animals continued in the study. EEG measurements were recorded untethered and only required the placement of a receiver (RPC-1; Data Sciences International, New Brighton, MN, USA) under the home cage of the animal. No other changes to the home cage environment or the well-being of the animal were required.

AChE Activity

At 1, 3, 7, and 14 days after DFP or VEH exposure, subsets of mice were deeply anesthetized with 4-5% isoflurane in medical-grade oxygen and transcardially perfused with 25 ml ice-cold PBS (3.6 mM Na_2HPO_4, 1.4 mM NaH_2PO_4, 150 mM NaCl, pH 7.2) using a Peri-Star Pro peristaltic pump (5 mL/min). Their brains were removed and dissected to isolate the hippocampus, somatosensory cortex, and cerebellum from both hemispheres. Brain regions were flash-frozen in individual cryotubes using liquid nitrogen and stored at -80ºC until use. AChE activity was measured in the hippocampus, cortex, cerebellum, and blood using the Ellman method (Ellman, Courtney et al. 1961). Tissue from each brain region was homogenized in cold sodium phosphate buffer (4ºC, 0.1M, pH = 8.0, 1% Triton X-100; 1 mL buffer:0.1g tissue), spun down in a centrifuge at 13.400xg for 1 min, and the supernatant collected. Blood plasma samples were diluted 1:25 in cold sodium phosphate buffer (4ºC, 0.1M, pH = 8.0, 0.03% Triton X-100) for the AChE assay. Supernatant and blood samples were plated in triplicate in a 96-well plate, and AChE activity was measured in each well using acetylthiocholine iodide (ASChI, Sigma) as the AChE substrate, and 5,5′-dithio-bis (2-nitrobenzoic acid) (DTNB, Sigma) as the colorimetric reagent. The hydrolysis of ASChI was quantified using a Synergy H1 Hybrid Plate Reader with

Gen5 2.0 software (BioTek Instruments, Winooski VT, USA) by measuring changes in absorbance at 405 nm over 15 min in each well. To specifically determine AChE activity versus total cholinesterase activity, all samples were run both in the absence and presence of the butyrylcholinesterase (BChE) inhibitor, tetraisopropyl pyrophosphoramide (100 µM). AChE activity was normalized against total protein concentration with the BCA assay according to the manufacturer's directions (Pierce, Rockford, IL, USA).

Histological Assessment

At 1, 7, and 28 days after exposure to DFP or VEH, mice assigned to histology cohorts were deeply anesthetized with 4-5% isoflurane in medical-grade oxygen and transcardially perfused with 25 ml ice-cold PBS (3.6 mM Na_2HPO_4, 1.4 mM NaH_2PO_4, 150 mM NaCl, pH 7.2) using a Peri-Star Pro peristaltic pump (5 ml/min). Their brains were removed and sliced coronally into 2 mm thick sections using a mouse coronal brain matrix (Zivic Instruments, #5325; Pittsburgh, PA, USA). Sections were placed into a 24-well plate so that each well contained 1-2 brain sections submerged in 1 mL 4% (w/v) paraformaldehyde (PFA; Sigma; St. Louis, MO, USA), covered and stored at 4ºC for 18-24 h. A disposable transfer pipette was used to replace the PFA in each well with a 30% sucrose solution. Plates were covered and stored again at 4ºC until brain tissue was fully saturated and sank to the bottom of the well. Brain sections were embedded in optimal cutting temperature medium (OCT; Fisher HealthCare; Waltham, MA, USA) and flash frozen. Blocked brain sections were stored at -80º C until cryosectioned with a Microm HM550 cryostat (Thermo Fisher Scientific; Waltham, MA, USA).

Ten micron thick coronal slices were mounted on Superfrost Plus microscope slides (Fisher HealthCare) that were stored at -80º C until used for immunohistochemistry.

Neurodegeneration was assessed at 1, 7, and 28 d after exposure to VEH or DFP using FluoroJade C (FJC; AG325, MilliporeSigma; Burlington, MA, USA) staining. Brain sections were incubated in 0.06% (w/v) $KMnO_4$ (Sigma) in distilled H_2O (dH_2O) for 10 min and then rinsed 3 times for 5 min in dH_2O. Slides were then incubated in FJC working solution containing FJC (0.00015%, v/v; Cat. #AG325, lot #2301303, Millipore, Billerica, MA, USA) and DAPI (0.5 µg/mL; Invitrogen; Carlsbad, CA, USA) in 0.1% acetic acid (v/v; Acros Organics; Geel, Belgium) in dH_2O for 10 min in the dark. Slides were rinsed 3 times for 5 min in dH_2O, then dipped in xylene (X5SK-4, Assay grade; Thermo Fisher Scientific) for 1 min and allowed to completely dry at 50ºC. Sections were cover slipped in Permount (Thermo Fisher Scientific) and imaged at 10-20X magnification on a high content ImageXpress XLS imaging system (Molecular Devices; Sunnyvale, CA, USA). The hippocampus, piriform cortex, and thalamus of VEH and DFP mice were assessed for the number of neurons positively labeled with FJC (per mm^2) using ImageJ (NIH, USA) thresholding and cell counting by a scorer blinded to animal identification number and experimental group.

Neuroinflammation was assessed at 1, 7, and 28 after exposure to VEH or DFP by immunohistochemistry. Sections were co-immunolabeled for GFAP and S100β to detect astrocytes or IBA1 and CD68 to detect microglia and phagocytic activity, as previously described (Guignet, Dhakal et al. 2020). Brain sections were removed from -80ºC storage, brought to room temperature, and submerged in PBS (3.6 mM Na_2HPO_4, 1.4 mM NaH_2PO_4, 150 mM NaCl, pH 7.2) for 5 min. Antigen retrieval was performed by submerging slides in 10 mM

sodium citrate buffer (pH = 6.0) and heating to 90ºC for 30 min in a vegetable steamer. After antigen retrieval, slides were washed 3 times for 5 min in PBS and then incubated in blocking buffer [PBS containing 10% normal goat serum (v/v; Vector Laboratories), 1% bovine serum albumin (w/v; Sigma), and 0.3% Triton X-100 (Thermo Fisher Scientific)] for 1 h at room temperature to prevent non-specific binding. Sections were next incubated in primary antibody diluted in blocking buffer at 4ºC for 18-24 h. Primary antibodies included rabbit anti-IBA1 (1:1000; 019–19741, Wako Laboratory Chemicals, Richmond, VA, USA; RRID:AB_839504), rat anti-CD68 (1:200, MCA1957, BIORAD, Hercules, CA, USA; RRID:AB_322219), mouse anti-GFAP (1:1000; 3670, Cell Signaling Technology, Danvers, MA, USA; RRID:AB_561049), and rabbit anti-S100β (1:300; ab52642, Abcam, Burlington, CA, USA; RRID:AB_882426). For negative controls, a subset of sections was incubated with blocking buffer instead of primary antibody and processed the same as the other sections. After primary incubation, sections were washed 3 times for 5 min with PBS and incubated with secondary antibody diluted in PBS with 0.3% Triton X-100 for 1 h at room temperature. Secondary antibodies included goat anti-rabbit IgG Alexa Fluor 568 (1:1000; A11036, Life Technologies; RRID:AB_10563566), goat anti-rat IgG Alexa Fluor 488 (1:500; A11006, Thermo Fisher Scientific; RRID:AB_2534074), goat anti-mouse IgG1 Alexa Fluor 568 (1:1000; A21124, Thermo Fisher Scientific; RRID:AB_2535766), and goat anti-rabbit Alexa Fluor 488 (1:600; A11034, Thermo Fisher Scientific; RRID:AB_2576217). Sections were then washed 3 times for 5 min with PBS and cover slipped using ProLong Gold Antifade Mountant with DAPI (Invitrogen, #P36931). Fluorescent images were acquired using a high content ImageXpress XLS imaging system (Molecular Devices, Sunnyvale, CA, USA) at 10-20X magnification. Positive immunostaining was determined as fluorescent intensity that was at least twice the background fluorescence levels in the negative

control samples, and all acquired images were used in the quantitative analysis. Two serial sections were analyzed for each animal in each brain region, and the total area of positive staining was averaged for each region between sections. The cortex, hippocampus, thalamus, and piriform cortex of VEH and DFP mice were analyzed using ImageJ to threshold and measure the percent area of positively labeled astrocytes and microglia by a scorer blinded to animal identification number and experimental group.

Behavioral Assessment

Open Field

At 27 days post-DFP intoxication, VEH and DFP mice were removed from their home cages and placed in a clean, empty, open field arena (48 cm x 48 cm x 48 cm) in a room with low lighting (~40 lx) and allowed to freely explore the arena in solitude for 30 min after the experimenter left the room. Ethovision video tracking software (EthoVision 10.1, Noldus Information Technology, Leesburg, VA, USA) was used to track the center point of the animal within the arena (3x3 zones) and measure the total distance traveled, average velocity, and time in center zone during the 30 min trial. After each test, the arena was cleaned with 70% ethanol and the vapor was allowed to evaporate before the next mouse was tested.

Home cage Reactivity

VEH and DFP mice were tested for anxiety-like behavior and hyperreactivity at 28 d post-intoxication using a modified home cage reactivity test, as previously described (Raffaele, Hughey et al. 1987, Guignet, Dhakal et al. 2020). A blinded experimenter used gloved hands

used a transfer pipette (13-711-7M, Thermo Fisher Scientific, Waltham, MA, USA) to apply the following five stimuli, in this order: [1] a puff of air to the back; [2] light pressure to the tail base; [3] light pressure to the back; [4] light pressure to the head; [5] picking up the animal by the tail. A score between 0 and 3 was assigned to each animal to quantify the reaction to each stimulus based on the following criteria: [0] little to no reaction; [1] forward or backward movement; [2] forward or backward movement with alertness, Straub tail; [3] movement with speed, facing experimenter, or tail shake. The behavioral scores for each stimulus were added together for each animal to produce an overall reactivity score.

Nesting Behavior

At 28 days post-DFP intoxication, the home cages of VEH and DFP mice were inspected to assess nesting behavior as determined by the animal's incorporation of a nesting pad (Nestlets, LabSupply, Fort Worth, Texas, USA) into the home cage paper nest. A blinded experimenter scored the nest in the home cage of each mouse according to the following criteria: [0] nesting pad was still intact; [1] nesting pad partially shredded; [2] nesting pad fully shredded, but not incorporated into the nest; and [3] if the nesting pad was fully shredded and incorporated into the nest.

Statistical Analyses

Biochemical assay data were analyzed using one-way ANOVA with Dunnett's multiple comparisons test as performed using Prism 8.0.1 (GraphPad Software, La Jolla, CA, USA). Behavioral data were analyzed using the Mann-Whitney test as performed by Prism 8.0.1. Key

outcomes considered in the histologic analyses included FJC labeling (number of cells/mm^2), % area of GFAP and S100β immunoreactivity, % area of GFAP and S100β colocalization, % area IBA1 and CD68 immunoreactivity, and % area of IBA1 and CD68 colocalization. Mixed effects models, including animal-specific random effects, were fit to assess differences between exposure groups. Primary factors of interest included exposure (DFP, VEH), region (thalamus, piriform cortex/amygdala, hippocampus, somatosensory cortex (except for FJC)), and time post-exposure (1, 7, 28 days). Interactions between the factors (treatment, region, and time point) were considered and the best model was chosen using Akaike Information Criterion. Outcomes, except for S100β and IBA1, were transformed using the natural logarithm after shifting all values by a small amount (0.1 for GFAP, GFAP/S100β colocalization, CD68 and IBA1/CD68 colocalization, and 1 for FJC) to enable the calculation for the animals with no positive staining to better meet the assumptions of the model. Contrasts for group differences, either overall or by time point or region, were constructed and tested using a Wald test. The Benjamini-Hochberg false discovery rate (FDR) was used within an outcome measure to account for multiple comparisons. Results are presented as geometric mean ratios (GMR) between exposure groups for the log-transformed outcomes and as differences between exposures for S100β and IBA1. Point estimates of the ratios or differences and 95% confidence intervals are presented in the figures. When the confidence interval for the GMR includes 1, there is no statistical evidence of a difference between groups; similarly, when the confidence interval for the differences includes 0, there is no statistical evidence of a difference between groups. All analyses were performed using SAS (version 9.4, SAS Institute, Inc., Cary, NC, USA), and graphics were created in R (version 3.6.3, R Core Team, Vienna, Austria) and alpha was set at 0.05; all reported results remained significant after the FDR procedure.

Results

Acute DFP intoxication causes *status epilepticus* in adult male mice

To confirm that acute exposure to DFP causes seizures that progress to SE in mice, seizure behavior was quantified using a seizure severity scale to score animals during the first 4 h after injection with VEH or DFP (Figure 3.2A). Scores were recorded for each animal in 5 min increments for the first 2 h after dosing, and every 20 min for the last 2 h of scoring. Symptoms of cholinergic nervous system activation, such as Straub tail and body shakes, were apparent in DFP-exposed mice within minutes of injection with DFP. Behaviors rapidly progressed to SE marked by continuous clonic or tonic seizures (seizure score ≥ 3; Figure 3.2B). DFP-exposed mice (n=12) had a mean seizure score of 3.2 ± SEM over the first 4 h of seizure scoring. VEH mice (n=12) did not display any cholinergic signs or seizure behaviors and were assigned a seizure score of 0 for each recorded time point. To confirm that animals exhibiting seizure behavior were experiencing electrographic seizures, a subset of mice were implanted with wireless EEG recording electrodes to monitor electrical activity in the brain and muscle, respectively. Relative to baseline recordings obtained from each animal immediately prior to DFP exposure, DFP injection causes robust electrographic seizures within minutes, confirming that behavioral seizure scores corresponded to electrographic seizures in the brains of DFP mice (Figure 3.2C). To monitor animal health and wellness after DFP exposure, the body weights of mice were recorded daily. Body weights of DFP mice decreased significantly compared to VEH control mice during the first 3 d post-exposure (DPE) but began to return to baseline by 4 DPE (Figure 3.2D).

Acute DFP intoxication causes persistent AChE inhibition in the mouse brain

AChE activity was measured in the blood and multiple brain regions up to 14 DPE to determine the extent and duration of AChE inhibition. AChE activity was significantly inhibited in the blood for at least 3 days and in the brain for at least 14 days in DFP-intoxicated mice relative to VEH controls (Figure 3.3). In the somatosensory cortex, AChE activity was inhibited by 91% on 1 DPE, 71% on 3 DPE, 77% on 7 DPE, and 57% on 14 DPE relative to VEH controls. In the hippocampus, AChE was inhibited by 83% on 1 DPE, 66% on 3 DPE, 54% on 7 DPE, and 41% on 14 DPE relative to VEH controls. In the cerebellum, AChE was inhibited by 73% on 1 DPE, 59% on 3 DPE, 49% on 7 DPE, and 29% on 14 DPE, relative to VEH controls. In the blood, AChE was inhibited by 92% on 1 DPE, 63% on 3 DPE, 24% on 7 DPE, and 19% on 14 DPE, relative to VEH controls.

Acute DFP intoxication causes persistent neurodegeneration

Fluorescent images acquired using semi-automated high-content imaging revealed significantly more FJC+ neurons in the hippocampus, piriform cortex, and thalamus of DFP mice relative to VEH controls at 1, 7, and 28 DPE (Figure 3.4A). No FJC labeling was observed in any brain region of VEH mice at any time point, and no FJC staining was observed in the somatosensory cortex of DFP-intoxicated mice. There was no significant interaction between exposure groups and either time point or brain region. Across brain regions and time points, there was consistently more neurodegeneration observed in the DFP mice than in the VEH mice (Figure 3.4B; GMR=125.2, 95% CI=102.9-152.2, $p < 0.001$). Raw data used to generate this figure are provided in the supplemental material (Figure S2).

Acute DFP intoxication causes persistent neuroinflammation

GFAP and S100β immunoreactivity were used as biomarkers to assess reactive astrogliosis (Eng and Ghirnikar 1994) and brain injury (Gonçalves, Concli Leite et al. 2008) in the somatosensory cortex, hippocampus, thalamus, and piriform cortex of DFP mice (Figure 3.5A). GFAP is a biomarker of astrocytosis (Eng and Ghirnikar 1994) and increased GFAP expression is associated with astrocytic responses to environmental challenge (Li, Liu et al. 2020). S100β is a biomarker of mature astrocytes (Raponi, Agenes et al. 2007) and has recently garnered interest as a potential biomarker for traumatic brain injury (Oris, Pereira et al. 2018). Because astrocytes undergo morphogenic changes in response to neurodegeneration or neuroinflammation (Liu, Li et al. 2012), the area of positive immunoreactivity for these biomarkers was quantified as a readout of reactive astrogliosis. For GFAP immunolabeling, there were significant interactions between group, time point and region ($p < 0.001$) suggesting that the difference between DFP and VEH varied temporally and spatially (Figure 3.5B). At 1 DPE, DFP mice had a 60%-120% increase in percent GFAP positive area relative to the VEH animals across all brain regions examined (cortex: GMR=2.0, 95% CI=1.5-2.5, $p < 0.001$; hippocampus: GMR=1.7, 95% CI=1.4-2.2, $p < 0.001$; piriform cortex: GMR=2.2, 95% CI=1.6-2.9, $p < 0.001$; thalamus: GMR=1.6, 95% CI=1.1-2.1, $p = 0.007$). Of the days studied, percent area of GFAP immunoreactivity in DFP animals peaked at 7 DPE, with the greatest elevation observed in the cortex (GMR=9.6, 95% CI=7.2-12.7, $p < 0.001$) and piriform cortex (GMR=6.6, 95% CI=5.4-8.2, $p < 0.001$) relative to the VEH mice. In these two regions, the extent of GFAP immunoreactivity decreased by 28 DPE (cortex: GMR=1.5, 95% CI=1.0-2.4, $p = 0.04$; piriform cortex: GMR=2.1, 95% CI=1.4-3.1, $p < 0.001$). In the hippocampus and thalamus, the increase in percent area of GFAP immunoreactivity in DFP-exposed animals relative to VEH animals

observed at 7 days (hippocampus: GMR=3.1, 95% CI=2.5-3.9, $p < 0.001$; thalamus: GMR=3.6, 95% CI=2.0-6.7, $p < 0.001$) persisted at 28 DPE (hippocampus: GMR=2.6, 95% CI=2.0-3.3, $p < 0.001$; thalamus: GMR=2.8, 95% CI=2.0-3.8, $p < 0.001$). Raw data used to generate this figure are provided in the supplemental material (Figure S3).

For S100β immunolabeling, there was no significant interaction between exposure group and either time point or brain region (Figure 3.5C). Across brain regions and time points, there was consistently more S100β immunoreactivity observed in the DFP mice than in the VEH mice (mean difference=5.1, 95% CI=3.6-6.6, $p < 0.001$). Raw data used to generate this figure are provided in the supplemental material (Figure S3).

IBA1 and CD68 immunoreactivity were quantified as biomarkers of microglia and phagocytosis, respectively (Ito, Imai et al. 1998, Hendrickx, van Eden et al. 2017), in the somatosensory cortex, hippocampus, thalamus, and piriform cortex of VEH and DFP mice (Figure 3.6A). The percent area of IBA1 immunoreactivity varied by brain region and time point (Figure 3.6B; $p < 0.001$). In the cortex, the percent area IBA1 immunoreactivity was elevated in DFP animals compared to VEH animals at 1 DPE (mean difference=7.6, 95% CI=4.4-10.7, $p < 0.001$), but not at 7 or 28 DPE. The percent area of IBA1 immunoreactivity was elevated in DFP-exposed mice relative to VEH controls across all three time points for the other three regions examined: Hippocampus: Day1 (diff=7.0, 95% CI=3.4-10.6, $p < 0.001$), Day 7 (diff=12.8, 95 %CI=7.6-18.0, $p < 0.001$), Day 28 (diff=7.6, 95% CI=4.4-10.7, $p < 0.001$); Piriform cortex: Day 1 (diff=9.0, 95% CI=5.6-12.3, $p < 0.001$), Day 7 (diff=11.9, 95% CI=6.4-17.4, $p < 0.001$), Day 28 (diff=6.3, 95% CI=0.4-12.2, $p = 0.04$); Thalamus: Day 1 (diff=4.0, 95 %CI=1.0-6.9, $p = 0.01$), Day 7 (diff=5.1, 95 %CI=1.1-9.0, $p = 0.01$), Day 28 (diff=5.4, 95% CI=1.1-9.7, $p = 0.01$).

Raw data used to generate this figure are provided in the supplemental material (Figure S4). The difference among groups in percent CD68 immunopositive area varied by brain region and time point (Figure 3.6C; $p < 0.01$). The percent area of CD68 immunoreactivity was over 5-fold higher in DFP-exposed mice relative to VEH animals across all four brain regions and three time points that were examined ($p < 0.001$). Raw data used to generate this figure are provided in the supplemental material (Figure S4).

For the colocalization of GFAP and S100β, there were significant interactions between group, time point and brain region ($p < 0.001$) suggesting that the difference in GFAP/S100β colocalization between DFP and VEH varied spatiotemporally (Figure 3.7A). Patterns were similar to those seen for percent area of GFAP immunoreactivity with elevated levels for DFP animals compared to VEH animals across all regions 1 DPE (cortex: GMR=2.4, 95% CI=1.5-3.9, $p < 0.001$; hippocampus: GMR=2.4, 95% CI=1.5-3.7, $p < 0.001$; piriform cortex: GMR=2.0, 95% CI=1.3-3.0, $p = 0.002$; thalamus: GMR=2.9, 95% CI=1.9-4.5, $p < 0.001$). By 7 DPE, colocalization was highest in the cortex of DFP-exposed animals relative to VEH animals (GMR=15.2, 95% CI=11.1-20.8, $p < 0.001$), followed by the piriform cortex (GMR=6.2, 95% CI=4.6-8.5, $p < 0.001$), thalamus (GMR=4.9, 95% CI=2.4-10.2, $p < 0.001$) and hippocampus (GMR=3.7, 95% CI=2.6-5.4, $p < 0.001$). The extent of colocalization was reduced by 28 DPE in the cortex (GMR=2.0, 95% CI=1.4-3.0, $p < 0.001$) and piriform cortex (GMR=2.3, 95% CI=1.6-3.3, $p < 0.001$), although levels remained elevated in the hippocampus (GMR=4.0, 95 %CI=3.0-5.2, $p < 0.001$) and thalamus (GMR=4.1, 95 %CI=2.4-7.0, $p < 0.001$). The difference among groups in percent IBA1/CD68 colocalization varied by brain region and time point (Figure 3.7B; $p < 0.01$). Colocalization was over 3.5 times higher in DFP exposed mice than in VEH animals across the time points and brain regions.

Acute DFP intoxication causes long-term behavioral deficits

Behavioral tests were performed 28 d after exposure to VEH or DFP. At 28 DPE, deficits in locomotor activity, reactivity, and nesting behavior were observed in DFP-exposed mice (Figure 3.8). In the open field test, DFP mice traveled a significantly greater distance in 30 min than VEH mice (Figure 3.8A; average 18.12 m ± 2.07 compared to an average of 10.69 m ± 2.05, respectively; $p < 0.0001$). Additionally, DFP mice traveled at a significantly greater average velocity (Figure 3.8A; 11.78 cm/s ± 2.26 versus 6.46 cm/s ± 1.31; $p < 0.0001$). DFP mice were also observed to spend significantly less percentage of time in the center zone of the open field arena (2.1% ± 1.2) relative to VEH controls (Figure 3.8A; 9.5% ± 5.4; $p < 0.0001$). In the reactivity test, DFP mice were observed to be significantly more reactive to tactile stimuli than VEH mice (Figure 3.8B; average reactivity score of 10.1 ± 2.92 compared to 5.63 ± 0.92, respectively; $p = 0.0035$). DFP mice were also observed to have deficits in nesting behavior relative to VEH controls. On a scale of 0-3, DFP mice averaged a score of 0.7 ± 0.95, whereas VEH mice scored an average of 3 with no nesting deficits noted (Figure 3.8B; $p < 0.0001$).

Discussion

Our findings indicate that the mouse model of acute DFP intoxication recapitulates many of the acute and chronic neurotoxic effects observed in rat models of acute DFP intoxication. Specifically, the DFP mice exhibited: (1) acute behavioral and electrographic responses consistent with SE; (2) neurodegeneration and neuroinflammation evident at 1 DPE that persisted at 28 DPE; and (3) deficits in locomotor and home-cage behavior at 28 DPE. Thus, we believe the adult male C57BL/6J mouse, which is the genetic background of many commercially

available transgenic mouse lines, can be used to investigate pathogenic mechanisms linking acute SE to long-term neurologic consequences and to test novel therapeutics for efficacy in mitigating chronic neurotoxic effects.

Previous studies using adult male rats to study acute DFP intoxication have demonstrated that rats exhibited signs of cholinergic crisis, including robust seizure behavior triggered within minutes of a single injection with DFP (Deshpande, Carter et al. 2010, Pouliot, Bealer et al. 2016, Guignet, Dhakal et al. 2020). Similarly, we observed that adult male mice acutely intoxicated with DFP showed symptoms of OP poisoning within minutes after exposure, including salivation, lacrimation, urination, and defecation (SLUD) and behavioral seizures that progressed rapidly to SE lasting for at least 4 h. It should be noted that the scale used to score seizure behavior in this study was modified from the scale used in the rat model (Deshpande, Carter et al. 2010) to include specific behaviors observed in the mouse: Straub tail and tonic limb extensions. Wireless EEG recordings confirmed electrographic seizures within minutes following DFP injection and these are similar to EEG recordings of DFP-intoxicated rats (Deshpande, Carter et al. 2010, Pouliot, Bealer et al. 2016). The loss of body weight in DFP mice during the first days after SE is also consistent with published observations of preclinical rat models of OP intoxication (Pessah, Rogawski et al. 2016, Rojas, McCarren et al. 2021). Additionally, the AChE inhibition observed in the brains of DFP mice was consistent with observations in rat models of acute DFP intoxication with respect to both the percent inhibition of AChE, and the persistence of decreased AChE activity to 14 DPE (Ferchmin, Andino et al. 2014, González, Rindy et al. 2020).

Prior studies in our lab of a rat model of DFP intoxication demonstrated that SE triggers progressive neuronal cell death in multiple brain regions starting at 12 h post-DFP that persists for at least 60 DPE (Sisó, Hobson et al. 2017). These findings confirmed previous reports showing progressive neurodegeneration in the days following DFP-induced SE (Li, Lein et al. 2011, Flannery, Bruun et al. 2016). The findings of the current study are consistent with these prior observations of rats in that DFP mice displayed persistent neurodegeneration in multiple brain regions starting as early as 1 DPE that persisted at 28 DPE. One notable difference in the spatiotemporal pattern of neurodegeneration observed in mice versus rats acutely intoxicated with DFP is that unlike rats, no FJC staining was observed in the somatosensory cortex of DFP-intoxicated mice. The reason for this difference is not known but suggests that persistent neurodegeneration is not directly linked to AChE inhibition since AChE remained significantly inhibited at 14 DPE in this brain region . Also unclear are the mechanism(s) underlying the neurodegeneration observed at delayed time points in mice. A positive correlation between seizure severity and neurodegeneration has been observed in the rat model of acute DFP intoxication (Sisó, Hobson et al. 2017), suggesting that excitotoxicity influences the extent of neurodegeneration. Spontaneous recurrent seizures (SRS) have also been reported in the rat DFP model within two weeks after exposure (Guignet, Dhakal et al. 2020), suggesting that repeated occurrence of seizures contributes to persistent neurodegeneration. Studies are currently ongoing to determine whether mice experience SRS in the days to weeks after acute DFP intoxication.

It is well documented that DFP-induced SE triggers a robust and persistent neuroinflammatory response in the rat brain (Liu, Li et al. 2012, Flannery, Bruun et al. 2016, Sisó, Hobson et al. 2017, Guignet, Dhakal et al. 2020) and mouse brain (Maupu, Enderlin et al. 2021). The findings of the current study are consistent with these reports. We observed

astrogliosis and microgliosis as early as 1 DPE that persisted at 28 DPE in multiple brain regions of DFP mice. Previous studies in the rat also demonstrated that the neuroinflammatory response induced by acute DFP intoxication varies spatiotemporally and is coincident with extensive neurodegeneration within the same brain regions (Li, Lein et al. 2011, Liu, Li et al. 2012, Rojas, Ganesh et al. 2015). Thus, due to the occurrence of severe neurodegeneration in the hippocampus, piriform cortex, and thalamus of DFP mice, it is not surprising that GFAP/S100β and IBA1/CD68 immunoreactivity remained significantly elevated in the same brain regions at 28 DPE. A significant increase in CD68 also corresponded to brain regions with elevated neurodegeneration, consistent with the suggestion that degenerating neurons trigger microglial phagocytosis. A notable difference in the spatial relationship between neurodegeneration and neuroinflammation was observed in the somatosensory cortex of DFP mice, where significant increases in GFAP/S100β and IBA1/CD68 were observed despite the absence of neurodegeneration. The reason for this discrepancy is not known, but it suggests that neurodegeneration is not the only mechanism driving a neuroinflammatory response in the brains of mice after DFP-induced SE. One possible explanation is that activated microglia in brain regions other than the somatosensory cortex triggered reactive astrogliosis and microglial activation in the somatosensory cortex through the secretion of soluble chemokines like Il-1α, TNFα, and C1q (Liddelow, Guttenplan et al. 2017). Testing this possibility is the goal of future studies. Significantly increased S100β immunoreactivity in the brains of DFP mice are intriguing because this protein is a reliable biomarker of brain injury in survivors of OP poisoning (Yardan, Baydin et al. 2013) and patients with epilepsy (Liang, Mu et al. 2019). Increased astrocytic expression of S100β has been associated with compromised blood brain barrier (BBB) integrity (Krishnan, Wu et al. 2020), suggesting that acute DFP intoxication

adversely impacts the BBB. Indeed, BBB breakdown has been reported in the cortex of rats 4 days after soman-induced SE (Rojas, McCarren et al. 2021), suggesting another mechanism of neuropathology in DFP mice. Future studies should investigate the potential disruption of the BBB during DFP intoxication in mice as a potential therapeutic target for OP poisoning.

It has been well established that DFP-induced SE in adult male rats causes delayed learning and memory deficits that can persist for as long as 2 months post-intoxication (Brewer, Troendle et al. 2013, Flannery, Bruun et al. 2016, Guignet, Dhakal et al. 2020). The tests used in these studies included the Morris water maze to assess spatial learning and reference memory and Pavlovian fear conditioning to assess contextual and cued learning and memory. These reports are consistent with human survivors of OP poisoning that report impaired learning and memory as one of the more common neurological consequences of acute OP intoxication (Okumura, Hisaoka et al. 2005, Chen 2012, Jett, Sibrizzi et al. 2020). Learning and memory tests (novel object recognition and Pavlovian fear conditioning) were performed with DFP mice at 28 DPE in this study, but the data were determined to be confounded by the observed locomotor hyperactivity in DFP mice at 28 DPE. Future studies should focus on identifying learning and memory tasks that are not confounded by hyperactivity to assess these behavioral domains in the DFP mice.

Preclinical studies of OP-induced SE in rats have also established long-term behavioral deficits in anxiety (Coubard, Beracochea et al. 2008) and hyperreactivity (Guignet, Dhakal et al. 2020), symptoms consistent with excessive arousal and post-traumatic stress disorder (Weston 2014, Figueiredo, Apland et al. 2018). These reports are consistent with clinical literature describing the occurrence of anxiety and excessive arousal in human survivors of OP poisoning

(Levin, Rodnitzky et al. 1976, Yokoyama, Araki et al. 1998, Salvi, Lara et al. 2003, Harrison and Ross 2016). Consistent with these reports, the DFP mice exhibited signs of anxiety as indicated by increased avoidance of the center zone in the open field arena relative to VEH controls (Prut and Belzung 2003). Elevated scores in reactivity to tactile stimuli at 7, 30, and 60 days have been previously reported in a rat model of acute DFP intoxication using an identical scoring paradigm as the current study (Guignet, Dhakal et al. 2020). The findings from the reactivity test in DFP mice are consistent with the rat model. Collectively, these findings that DFP-induced SE caused signs of hyperarousal and anxiety in mice at 28 DPE are consistent with the human and rat literature.

The open field test revealed that DFP mice were hyperactive as evidenced by significantly increased total distance traveled and rate of travel relative to VEH controls at 28 DPE. This locomotor deficit is inconsistent with what has been previously shown in the DFP rat model, in which no deficits in locomotor activity were observed in the open field at 1 month post-DFP (Guignet, Dhakal et al. 2020). The reason for the difference between models in OP-induced locomotor effects is unclear. Previous observations of hyperactivity in mice after OP exposure have been attributed to OP-induced inhibition of neuropathy target esterase (NTE; Winrow, Hemming et al. 2003). Whether this explains the hyperactivity in DFP mice is not known since NTE was not assessed in the current study; however, previous studies have demonstrated that DFP can significantly inhibit NTE activity (Lotti, Caroldi et al. 1987, Correll and Ehrich 1991). Additional studies are needed to quantify NTE activity in the brains of DFP mice to determine if this is a mechanism contributing to the locomotor hyperactivity in the DFP mouse model.

While decreased ability for nesting behavior has not been previously reported in DFP mice specifically, nesting deficits have been observed in several mouse models of SE induced by either pilocarpine or kainic acid that also produce hippocampal damage (Jiang, Quan et al. 2013, Jiang, Yang et al. 2015, Jiang, Yu et al. 2019). Because brain damage or lesions in the hippocampus of mice is known to be associated with impaired nesting (Deacon 2006), it is not surprising that DFP mice do not successfully nest at 28 DPE when the hippocampus is still exhibiting significant neurodegeneration. More long-term studies of DFP mice are needed to fully characterize the timeline of OP-induced nesting deficits in this model species relative to the persistence of hippocampal damage.

In conclusion, the findings of the current study support the hypothesis that the adult male C57BL/6J mouse DFP model recapitulates many of the acute and chronic neurotoxic effects observed in rats and humans following acute OP intoxication. Since this is the genetic background of many currently available transgenic mouse strains, this model may be ideally suited to investigate the molecular mechanisms of DFP-induced SE, neuropathology, and behavioral deficits.

Acknowledgments

The authors gratefully acknowledge Dr. Suzette Smiley-Jewell for assistance with manuscript preparation. This research was supported by the CounterACT Program, National Institutes of Health Office of the Director, and the National Institute of Neurological Disorders and Stroke (NINDS) under Grant U54 NS079202. J.J.C. was supported by a predoctoral fellowship from the UC Davis School of Veterinary Medicine; E.A.G., by predoctoral fellowships from the National Institute of Neurological Disorders and Stroke [grant number F31 NS110522] and the National Institutes of Health Initiative for Maximizing Student Development [grant number R25 GM5676520]; and M.A.G., by predoctoral fellowships from the National Institute of General Medical Sciences [grant number T32 GM099608], and the David and Dana Loury Foundation. This project used core facilities supported by the UC Davis MIND Institute Intellectual and Developmental Disabilities Research Center (Eunice Kennedy Shriver National Institute of Child Health and Human Development grant U54 HD079125). The sponsors were not involved in the study design, in the collection, analysis, or interpretation of data, in the writing of the report, or in the decision to submit the paper for publication.

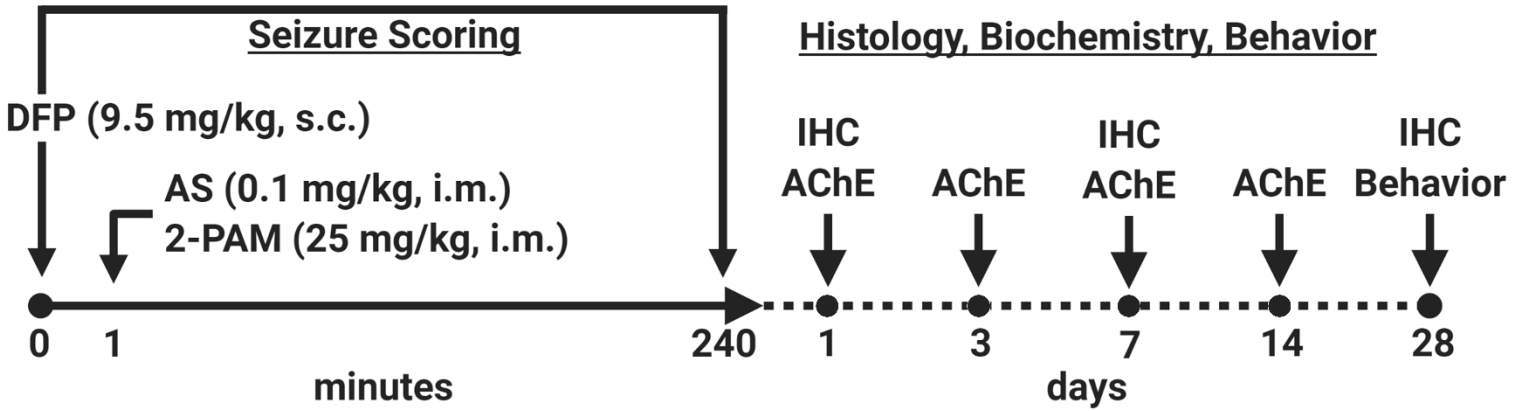
Seizure Scoring
Histology, Biochemistry, Behavior
DFP (9.5 mg/kg, s.c.)
AS (0.1 mg/kg, i.m.)
2-PAM (25 mg/kg, i.m.)
IHC
AChE
AChE
IHC
AChE
AChE
IHC
Behavior
0
1
240
1
3
7
14
28
minutes
days

Figure 3.1. Schematic of experimental design. Adult male C57BL/6 mice were injected subcutaneously with vehicle (VEH, saline) or DFP followed one minute later by intramuscular injection of atropine sulfate (AS) and 2-pralidoxime (2-PAM). Seizure behavior was manually scored for 4 h after DFP injection, and surviving mice were randomly assigned to cohorts for histological, biochemical, or behavioral assessment at 1, 3, 7, 14, and 28 days post-exposure. AChE=acetylcholinesterase assay; DFP=diisopropylfluorophosphate; IHC=immunohistochemistry. Created with BioRender.com.

A.

Score	Behavior
5	Falling with loss of righting reflex
4	Rearing, falling, tonic extensions
3	Forelimb or hindlimb clonus
2	Muscle tremors, head nod
1	Straub tail, SLUD
0	No abnormal symptoms

B.

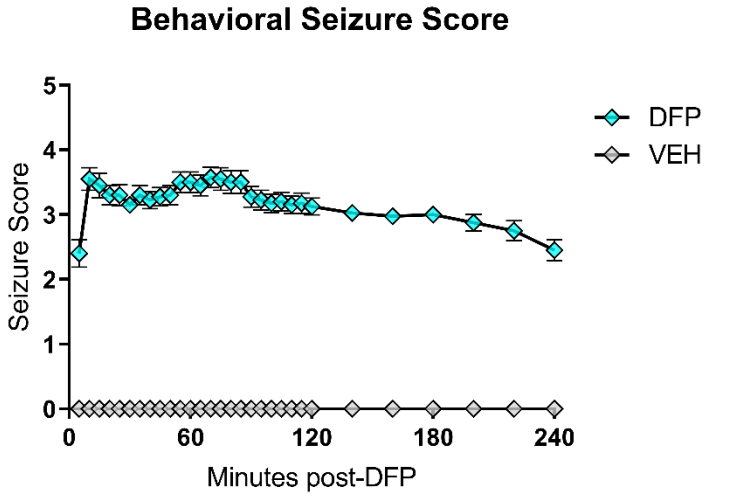

C.

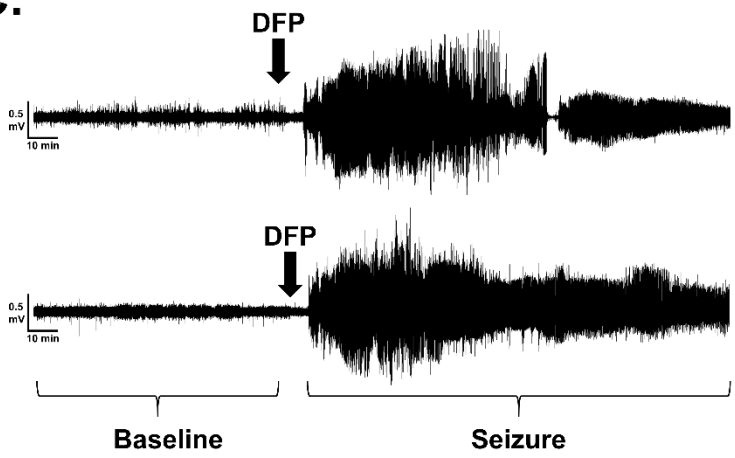

D.

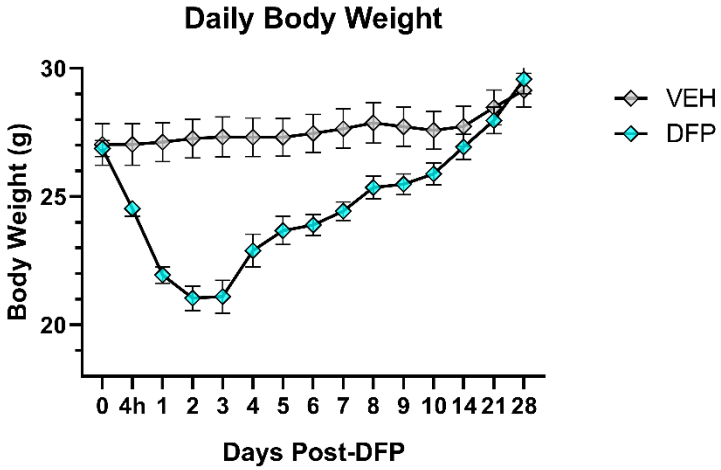

Figure 3.2. Acute DFP intoxication caused robust seizure behavior, electrographic abnormalities, and weight loss in adult mice. (A) The behavioral scoring scale used to evaluate seizure behavior after DFP injection. SLUD=salivation, lacrimation, urination, defecation. (B) Resulting seizure scores for the first 4 h after DFP or VEH injection. Data points represent the mean seizure score (± SEM) for each treatment group at each time point (n = 12 mice/group). (C) Representative EEG traces of 2 individual DFP mice over 100 min of baseline and seizure recording. (D) Body weights of mice over the 28 d after injection with DFP or VEH. Data points represent the mean body weight (± SEM) for each group at each time point (n = 12 mice/group).

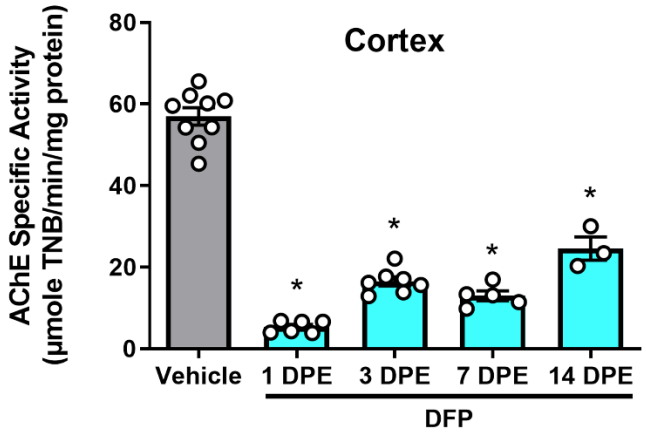
Cortex
AChE Specific Activity
(µmole TNB/min/mg protein)
80
60
40
20
0
Vehicle
1 DPE
3 DPE
7 DPE
14 DPE
DFP

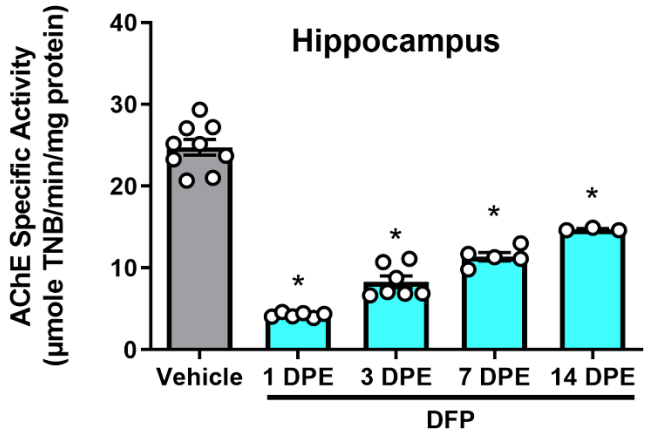
Hippocampus
AChE Specific Activity
(µmole TNB/min/mg protein)
40
30
20
10
0
Vehicle
1 DPE
3 DPE
7 DPE
14 DPE
DFP

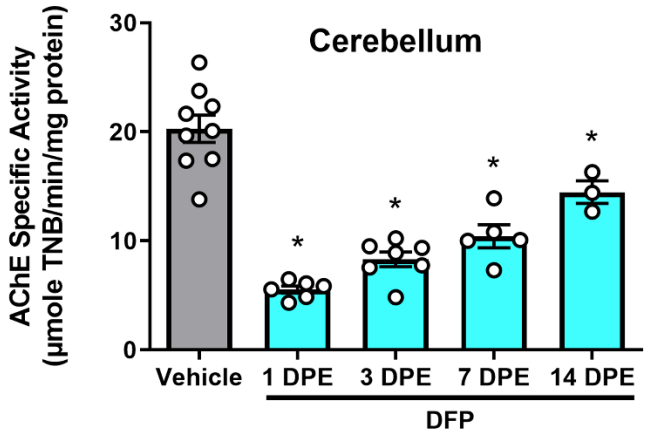
Cerebellum
AChE Specific Activity
(µmole TNB/min/mg protein)
30
20
10
0
Vehicle
1 DPE
3 DPE
7 DPE
14 DPE
DFP

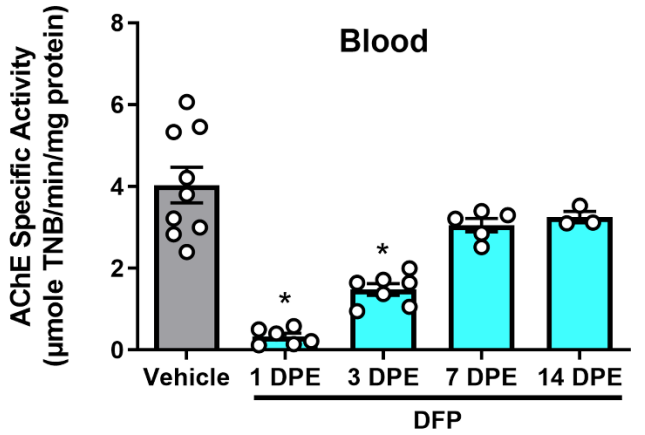
Blood
AChE Specific Activity
(µmole TNB/min/mg protein)
8
6
4
2
0
Vehicle
1 DPE
3 DPE
7 DPE
14 DPE
DFP

Figure 3.3. Acute DFP intoxication causes persistent inhibition of AChE activity in the brain and blood. Bars reflect the mean specific activity of AChE (± SEM) for VEH and DFP mice at each time point (n = 3-9 per time point). *Significantly different from VEH at $p < 0.05$ as determined by one-way ANOVA with Dunnett's multiple comparison test. DPE=days post-exposure.

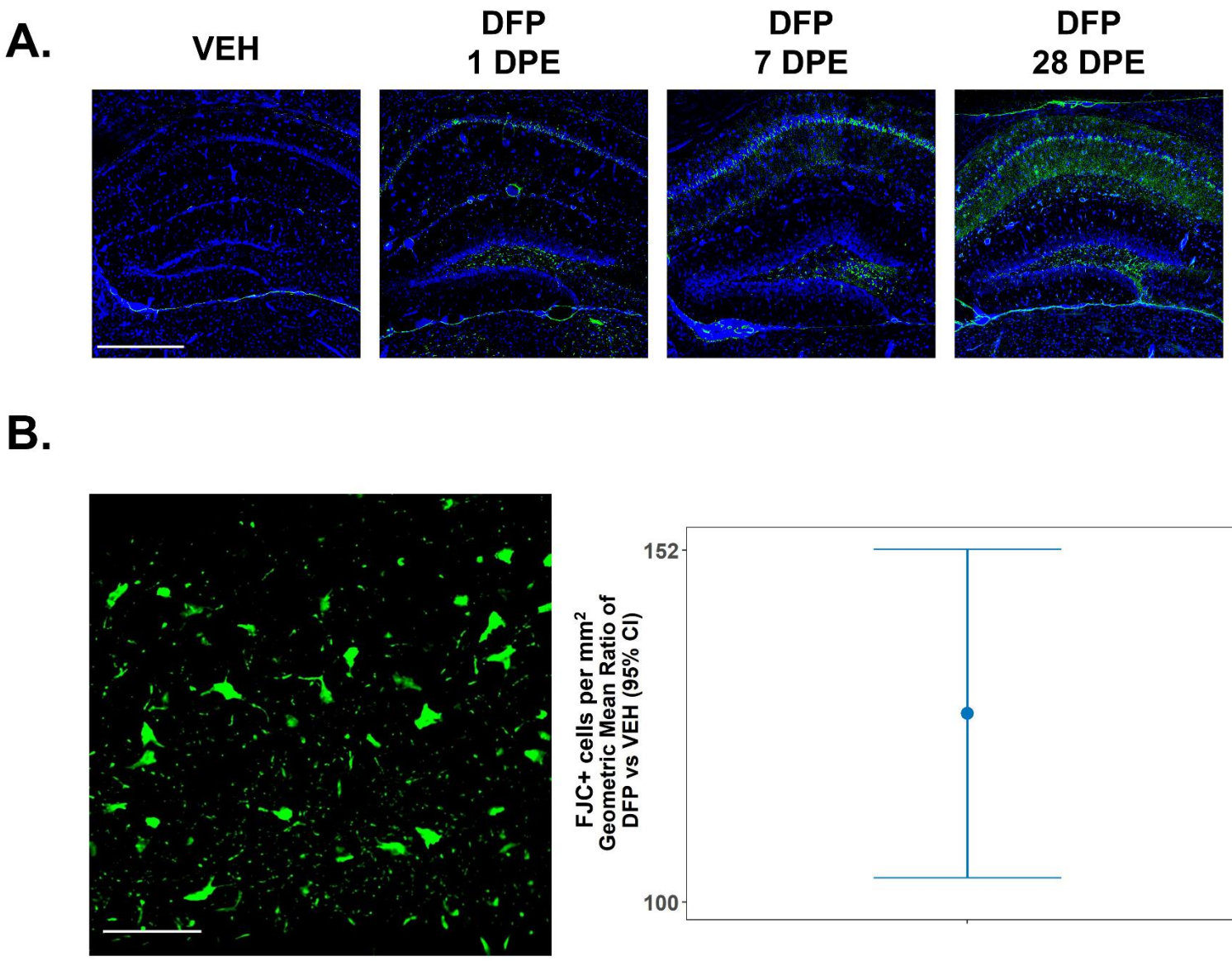
A.
VEH
DFP
1 DPE
DFP
7 DPE
DFP
28 DPE
B.
FJC+ cells per mm2
Geometric Mean Ratio of
DFP vs VEH (95% CI)
152
100

Figure 3.4. Acute DFP intoxication causes persistent neurodegeneration in multiple brain regions. (A) Representative photomicrographs of the hippocampus from VEH and DFP mice stained with FluoroJade C (FJC, green) and counterstained with DAPI (blue) to label all cell nuclei. Scale bar = 1mm. (B) Representative high magnification image of FJC+ neurons from the hippocampus of DFP mice at 7 DPE. Scale bar = 50 µm. Geometric mean ratio (dot) and 95% confidence interval (bars) of the number of FJC+ cells in the hippocampus, piriform cortex, and thalamus of DFP mice relative to VEH controls at 1, 7, and 28 DPE with 95% confidence intervals (bars). The y-axis is a log scale. Confidence intervals that do not include 1 indicate a significant difference between DFP and VEH groups. No statistically significant differences between region or days post-exposure (DPE) were found, so all brain regions and time points were collapsed. Individual data points used to generate this figure can be found in the supplemental material (Figure S2).

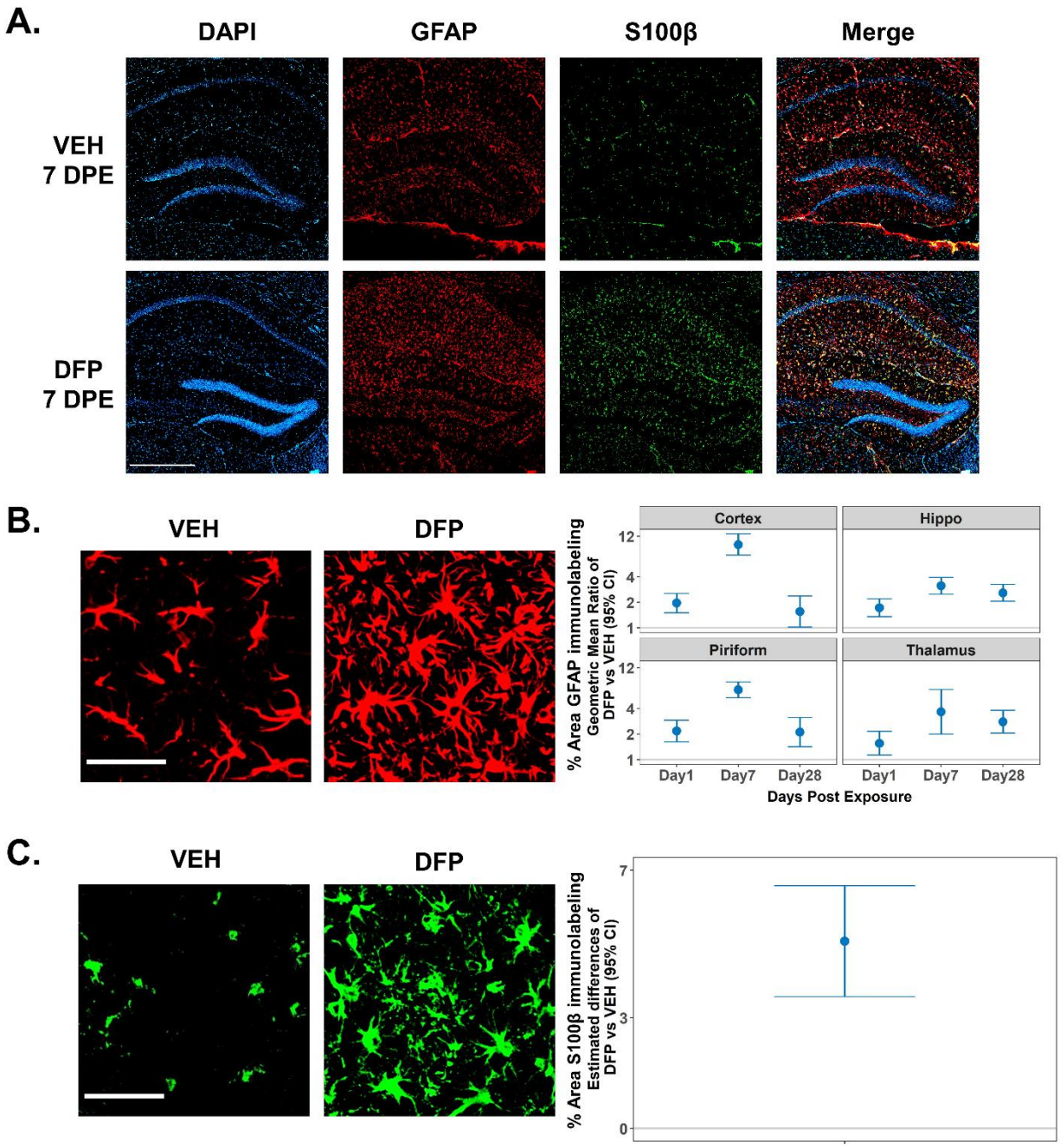
A.
DAPI
GFAP
S100β
Merge
VEH
7 DPE
DFP
7 DPE
B.
VEH
DFP
% Area GFAP immunolabeling
Geometric Mean Ratio of
DFP vs VEH (95% CI)
Cortex
Hippo
Piriform
Thalamus
12
4
2
1
Day1
Day7
Day28
Days Post Exposure
C.
VEH
DFP
% Area S100β immunolabeling
Estimated differences of
DFP vs VEH (95% CI)
7
3
0

Figure 3.5. DFP-induced SE caused persistent reactive astrogliosis in multiple brain regions. (A) Representative photomicrographs of the hippocampus 7 days after exposure to VEH or DFP. Coronal brain sections were immunolabeled GFAP (red) and S100β (green) to detect astrocytes, and counterstained with DAPI (blue) to detect nuclei. Scale bar = 1 mm. (B) Representative high magnification images of GFAP labeling in the hippocampus of VEH and DFP mice at 7 DPE. Scale bar = 500 µm. Geometric mean ratio (dot) of the percent area of GFAP immunoreactivity in the brain of DFP mice relative to VEH controls with 95% confidence intervals (bars) (n = 6-8 per group). The y-axis is a log scale. Confidence intervals that do not include 1 (identified as the gray line) indicate a significant difference between DFP and VEH groups. (C) Representative high magnification images of S100β labeling in the hippocampus of VEH and DFP mice at 7 DPE. Scale bar = 500 µm. Estimated difference (dot) of the percent area of positive S100β immunolabeling in the brain of DFP mice relative to VEH controls with 95% confidence intervals (bars) (n = 6-8 per group). Confidence intervals that do not include 0 (identified as the gray line) indicate a significant difference between DFP and VEH groups. No statistically significant differences were identified between brain regions (cortex, hippocampus, thalamus, and piriform cortex) or days post-exposure (1, 7, and 28 days), so data from all brain regions and time points were collapsed. Individual data points used to generate this figure can be found in the supplemental material (Figure S3)

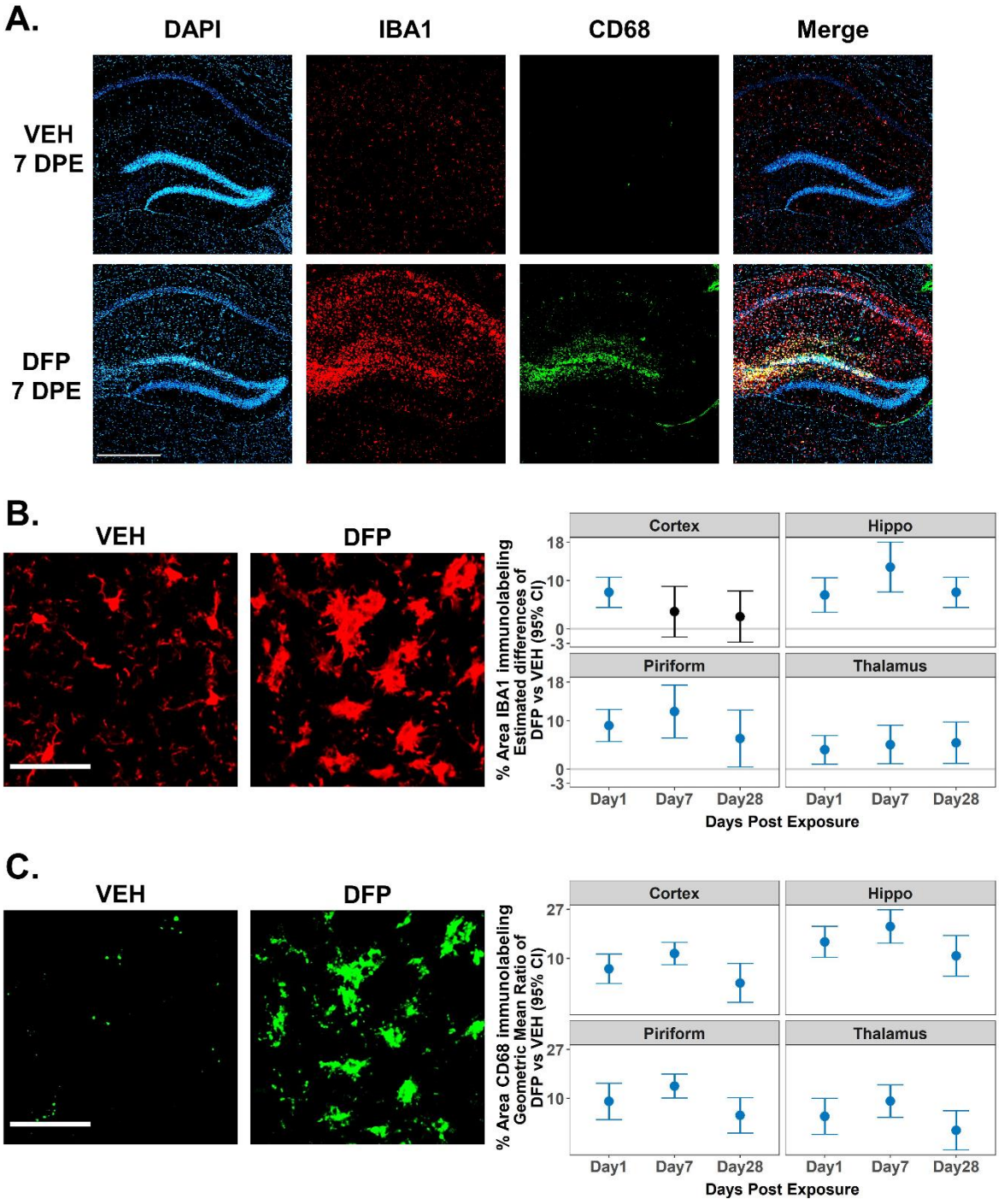
A.
DAPI
IBA1
CD68
Merge
VEH
7 DPE
DFP
7 DPE
B.
VEH
DFP
Cortex
Hippo
Piriform
Thalamus
% Area IBA1 immunolabeling
Estimated differences of
DFP vs VEH (95% CI)
18
10
0
-3
Day1
Day7
Day28
Days Post Exposure
C.
VEH
DFP
Cortex
Hippo
Piriform
Thalamus
% Area CD68 immunolabeling
Geometric Mean Ratio of
DFP vs VEH (95% CI)
27
10
Day1
Day7
Day28
Days Post Exposure

Figure 3.6. DFP-induced SE caused persistent microgliosis. (A) Representative photomicrographs of the hippocampus 7 days after injection with VEH or DFP. Coronal brain sections were immunolabeled with IBA1 to detect microglia, and CD68 to detect phagocytic cells and counterstained with DAPI to detect nuclei. Bar = 1 mm. (B) Representative high magnification image of IBA1 immunoreactivity in the hippocampus of VEH and DFP mice at 7 DPE. Scale bar = 500 µm. Estimated difference (dot) of the percent area of IBA1 immunolabeling in DFP mice relative to VEH controls with 95% confidence intervals (bars) (n = 6-8 per group). Confidence intervals that do not include 0 (identified as the gray line) indicate a significant difference between DFP and VEH groups (colored blue). (C) Representative high magnification image of CD68 immunolabeling in the hippocampus of VEH and DFP mice at 7 DPE. Scale bar = 500 µm. Geometric mean ratio (dot) of the percent area of positive CD68 immunolabeling in DFP mice relative to VEH controls with 95% confidence intervals (bars) (n = 6-8 per group). The y-axis is a log scale. Confidence intervals that are above and do not include 1 indicate a significant difference between DFP and VEH groups. Individual data points used to generate this figure are provided in the supplemental material (Figure S4).

A. GFAP/S100β colocalization

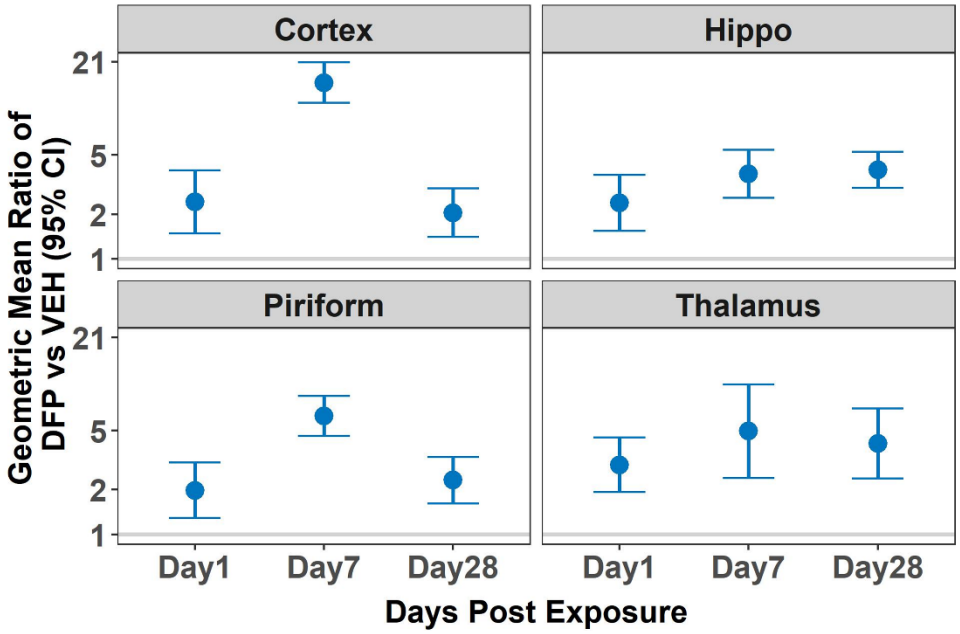

B. IBA1/CD68 colocalization

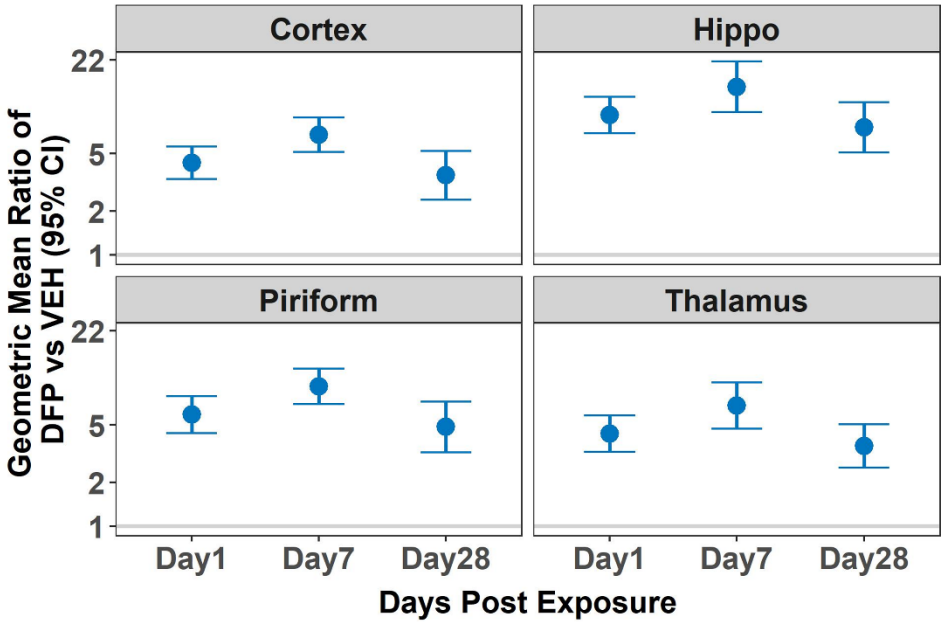

Figure 3.7. Quantitative analyses of the colocalization of biomarkers for astrocytes (GFAP and S100β) and microglia (IBA1 and CD68). (A) Geometric mean ratio (dot) of the percent area of positive GFAP and positive S100β immunolabeling in the brain regions of DFP mice relative to VEH controls with 95% confidence intervals (bars) (n = 6-8 per group). (B) Geometric mean ratio (dot) of the percent area of co-labeling for IBA1 and positive CD68 immunoreactivity in DFP mice relative to VEH controls with 95% confidence intervals (bars) (n = 6-8 per group). In both panels, the y-axis is a log scale. Confidence intervals that do not include 1 (identified as the gray line) indicate a significant difference between DFP and VEH groups. Individual data points used to generate this figure can be found in the supplemental material (Figures S2 and S3).

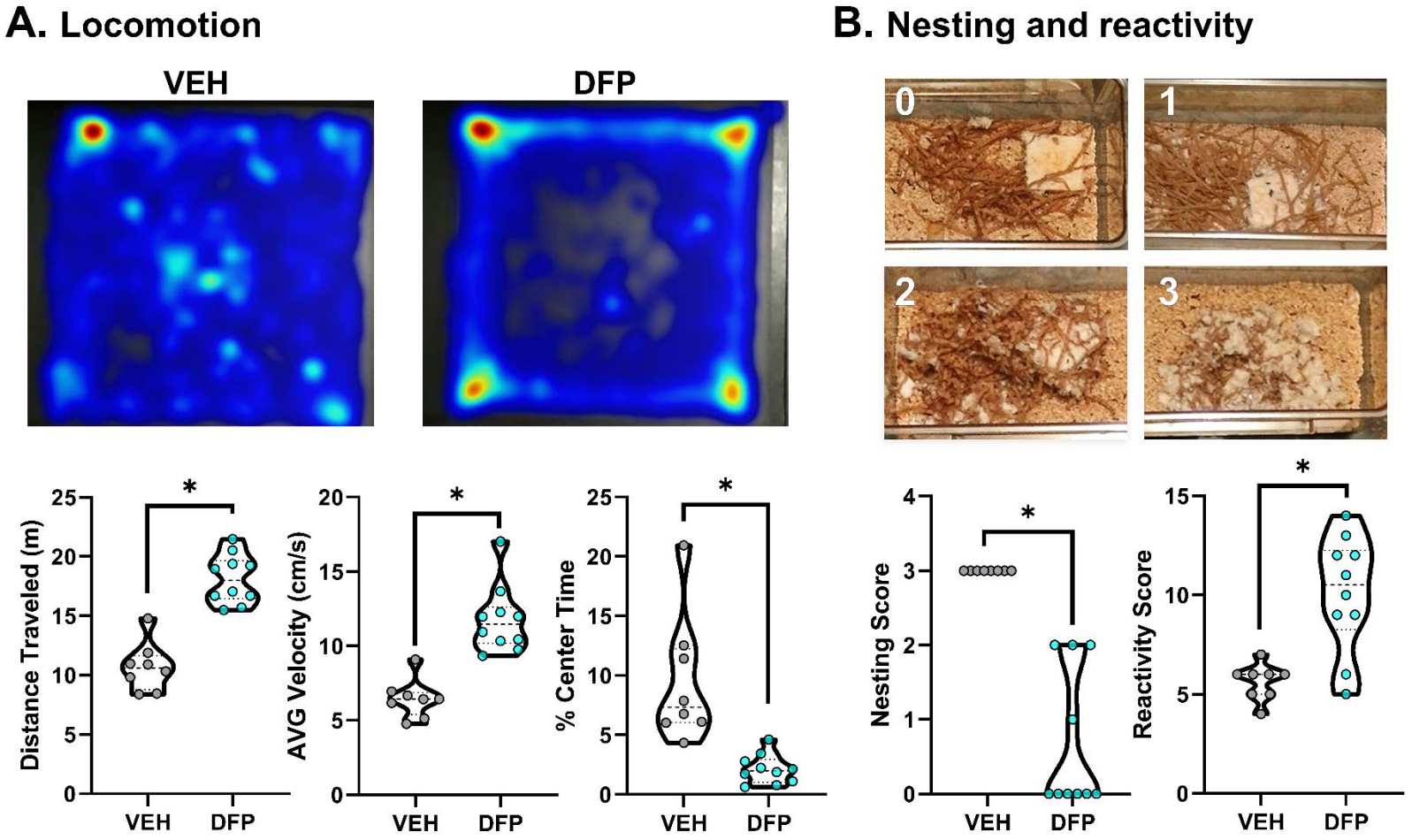
A. Locomotion
VEH
DFP
Distance Traveled (m)
AVG Velocity (cm/s)
% Center Time
B. Nesting and reactivity
0
1
2
3
Nesting Score
Reactivity Score
VEH
DFP
*

Figure 3.8. Behavioral assessments of locomotion, reactivity, and nesting at 28 d post-exposure. (A) Representative heat maps generated from 30 min in the open field assessment for a VEH and DFP mouse. Open field distance traveled (m), velocity (cm/s), and percent time spent in arena center during 30 min isolation in an open field arena. Violin plots represent the median and quartiles for distance traveled, average velocity, and percent time in center zone for VEH and DFP mice with each dot representing an individual animal (n = 8-10 per group). *Significantly different at $p < 0.0001$ as determined by an unpaired two-tailed t-test. (B) Representative images of the nesting pads illustrating each nesting score. Reactivity and nesting scores for VEH and DFP mice, with violin plots representing the median and quartiles and each dot representing an individual animal (n = 8-10 per group). *Significantly different at $p < 0.005$ as determined by an unpaired two-tailed t-test.

Table 1. Current mouse models of organophosphate-induced seizures

Mouse Strain	OP	Exposure Paradigm	SE	OP-induced Neuropathology	Brain Regions	OP-induced Deficits	Citation
Male C57 (8-10 weeks)	***DFP***	***DFP (9.5 mg/kg, s.c.) AS (0.1 mg/kg, i.m.) 1 min post 2-PAM (25 mg/kg, i.m.) 1 min post***	***>4 h***	***↑ FJC at 1, 7, 28 DPE ↑ Astrogliosis at 1, 7, 28 DPE ↑ Microgliosis at 1, 7, 28 DPE***	***SS cortex Hippocampus Thalamus Piriform***	***↑ Locomotor ↑ Reactivity ↑ Anxiety ↑ Weight loss ↓ Nesting***	***Current study***
Male NIH (8 weeks)	DFP	DFP (9.93 mg/kg, s.c.) AS (3 mg/kg, i.p.) 1 min post-DFP HI-6 (50 mg/kg, i.p.) 1 min post-DFP DZP (10 mg/kg, i.p.) 80 min post-DFP	1 h	↑ astrogliosis at 1, 3 DPE ↑ microgliosis at 1, 3 DPE	CA1 CA3 DG	N/A	(Maupu, Enderlin et al. 2021)
Male NIH (7-8 weeks)	DFP	DFP (9.93 mg/kg, s.c.) AS (3 mg/kg, i.p.) 1 min post-DFP HI-6 (50 mg/kg, i.p.) 1 min post-DFP	≤11 h	↑ c-Fos at 1 HPE ↑ FJC at 1 DPE	CA1 CA3 DG	↑ ECoG	(Enderlin, Igert et al. 2020)
Male C57 (8-10 weeks)	Paraoxon	Paraoxon (0.5 mg/kg, s.c.) AS (1.5 mg/kg, i.p.) 4 min post-PXN Obidoxime (20 mg/kg, i.p.) 4 min post-PXN	>1 h	↑ thrombin activity at 10 min ↑ pERK/ERK2 levels at 10 min ↑ PAR-1/actin ratio at 30 min	CA1 CA3	↑ spike amplitude ↑ spontaneous activity (hippocampal slice)	(Golderman, Shavit-Stein et al. 2019)
Male C57 (12-13 weeks)	Soman	HI-6 (50 mg/kg, i.p.) 5 min pre-soman Soman (172 µg/kg, s.c.) AMN (0.5 mg/kg, i.p.) 1 min post-soman DZP (5 mg/kg, i.p.) 2 h post-soman	>2 h	↑ histopathological lesions at 43 DPE	amygdala CA1 DG piriform	↑ Mortality ↑ SRS	(McCarren, Eisen et al. 2020)
Male NIH (weight=30 g)	Soman	HI-6 (50 mg/kg, i.p.) 5 min pre-soman Soman (172 µg/kg, s.c.) AS (10 mg/kg, i.p.) 30 or 60 min post-soman KET (25 mg/kg, i.p.) 30 or 60 min post-soman	≤1 h	↑ astrogliosis at 2, 7 DPE ↑ microgliosis at 2, 7 DPE	lateral septum piriform amygdala CA1 CA3	↑ Mortality ↑ Weight loss	(Dhote, Carpentier et al. 2012)
Male B6D (9 weeks)	Soman	Soman (110 µg/kg, s.c.) AMN (5 mg/kg, i.p.) 1 min post-soman	≥2 h	↑ neuronal death at 1, 30 DPE	amygdala	↑ Anxiety ↑ Fear Conditioning	(Collombet, Pierard et al. 2008, Coubard, Beracochea et al. 2008)
Male NIH (weight=30 g)	Soman	HI-6 (50 mg/kg, i.p.) 5 min pre-soman Soman (172 µg/kg, s.c.)	>3 h	↑ inflammatory gene levels up to 7 DPE	cortex hippocampus cerebellum	N/A	(Dhote, Peinnequin et al. 2007)

2PAM=2-pralidoxime; AMN=atropine methyl nitrate; AS=atropine sulfate; B6D=B6D2F1/j@rj; C57=C57BL/6; DFP = diisopropylfluorophosphate; DG=dentate gyrus; DPE=days post exposure; DZP=diazepam; EcoG= electrocorticography; FJC=fluoro jade C; HPE=hours post exposure; i.m.=intramuscular; i.p.=intraperitoneal; KET=ketamine; N/A=not applicable; NIH=NIH Swiss; OP=organophosphate; PXN = paraoxon; s.c.=subcutaneous; SE=*status epilepticus*; SRS=spontaneous recurrent seizures.

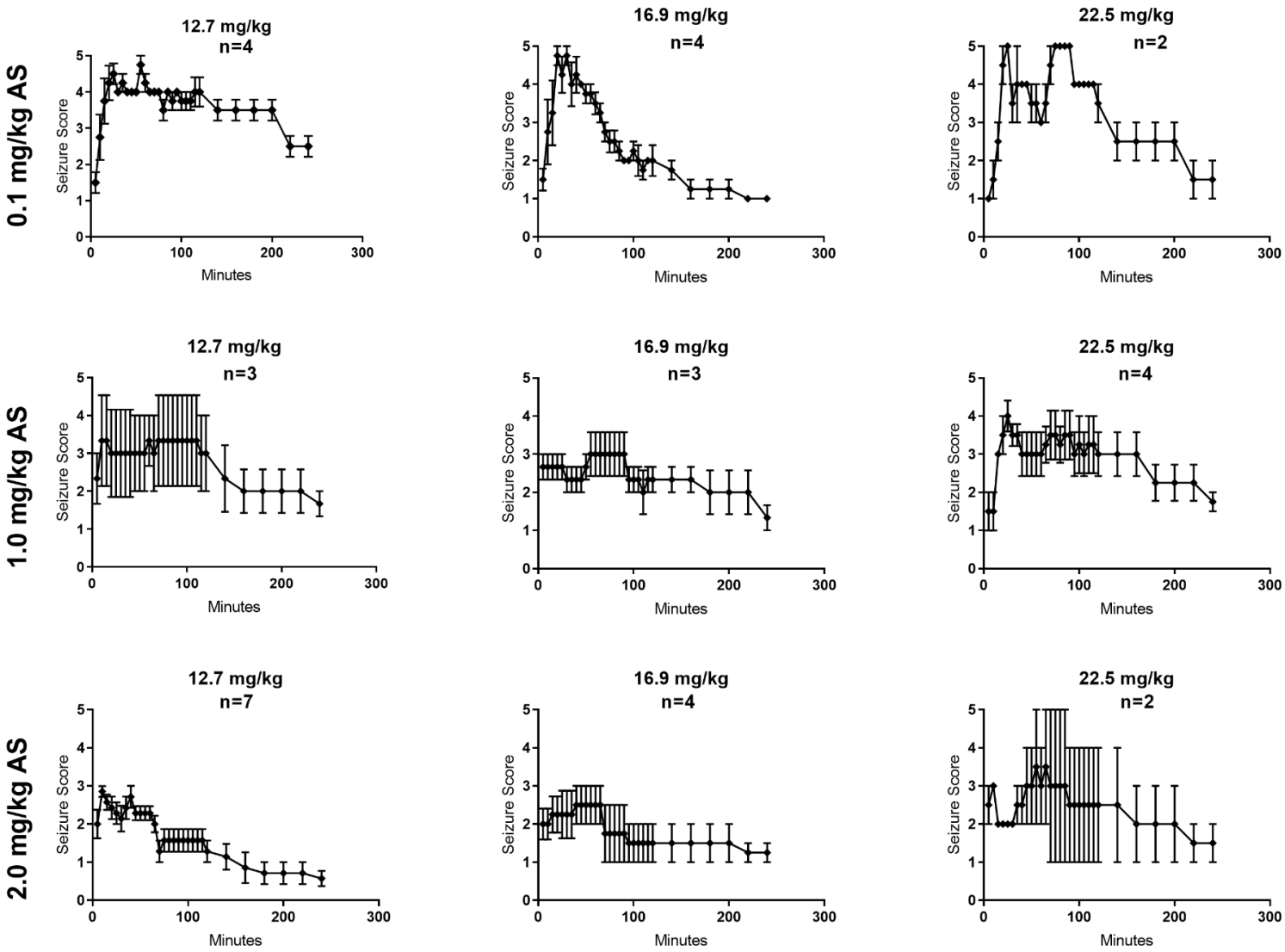
0.1 mg/kg AS
1.0 mg/kg AS
2.0 mg/kg AS
12.7 mg/kg
n=4
16.9 mg/kg
n=4
22.5 mg/kg
n=2
12.7 mg/kg
n=3
16.9 mg/kg
n=3
22.5 mg/kg
n=4
12.7 mg/kg
n=7
16.9 mg/kg
n=4
22.5 mg/kg
n=2
Seizure Score
Minutes
0
1
2
3
4
5
0
100
200
300

Figure S1. Seizure scores from preliminary dose-finding experiments for mice in this study. A range of diisopropylfluorophosphate (DFP) doses was used to produce continuous seizures in DFP-exposed mice (12.7, 16.9, or 22.5 mg/kg, s.c.). A range of atropine sulfate (AS) doses (0.1, 1.0, or 2.0 mg/kg, i.m.) were compared to determine which dose to use for DFP-exposed mice. Data points represent the mean seizure score (± SEM) for each treatment group at each time point (n = 2-7 mice/group).

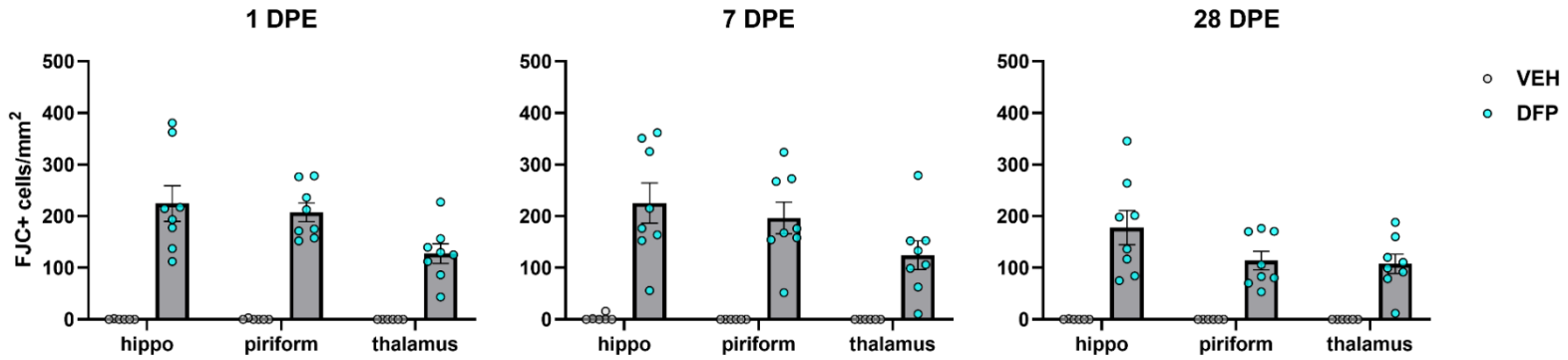
1 DPE
7 DPE
28 DPE
FJC+ cells/mm2
500
400
300
200
100
0
hippo
piriform
thalamus
VEH
DFP

Figure S2. Acute DFP intoxication causes robust FJC staining at 1, 7, and 28 days post-exposure (DPE) in the hippocampus, piriform cortex, and thalamus of DFP-treated mice relative to VEH controls (n=6-8 per group). Bars represent the mean ± SEM of positively labeled FJC cells per square millimeter of brain tissue. hippo=hippocampus; piriform=piriform cortex.

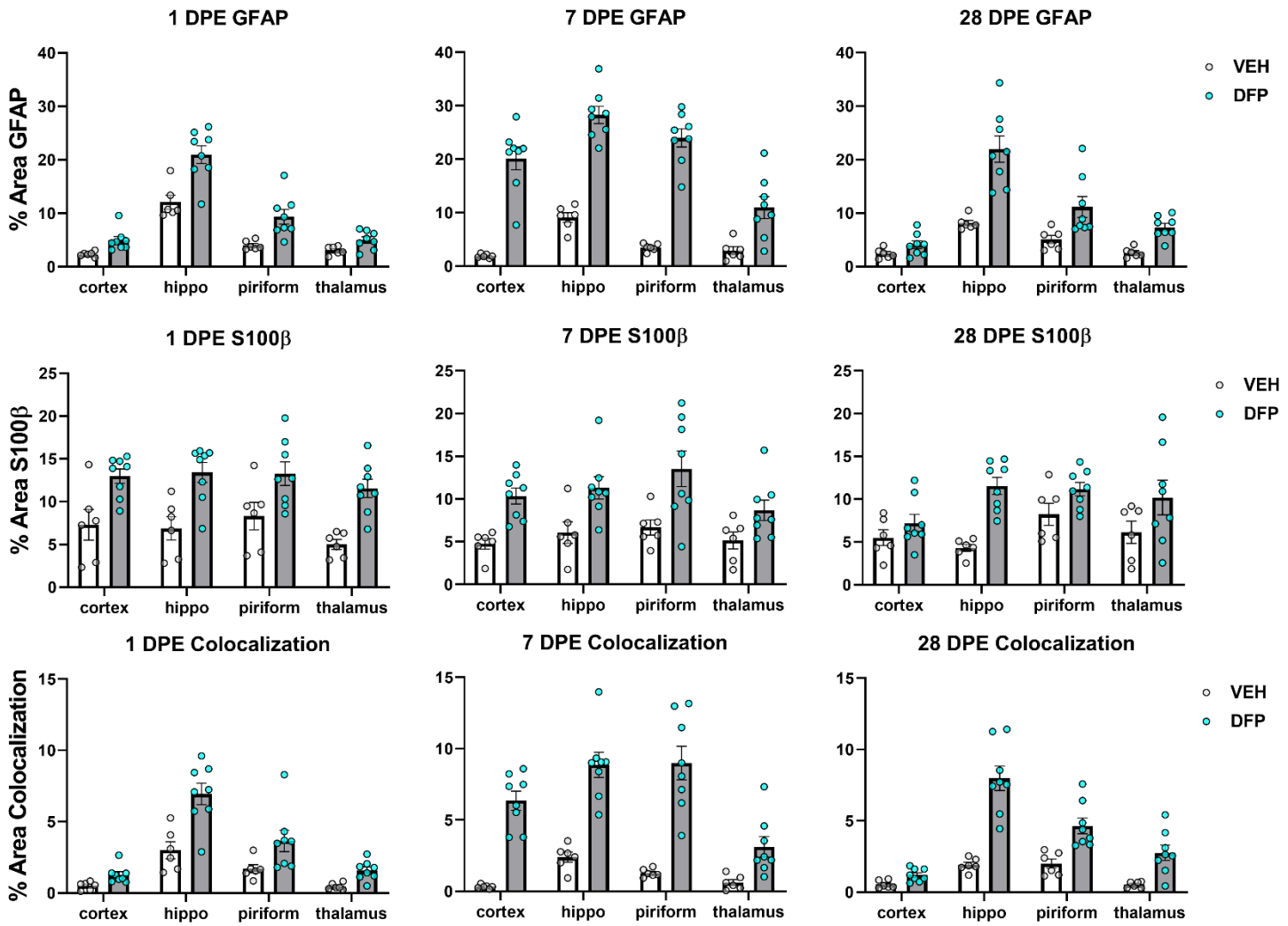
1 DPE GFAP
7 DPE GFAP
28 DPE GFAP
% Area GFAP
1 DPE S100β
7 DPE S100β
28 DPE S100β
% Area S100β
1 DPE Colocalization
7 DPE Colocalization
28 DPE Colocalization
% Area Colocalization
cortex
hippo
piriform
thalamus
VEH
DFP

Figure S3. Individual data points of GFAP and S100β immunolabeling in this study. Percent of the area of brain region immunolabeled with GFAP, S100β, and colocalization of these markers at 1, 7, and 28 d after injection with VEH or DFP. Bars represent the mean percent area ± SEM for each brain region by treatment group (n=6-8 per group). DPE=days post-exposure, cortex= somatosensory cortex, hippo=hippocampus, piriform=piriform cortex.

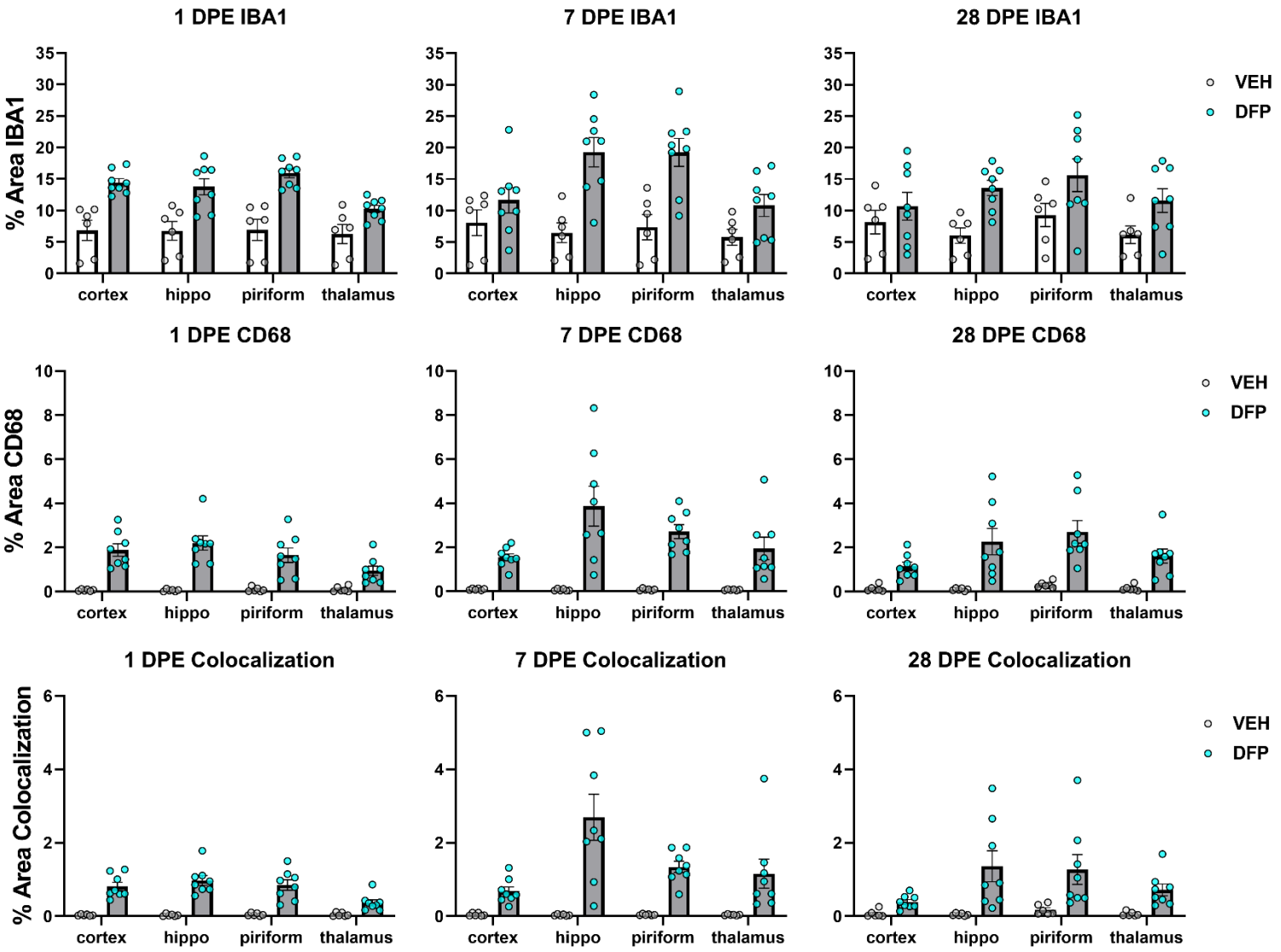
1 DPE IBA1
7 DPE IBA1
28 DPE IBA1
% Area IBA1
1 DPE CD68
7 DPE CD68
28 DPE CD68
% Area CD68
1 DPE Colocalization
7 DPE Colocalization
28 DPE Colocalization
% Area Colocalization
cortex
hippo
piriform
thalamus
VEH
DFP

Figure S4. Percent area of IBA and CD68 immunoreactivity in specific brain regions at 1, 7, and 28 d after injection with VEH or DFP. Bars represent the mean percent area ± SEM for each brain region by treatment group (n=6-8 per group). cortex= somatosensory cortex; DPE=days post-exposure; hippo=hippocampus, piriform=piriform cortex.

References

Adeyinka, A., E. Muco and L. Pierre (2020). Organophosphates, StatPearls Publishing, Treasure Island (FL).

Aroniadou-Anderjaska, V., T. H. Figueiredo, J. P. Apland and M. F. Braga (2020). "Targeting the glutamatergic system to counteract organophosphate poisoning: A novel therapeutic strategy." Neurobiol Dis **133**: 104406.

Brewer, K. L., M. M. Troendle, L. Pekman and W. J. Meggs (2013). "Naltrexone prevents delayed encephalopathy in rats poisoned with the sarin analogue diisopropylflurophosphate." Am J Emerg Med **31**(4): 676-679.

Chai, P. R., B. D. Hayes, T. B. Erickson and E. W. Boyer (2018). "Novichok agents: a historical, current, and toxicological perspective." Toxicology communications **2**(1): 45-48.

Chen, Y. (2012). "Organophosphate-induced brain damage: mechanisms, neuropsychiatric and neurological consequences, and potential therapeutic strategies." Neurotoxicology **33**(3): 391-400.

Collombet, J. M., C. Pierard, D. Beracochea, S. Coubard, M. F. Burckhart, E. Four, C. Masqueliez, D. Baubichon and G. Lallement (2008). "Long-term consequences of soman poisoning in mice Part 1. Neuropathology and neuronal regeneration in the amygdala." Behav Brain Res **191**(1): 88-94.

Correll, L. and M. Ehrich (1991). "A microassay method for neurotoxic esterase determinations." Fundam Appl Toxicol **16**(1): 110-116.

Coubard, S., D. Beracochea, J. M. Collombet, J. N. Philippin, A. Krazem, P. Liscia, G. Lallement and C. Pierard (2008). "Long-term consequences of soman poisoning in mice: part 2. Emotional behavior." Behav Brain Res **191**(1): 95-103.

Deacon, R. M. (2006). "Assessing nest building in mice." Nature protocols **1**(3): 1117-1119.

Deshpande, L. S., D. S. Carter, R. E. Blair and R. J. DeLorenzo (2010). "Development of a prolonged calcium plateau in hippocampal neurons in rats surviving status epilepticus induced by the organophosphate diisopropylfluorophosphate." Toxicological sciences **116**(2): 623-631.

Dhote, F., P. Carpentier, L. Barbier, A. Peinnequin, V. Baille, F. Pernot, G. Testylier, C. Beaup, A. Foquin and F. Dorandeu (2012). "Combinations of ketamine and atropine are neuroprotective and reduce neuroinflammation after a toxic status epilepticus in mice." Toxicol Appl Pharmacol **259**(2): 195-209.

Dhote, F., A. Peinnequin, P. Carpentier, V. Baille, C. Delacour, A. Foquin, G. Lallement and F. Dorandeu (2007). "Prolonged inflammatory gene response following soman-induced seizures in mice." Toxicology **238**(2-3): 166-176.

Eddleston, M., N. A. Buckley, P. Eyer and A. H. Dawson (2008). "Management of acute organophosphorus pesticide poisoning." The Lancet **371**(9612): 597-607.

Ellman, G. L., K. D. Courtney, V. Andres and R. M. Featherstone (1961). "A new and rapid colorimetric determination of acetylcholinesterase activity." Biochemical Pharmacology **7**(2): 88-95.

Enderlin, J., A. Igert, S. Auvin, F. Nachon, G. Dal Bo and N. Dupuis (2020). "Characterization of organophosphate-induced brain injuries in a convulsive mouse model of diisopropylfluorophosphate exposure." Epilepsia **61**(6): e54-e59.

Eng, L. F. and R. S. Ghirnikar (1994). "GFAP and astrogliosis." Brain Pathol **4**(3): 229-237.

Ferchmin, P., M. Andino, R. R. Salaman, J. Alves, J. Velez-Roman, B. Cuadrado, M. Carrasco, W. Torres-Rivera, A. Segarra and A. H. Martins (2014). "4R-cembranoid protects against diisopropylfluorophosphate-mediated neurodegeneration." Neurotoxicology **44**: 80-90.

Figueiredo, T. H., J. P. Apland, M. F. Braga and A. M. Marini (2018). "Acute and long-term consequences of exposure to organophosphate nerve agents in humans." Epilepsia **59**: 92-99.

Flannery, B. M., D. A. Bruun, D. J. Rowland, C. N. Banks, A. T. Austin, D. L. Kukis, Y. Li, B. D. Ford, D. J. Tancredi, J. L. Silverman, S. R. Cherry and P. J. Lein (2016). "Persistent neuroinflammation and cognitive impairment in a rat model of acute diisopropylfluorophosphate intoxication." J Neuroinflammation **13**(1): 267.

Gao, J., S. X. Naughton, H. Wulff, V. Singh, W. D. Beck, J. Magrane, B. Thomas, N. A. Kaidery, C. M. Hernandez and A. V. Terry (2016). "Diisopropylfluorophosphate impairs the transport of membrane-bound organelles in rat cortical axons." Journal of Pharmacology and Experimental Therapeutics **356**(3): 645-655.

Golderman, V., E. Shavit-Stein, O. Gera, J. Chapman, A. Eisenkraft and N. Maggio (2019). "Thrombin and the Protease-Activated Receptor-1 in Organophosphate-Induced Status Epilepticus." J Mol Neurosci **67**(2): 227-234.

Gonçalves, C.-A., M. Concli Leite and P. Nardin (2008). "Biological and methodological features of the measurement of S100B, a putative marker of brain injury." Clinical Biochemistry **41**(10): 755-763.

González, E. A., A. C. Rindy, M. A. Guignet, J. J. Calsbeek, D. A. Bruun, A. Dhir, P. Andrew, N. Saito, D. J. Rowland and D. J. Harvey (2020). "The chemical convulsant diisopropylfluorophosphate (DFP) causes persistent neuropathology in adult male rats independent of seizure activity." Archives of toxicology **94**(6): 2149-2162.

Guignet, M., K. Dhakal, B. M. Flannery, B. A. Hobson, D. Zolkowska, A. Dhir, D. A. Bruun, S. Li, A. Wahab, D. J. Harvey, J. L. Silverman, M. A. Rogawski and P. J. Lein (2020). "Persistent behavior deficits, neuroinflammation, and oxidative stress in a rat model of acute organophosphate intoxication." Neurobiol Dis **133**: 104431.

Haley, N. (2018). "Remarks at an Emergency UN Security Council Briefing on Chemical Weapons Use by Russia in the United Kingdom." United States Mission to the United Nations.

Harrison, V. and S. M. Ross (2016). "Anxiety and depression following cumulative low-level exposure to organophosphate pesticides." Environmental research **151**: 528-536.

Hendrickx, D. A., C. G. van Eden, K. G. Schuurman, J. Hamann and I. Huitinga (2017). "Staining of HLA-DR, Iba1 and CD68 in human microglia reveals partially overlapping expression depending on cellular morphology and pathology." Journal of neuroimmunology **309**: 12-22.

Hobson, B. A., D. J. Rowland, S. Siso, M. A. Guignet, Z. T. Harmany, S. B. Bandara, N. Saito, D. J. Harvey, D. A. Bruun, J. R. Garbow, A. J. Chaudhari and P. J. Lein (2019). "TSPO PET Using [18F]PBR111 Reveals Persistent Neuroinflammation Following Acute Diisopropylfluorophosphate Intoxication in the Rat." Toxicol Sci **170**(2): 330-344.

HRW. (2021). "The Syrian Government's Widespread and Systematic Use of Chemical Weapons." from https://www.hrw.org/report/2017/05/01/death-chemicals/syrian-governments-widespread-and-systematic-use-chemical-weapons.

Hulse, E. J., J. O. Davies, A. J. Simpson, A. M. Sciuto and M. Eddleston (2014). "Respiratory complications of organophosphorus nerve agent and insecticide poisoning. Implications for respiratory and critical care." American journal of respiratory and critical care medicine **190**(12): 1342-1354.

Ito, D., Y. Imai, K. Ohsawa, K. Nakajima, Y. Fukuuchi and S. Kohsaka (1998). "Microglia-specific localisation of a novel calcium binding protein, Iba1." Molecular brain research **57**(1): 1-9.

Jett, D. A., C. A. Sibrizzi, R. B. Blain, P. A. Hartman, P. J. Lein, K. W. Taylor and A. A. Rooney (2020). "A national toxicology program systematic review of the evidence for long-term effects after acute exposure to sarin nerve agent." Crit Rev Toxicol **50**(6): 474-490.

Jett, D. A. and S. M. Spriggs (2020). "Translational research on chemical nerve agents." Neurobiology of disease **133**: 104335.

Jiang, J., Y. Quan, T. Ganesh, W. A. Pouliot, F. E. Dudek and R. Dingledine (2013). "Inhibition of the prostaglandin receptor EP2 following status epilepticus reduces delayed mortality and brain inflammation." Proceedings of the National Academy of Sciences **110**(9): 3591-3596.

Jiang, J., M.-s. Yang, Y. Quan, P. Gueorguieva, T. Ganesh and R. Dingledine (2015). "Therapeutic window for cyclooxygenase-2 related anti-inflammatory therapy after status epilepticus." Neurobiology of disease **76**: 126-136.

Jiang, J., Y. Yu, E. R. Kinjo, Y. Du, H. P. Nguyen and R. Dingledine (2019). "Suppressing pro-inflammatory prostaglandin signaling attenuates excitotoxicity-associated neuronal inflammation and injury." Neuropharmacology **149**: 149-160.

Krishnan, A., H. Wu and V. Venkataraman (2020). "Astrocytic S100B, Blood-Brain Barrier and Neurodegenerative Diseases." Glia Health Dis.

Levin, H. S., R. L. Rodnitzky and D. L. Mick (1976). "Anxiety associated with exposure to organophosphate compounds." Archives of General Psychiatry **33**(2): 225-228.

Li, D., X. Liu, T. Liu, H. Liu, L. Tong, S. Jia and Y. F. Wang (2020). "Neurochemical regulation of the expression and function of glial fibrillary acidic protein in astrocytes." Glia **68**(5): 878-897.

Li, Y., P. J. Lein, C. Liu, D. A. Bruun, T. Tewolde, G. Ford and B. D. Ford (2011). "Spatiotemporal pattern of neuronal injury induced by DFP in rats: a model for delayed neuronal cell death following acute OP intoxication." Toxicol Appl Pharmacol **253**(3): 261-269.

Liang, K.-G., R.-Z. Mu, Y. Liu, D. Jiang, T.-T. Jia and Y.-J. Huang (2019). "Increased serum S100B levels in patients with epilepsy: a systematic review and meta-analysis study." Frontiers in neuroscience **13**: 456.

Liddelow, S. A., K. A. Guttenplan, L. E. Clarke, F. C. Bennett, C. J. Bohlen, L. Schirmer, M. L. Bennett, A. E. Münch, W.-S. Chung and T. C. Peterson (2017). "Neurotoxic reactive astrocytes are induced by activated microglia." Nature **541**(7638): 481-487.

Liu, C., Y. Li, P. J. Lein and B. D. Ford (2012). "Spatiotemporal patterns of GFAP upregulation in rat brain following acute intoxication with diisopropylfluorophosphate (DFP)." Current neurobiology **3**(2): 90.

Lotti, M., S. Caroldi, A. Moretto, M. K. Johnson, C. J. Fish, C. Gopinath and N. L. Roberts (1987). "Central-peripheral delayed neuropathy caused by diisopropyl phosphorofluoridate (DFP): segregation of peripheral nerve and spinal cord effects using biochemical, clinical, and morphological criteria." Toxicol Appl Pharmacol **88**(1): 87-96.

Lumley, L., D. Miller, W. T. Muse, B. Marrero-Rosado, M. de Araujo Furtado, M. Stone, J. McGuire and C. Whalley (2019). "Neurosteroid and benzodiazepine combination therapy reduces status epilepticus and long-term effects of whole-body sarin exposure in rats." Epilepsia open **4**(3): 382-396.

Marrero-Rosado, B. M., M. de Araujo Furtado, E. R. Kundrick, K. A. Walker, M. F. Stone, C. R. Schultz, D. A. Nguyen and L. A. Lumley (2020). "Ketamine as adjunct to midazolam treatment following soman-induced status epilepticus reduces seizure severity, epileptogenesis, and brain pathology in plasma carboxylesterase knockout mice." Epilepsy & Behavior **111**: 107229.

Masson, P. (2011). "Evolution of and perspectives on therapeutic approaches to nerve agent poisoning." Toxicology letters **206**(1): 5-13.

Maupu, C., J. Enderlin, A. Igert, M. Oger, S. Auvin, R. Hassan-Abdi, N. Soussi-Yanicostas, X. Brazzolotto, F. Nachon, G. Dal Bo and N. Dupuis (2021). "Diisopropylfluorophosphate-induced

status epilepticus drives complex glial cell phenotypes in adult male mice." Neurobiol Dis **152**: 105276.

McCarren, H. S., M. R. Eisen, D. L. Nguyen, P. B. Dubee, C. E. Ardinger, E. N. Dunn, K. M. Haines, A. N. Santoro, P. M. Bodner, C. A. Ondeck, C. L. Honnold, J. H. McDonough, P. H. Beske and P. M. McNutt (2020). "Characterization and treatment of spontaneous recurrent seizures following nerve agent-induced status epilepticus in mice." Epilepsy Res **162**: 106320.

McDonough, J. H., L. D. Zoeffel, J. McMonagle, T. L. Copeland, C. D. Smith and T.-M. Shih (1999). "Anticonvulsant treatment of nerve agent seizures: anticholinergics versus diazepam in soman-intoxicated guinea pigs." Epilepsy Research **38**(1): 1-14.

Munro, N. (1994). "Toxicity of the organophosphate chemical warfare agents GA, GB, and VX: implications for public protection." Environmental health perspectives **102**(1): 18-37.

Okumura, T., T. Hisaoka, T. Naito, H. Isonuma, S. Okumura, K. Miura, H. Maekawa, S. Ishimatsu, N. Takasu and K. Suzuki (2005). "Acute and chronic effects of sarin exposure from the Tokyo subway incident." Environmental toxicology and pharmacology **19**(3): 447-450.

OPCW (2018). Statement by h.e. ambassador Ahmad Nazri Yusof permanent representative of malaysia to the OPCW at the eighty-seventh session of the executive council

OPCW. (2020). "OPCW Issues Report on Technical Assistance Requested by Germany; Alexei Navalny." from https://www.opcw.org/media-centre/news/2020/10/opcw-issues-report-technical-assistance-requested-germany.

Oris, C., B. Pereira, J. Durif, J. Simon-Pimmel, C. Castellani, S. Manzano, V. Sapin and D. Bouvier (2018). "The Biomarker S100B and Mild Traumatic Brain Injury: A Meta-analysis." Pediatrics **141**(6).

Pessah, I. N., M. A. Rogawski, D. J. Tancredi, H. Wulff, D. Zolkowska, D. A. Bruun, B. D. Hammock and P. J. Lein (2016). "Models to identify treatments for the acute and persistent effects of seizure-inducing chemical threat agents." Annals of the New York Academy of Sciences **1378**(1): 124.

Pouliot, W., S. Bealer, B. Roach and F. Dudek (2016). "A rodent model of human organophosphate exposure producing status epilepticus and neuropathology." Neurotoxicology **56**: 196-203.

Prut, L. and C. Belzung (2003). "The open field as a paradigm to measure the effects of drugs on anxiety-like behaviors: a review." Eur J Pharmacol **463**(1-3): 3-33.

Raffaele, K., D. Hughey, G. Wenk, D. Olton, H. Modrow and J. McDonough (1987). "Long-term behavioral changes in rats following organophosphonate exposure." Pharmacology Biochemistry and Behavior **27**(3): 407-412.

Raponi, E., F. Agenes, C. Delphin, N. Assard, J. Baudier, C. Legraverend and J.-C. Deloulme (2007). "S100B expression defines a state in which GFAP-expressing cells lose their neural stem cell potential and acquire a more mature developmental stage." Glia **55**(2): 165-177.

Rojas, A., T. Ganesh, N. Lelutiu, P. Gueorguieva and R. Dingledine (2015). "Inhibition of the prostaglandin EP2 receptor is neuroprotective and accelerates functional recovery in a rat model of organophosphorus induced status epilepticus." Neuropharmacology **93**: 15-27.

Rojas, A., H. S. McCarren, J. Wang, W. Wang, J. Abreu-Melon, S. Wang, J. H. McDonough and R. Dingledine (2021). "Comparison of neuropathology in rats following status epilepticus induced by diisopropylfluorophosphate and soman." Neurotoxicology **83**: 14-27.

Salvi, R. M., D. R. Lara, E. S. Ghisolfi, L. V. Portela, R. D. Dias and D. O. Souza (2003). "Neuropsychiatric evaluation in subjects chronically exposed to organophosphate pesticides." Toxicological Sciences **72**(2): 267-271.

Shih, T. (2000). "Anticonvulsant treatment of nerve agent seizures: anticholinergics vs diazepam in soman-intoxicated guinea pigs." Epilepsy Res **38**: 114National.

Sisó, S., B. A. Hobson, D. J. Harvey, D. A. Bruun, D. J. Rowland, J. R. Garbow and P. J. Lein (2017). "Editor's highlight: Spatiotemporal progression and remission of lesions in the rat brain following acute intoxication with diisopropylfluorophosphate." Toxicological sciences **157**(2): 330-341.

UN. (2020). "Independent International Commission of Inquiry on the Syrian Arab Republic." Retrieved March 14, 2021, from https://www.ohchr.org/EN/HRBodies/HRC/Pages/NewsDetail.aspx?NewsID=21481&LangID=E.

Weston, C. S. (2014). "Posttraumatic stress disorder: a theoretical model of the hyperarousal subtype." Frontiers in psychiatry **5**: 37.

Winrow, C. J., M. L. Hemming, D. M. Allen, G. B. Quistad, J. E. Casida and C. Barlow (2003). "Loss of neuropathy target esterase in mice links organophosphate exposure to hyperactivity." Nature genetics **33**(4): 477-485.

Yardan, T., A. Baydin, E. Acar, F. Ulger, D. Aygun, A. Duzgun and R. Nar (2013). "The role of serum cholinesterase activity and S100B protein in the evaluation of organophosphate poisoning." Human & experimental toxicology **32**(10): 1081-1088.

Yokoyama, K., S. Araki, K. Murata, M. Nishikitani, T. Okumura, S. Ishimatsu, N. Takasu and R. F. White (1998). "Chronic neurobehavioral effects of Tokyo subway sarin poisoning in relation to posttraumatic stress disorder." Archives of Environmental Health: An International Journal **53**(4): 249-256.

Chapter 4

Mechanistic role of nicotinic receptors in *status epilepticus* caused by acute organophosphate intoxication in adult mice

Based on a submission to *Archives of Toxicology* under the same title with the following authors:

Jonas J. Calsbeek[1], Eduardo A. González[1], Brandon Pressly[2], Nycole A. Copping[3,4], Mallory E. Dawson[1], Jeremy A. MacMahon[1], Alexandria J. Yu[1], Gene G. Gurkoff[5], Jill L. Silverman[3,4], Isaac N. Pessah[1], Pamela J. Lein[1,4]

[1]Department of Molecular Biosciences, University of California, Davis, School of Veterinary Medicine, Davis, CA 95616, USA (jcalsbeek@ucdavis.edu, azgonzalez@ucdavis.edu, medawson@ucdavis.edu, jamacmahon@ucdavis.edu, ajyu@ucdavis.edu, inpessah@ucdavis.edu, pjlein@ucdavis.edu); [2]Department of Pharmacology, University of California, Davis, School of Medicine, Davis, CA 95616, USA (bpressly@ucdavis.edu); [3]Department of Psychiatry and Behavioral Sciences, School of Medicine, University of California, Davis, Sacramento, CA 95817, USA (nacopping@ucdavis.edu, jsilverman@ucdavis.edu); [4]MIND Institute, School of Medicine, University of California, Davis, Sacramento, CA 95817, USA. [5]Department of Neurological Surgery, University of California, Davis School of Medicine, 4800 Y St Suite 3740, Sacramento, CA 95817, USA (gggurkoff@ucdavis.edu).

Corresponding Author:
Dr. Pamela J. Lein
Department of Molecular Biosciences
University of California Davis School of Veterinary Medicine
1089 Veterinary Medicine Drive, 2009 VM3B
Davis, CA 95616
Telephone: (530) 752-1970 Fax: (530) 752-7690
Email: pjlein@ucdavis.edu

Abstract:

Acute intoxication with organophosphate (OP) nerve agents and pesticides can cause *status epilepticus* (SE) and death by inhibiting acetylcholinesterase (AChE), an enzyme that regulates cholinergic signaling in the nervous system through hydrolysis of acetylcholine (ACh). Excessive accumulation of ACh at central and peripheral synapses induces a toxidrome known as cholinergic crisis, which is a consequence of nicotinic and muscarinic overstimulation. The standard of care for acute OP intoxication, which includes atropine to block muscarinic receptors and oximes to regenerate AChE, notably does not include therapeutics that target nicotinic cholinergic receptors (nAChR). Here, we test the hypothesis that nAChR activation is involved in the initiation and/or maintenance of SE in a mouse model of acute intoxication with the OP diisopropylfluorophosphate (DFP). Administration of the non-selective nicotinic antagonist mecamylamine (MEC, 9.5 mg/kg, s.c.) 10 min before or 10 min after, but not 40 min after, DFP (9.5 mg/kg, s.c.) significantly reduced seizure severity, seizure duration, and weight loss relative to untreated DFP controls. Pre-treatment with the α4 subunit-selective antagonist dihydro-β-erythroidine (DHβE) also significantly reduced seizure severity, duration and weight loss, but pretreatment with the α7 subunit-selective antagonist methyllycaconitine **(**MLA) did not. Consistent with the pharmacologic data, genetic deletion of the α4, but not the α7, nAChR subunit reduced behavioral seizure scores and electrographic seizure activity relative to wildtype mice. Collectively, these data identify a mechanistic role for α4-containing nAChR in the initiation and/or progression of seizures following acute OP intoxication, and support further investigation of nicotinic antagonists as prophylactics for OP-induced SE.

Keywords: Cholinergic crisis, diisopropylfluorophosphate, mecamylamine, seizure

Abbreviations

ACh = acetylcholine

AChE = acetylcholinesterase

DFP = diisopropylfluorophosphate

DHβE = dihydro-β-erythroidine

DPE = days post-exposure

KO = knockout

MEC = mecamylamine

MLA = methyllycaconitine

nAChR = nicotinic cholinergic receptor

SE = *status epilepticus*

SLUD = salivation, lacrimation, urination, defecation

VEH = vehicle

WT = wildtype

Introduction

Organophosphates (OPs) are a class of synthetic neurotoxic chemicals that can cause seizures and death via acetylcholinesterase (AChE) inhibition (Colovic, Krstic et al. 2013, Pope and Brimijoin 2018). OP-induced seizures, which are triggered by hypercholinergic signaling resulting from AChE inhibition, can rapidly progress to *status epilepticus* (SE). OPs remain a significant public health concern. OP nerve agents were deployed as weapons of war against civilians in Syria in 2017 (HRW 2021), and their use has been confirmed in multiple high-profile assassination attempts in the UK, Malaysia, and Russia (Chai, Hayes et al. 2018, Haley 2018, OPCW 2018, OPCW 2020). OP pesticides account for hundreds of thousands of suicidal deaths every year (Eddleston 2019). Of significant concern given the threat these chemicals pose to human health, current medical countermeasures are insufficient protect survivors against the acute neurotoxic effects of acute OP poisoning (Jett and Spriggs 2020). There is, therefore, an urgent need to understand better the cellular and molecular mechanisms of OP-induced SE to identify novel therapeutic targets for protecting against acute OP neurotoxicity.

During a cholinergic crisis, excessive accumulation of ACh causes overstimulation of nicotinic and muscarinic receptors (Adeyinka and Kondamudi 2019). However, the current standard of care for OP intoxication does not protect against overstimulation of nicotinic receptors (nAChRs) during OP intoxication. The nAChR is a pentameric, ionotropic receptor made of α and/or β subunits, which upon ligand binding allow the influx of cations including sodium or calcium into the postsynaptic cell (Davis and de Fiebre 2006). Within the central nervous system, α4 and α7 are the predominant nAChR subtypes expressed (Davis and de Fiebre 2006). The α4β2 nAChR is a heteropentamer with the agonist binding site for ACh located at the extracellular α4 and β2 interface. Mutations in the α4 subunit are linked to epilepsy (Steinlein,

Mulley et al. 1995), and transgenic mice with hypersensitive α4 receptor subtypes display higher vulnerability to agonist-induced seizures (Fonck, Nashmi et al. 2003). The α7 nAChR is a homopentamer, and the ACh binding site is found between each interface of the extracellular subunits, allowing five active domains for ligand binding ACh (Davis and de Fiebre 2006). When activated, these receptors can influence synaptic remodeling and downstream neurotransmitter release (Orr-Urtreger, Goldner et al. 1997).

Earlier reports in the literature suggest nAChR may be involved in OP-induced seizures (Sheridan, Smith et al. 2005). In a rat model of DFP intoxication (3.3 mg/kg, i.v.), 30 min pretreatment with a combination of atropine (0.79 mg/kg, i.m.), mecamylamine (0.79 mg/kg, i.m.), and either pyridostigmine (0.056 mg/kg, i.m.) or physostigmine (0.026 mg/kg, i.m.) protected against the lethal effects of DFP (Harris and Stitcher 1984). Because this study did not assess nicotinic antagonism alone compared to the combinatorial therapy, the observed therapeutic benefits could not be attributed to nicotinic antagonism alone. However, in a soman intoxication model, mecamylamine (5 mg/kg, s.c.) treatment 5 min post-soman (250 μg/kg, s.c.) reduced fasciculations and respiratory irregularities in rats that were pretreated with scopolamine (30 min pre-soman; 20 mg/kg, s.c.) relative to scopolamine pretreatment alone (Hassel 2006). When the α7 nAChR antagonist 4R-cembranoid was injected (4R; 6 mg/kg, s.c.) either 1 h before, 5 h after, or 24 h after DFP (9 mg/kg, i.p.), a significant reduction in neurodegeneration and neuroinflammation was observed at 48 h post-DFP (Ferchmin, Andino et al. 2014). It should be noted that this study did not observe any antiseizure effects of the 1 h pretreatment with 4R, suggesting the α7 subunit may not be involved in DFP-induced seizures, but rather in downstream consequences of the cholinergic crisis.

In the present study, we targeted α4- and α7-containing nAChRs because of their predominant expression in the brain and because both subunits have been implicated in either preclinical seizure models or in epilepsy (Damaj, Glassco et al. 1999, Ghasemi and Hadipour-Niktarash 2015). To address the question of what role nicotinic receptors play in OP-induced seizures, we leveraged a mouse model of acute intoxication with DFP (Calsbeek, González et al. 2021, under review) to evaluate the effects of pharmacologic antagonism and genetic deletion of nAChR on seizure severity and duration. We also measured weight loss as an indirect indicator of the severity of peripheral cholinergic symptoms, specifically, salivation, lacrimation, urination, and defecation (SLUD) (Adeyinka and Kondamudi 2019).

Materials and Methods

Animals

All studies involving animals conformed to the ARRIVE guidelines and were conducted in accordance with protocols approved by the UC Davis Institutional Animal Care and Use Committee that were designed to minimize pain and suffering. All animals were housed in facilities accredited by the American Association for Accreditation of Laboratory Animal Care (AAALAC) International. Adult male C57BL/6 mice (8-10 weeks old; 20-30 g; The Jackson Laboratory, Sacramento, CA) were maintained on a 12:12 light:dark cycle in a temperature and humidity-controlled vivarium (22 ± 2ºC; 40-50% humidity). Mice were group housed (up to 4 mice per cage) in standard plastic mouse cages with corncob bedding, provided standard rodent chow (LabDiet #5058) and tap water *ad libitum*, and allowed to acclimate for at least 7 days prior to experimentation. Three pairs of male and female heterozygous α4-nAChR knockout (KO) mice on a C57BL/6J genetic background were obtained from the California Institute of

Technology (CalTech; Pasadena, CA, USA) and paired for breeding. Litters were genotyped at weaning (postnatal day 21) and homozygous offspring were paired for breeding to produce homozygous α4-nAChR subunit KO mice for this study. Three breeding pairs of male and female homozygous α7-nAChR subunit KO mice on a C57BL/6J genetic background were obtained from The Jackson Laboratories (Sacramento, CA, USA). Age-matched wildtype (WT) C57BL/6J mice were obtained from The Jackson Laboratories (Sacramento, CA, USA) as the control group for genetic investigation.

Dosing Paradigm

DFP was purchased from Sigma (St. Louis, MO, USA), stored at -80ºC, and confirmed to be at least 90% pure using NMR methods as previously described (Gao, Naughton et al. 2016). Atropine sulfate (AS) and 2-pralidoxime (2-PAM) were purchased from Sigma, stored at room temperature, and certificates of analysis provided by the manufacturers indicated the purity of AS to be >97% (lot #BCBM6966V) and of 2-PAM to be >99% (lot #MKCG3184). Adult male mice were injected with DFP (9.5 mg/kg in sterile saline, s.c.; 100 μL), followed 1 min later by injection of AS (0.1 mg/kg in sterile saline, i.m.) and 2-PAM (25 mg/kg in sterile saline, i.m.) to prevent peripheral toxicity. To assess the role of nAChRs in DFP-induced SE, mice were injected with the broad nicotinic antagonist mecamylamine hydrochloride (MEC; AK Scientific, Union City, CA, USA) or vehicle (sterile saline) either 10 min before, 10 min after, or 40 min after DFP injection. The α4-selective nAChR antagonist dihydro-β-erythroidine hydrobromide (DHβE; Tocris, Bristol, UK) or the α7-selective nAChR antagonist methyllycaconitine citrate (MLA; Tocris) was injected in sterile saline 10 min before DFP to assess the role of specific nAChR subunits in DFP-induced SE. Certificates of analysis provided by the manufacturers

confirmed the purity of MEC to ≥98% (lot #TC24203), DHβE to be ≥98% (batch #11A/249912), and MLA to be ≥98% (batch #23A/251394). DFP control mice were injected with an equal volume of sterile saline vehicle in place of the nAChR antagonists. Initial doses for the nAChR antagonists were selected based on a previous study using them as pretreatments for nicotine-induced seizures in adult mice (Damaj, Glassco et al. 1999).

Seizure behavior in mice was quantified after DFP injection using a behavioral seizure scoring scale from 0 to 5 ranked in order of symptom severity (Figure 4.1). Seizures were scored every 5 min for the first 120 min, and every 20 min from 120-240 min after DFP to quantify the onset, duration, and severity of SE. After 4 h of seizure scoring, mice were injected with dextrose (5% in saline; 1 mL, s.c.) and singly housed with wet food. Mice were weighed daily and given additional wet food and dextrose as needed (5% in saline (v/v); 1 mL, s.c.; daily) until body weight returned to pre-DFP baseline levels (typically within 4-7 days).

Electroencephalogram Recording

A small cohort of mice (3 experimental groups, n=2-4 per group) were instrumented with wireless (electroencephalogram) EEG telemetry devices (HDX02; Data Sciences International, St. Paul, MN, USA) in accordance with the UC Davis Survivable Rodent Surgery guidelines, as previously described (Copping and Silverman 2021). Briefly, mice were deeply anesthetized with isoflurane (4-5% for induction, 1-3% for maintenance) as confirmed by foot pinch before the skull was exposed to drill small holes for placement of electrodes. Stereotaxic coordinates were used to position the front edge of the implant 3.0-3.5 mm anterior of bregma. After securing the implant with anchor screws, the skin incision was sutured closed, and the head mount was fixed with dental cement. Implanted mice were returned to their home cage and

allowed to recover for at least 7 days prior to experimentation. Untethered EEG recordings were acquired using a receiver (RPC-1; Data Sciences International, St. Paul, MN, USA) placed under the home cage of the animal. EEG traces were analyzed for the root mean square of spike amplitude (per second) during 1 h epochs before and after DFP injection.

Statistical Analyses

Seizure scores were used to calculate the mean 4 h seizure score for each experimental group and analyzed using GraphPad Prism (version 8.1.2, alpha=0.5). Statistical comparisons between two experimental groups were performed using unpaired, two-tailed, t-test with *post-hoc* Mann Whitney test. Statistical comparisons between multiple (>2) experimental groups were performed using one-way ANOVA with *post-hoc* Dunnett's multiple comparisons test. Statistical comparisons between EEG experimental groups were performed using a two-way ANOVA with *post-hoc* Sidak's multiple comparisons test.

Results

Mecamylamine (MEC) pretreatment prevented DFP-induced SE

To determine whether nAChR were involved in initiation of OP-induced seizures, animals were administered varying doses (0.3-9.5 mg/kg, s.c.) of the non-selective nAChR antagonist MEC 10 min prior to being exposed to DFP (9.5 mg/kg, s.c.). A higher dose of MEC (30 mg/kg, s.c.) was also tested, but was observed to cause lethality before DFP was administered, confirming previously published concerns with high doses of mecamylamine (Hassel 2006). Using the seizure scale shown in Figure 4.1, seizure behavior was scored during the first 4 h after DFP injection. MEC caused a dose-dependent reduction in seizure scores

relative to untreated DFP controls (Figure 4.2A). Specifically, MEC-treated mice displayed reduced seizure behavior scores and SLUD that were apparent immediately after DFP, as manifested by attenuated convulsive behavior and minimal release of urine and feces. Similarly, the mean 4 h seizure score was significantly reduced in MEC-treated mice relative to untreated DFP controls, with the greatest seizure protection observed in DFP animals pretreated with MEC at 9.5 mg/kg (Figure 4.2B). The percentage of animals within each group that experienced a seizure score ≥ 3 at any time during the 4 h scoring period was the least in the 9.5 mg/kg MEC group, identifying this dose of MEC as the most efficacious in protecting against DFP-induced SE.

Mecamylamine terminated seizure behavior when administered early after DFP exposure

To evaluate a role for nAChR in propagating OP-induced seizures, MEC (9.5 mg/kg, s.c.) was administered 10 min after exposure to DFP. In all groups, seizures began within minutes of DFP injection; however, in DFP animals treated with MEC, seizures stopped within minutes of MEC injection (Figure 4.3A). The mean 4 h seizure score was also significantly reduced in MEC-treated mice relative to DFP controls (Figure 4.3B). Symptoms of SLUD appeared reduced in MEC-treated mice relative to untreated mice that displayed excessive nasal secretions, urination and defecation. MEC-treated mice lost significantly less weight relative to untreated DFP controls when assessed at 4 h (Figure 4.3C) and 24 h after DFP (Figure 4.3D). In contrast, administration of MEC (9.5 mg/kg, s.c.) at 40 min after DFP did not significantly reduce seizure scores (Figure 4.4A, B) or weight loss (Figure 4.4C, D) relative to untreated DFP controls.

The α4 but not α7 nAChR subunit is involved in DFP-induced SE

To assess the contribution of specific nAChR subunits to DFP-induced SE, the subunit-selective nicotinic antagonists DHβE (α4-selective) or MLA (α7-selective) were injected 10 min before DFP. Immediately after DFP injection, seizure behavior was reduced in DhβE-treated mice, and reached a stable seizure score of 1.0 at 65 min post-DFP. A significant reduction in mean seizure score was observed in mice treated with 5 mg/kg of DHβE relative to untreated DFP control mice (Figure 4.5A). Pretreatment with DhβE also significantly reduced body weight loss at 4 and 24 h after DFP exposure (Figure 4.5B). In contrast, pretreatment with MLA did not protect against DFP-induced SE (Figure 4.5C) or weight loss (Figure 4.5D).

To verify that effects observed using nAChR subunit-selective pharmacologic antagonism were not due to off-target effects, we compared DFP-induced seizures and weight loss in knockout (KO) mice that lacked either the α4 or α7 nicotinic receptor subunit relative to wildtype (WT) mice. Regardless of genotype, all mice exhibited seizure behavior within minutes of the DFP injection (Figure 4.6A); however, seizure scores dropped in α4KO mice between 40-45 min post-DFP and remained at ~2.0 for the remainder of the scoring period s. The mean 4 h seizure score was significantly reduced in the α4-AChR subunit KO mice compared to WT DFP controls or α7- KNO mice (Figure 4.6B). The mean seizure score for heterozygous α4 KO mice was also significantly lower than WT DFP controls but higher than homozygous α4 KO mice. EEG recordings from a separate cohort of mice (n=2-4 per genotype) indicated that DFP caused significant electroencephalographic seizure activity in WT mice, but not in α4 KO mice (Figure 4.6C). The root mean square (per second) of spike amplitude following DFP was significantly increased relative to baseline in WT DFP but not in α4 KO mice (Figure 4.6D).

Discussion

The findings of this study support the hypothesis that nAChRs, in particular α4 subunit containing nAChRs, are involved in OP-induced seizures. The most direct evidence in support of this includes results from pharmacologic antagonism of nicotinic receptors 10 min before or after DFP, and the attenuated effects of DFP in mice that do not express the α4 nAChR subunit. Treatment with MEC was effective in preventing or terminating severe seizure behavior when given 10 min before or after DFP, but when injected at 40 min post-DFP, MEC did not reduce the severity of seizure behavior. This is consistent with evidence in the literature describing a shift from hypercholinergic signaling driving seizure activity to sustained glutamatergic signaling that occurs within minutes following OP intoxication to maintain seizure activity (Aroniadou-Anderjaska, Figueiredo et al. 2020). This could explain the limited efficacy of MEC at 40 min post-DFP in the current study. Another plausible explanation is that overactivation of nAChRs caused receptor internalization or desensitization in response to excessive signaling (Giniatullin, Nistri et al. 2005). Similarly, SE become refractory to benzodiazepines after 20-30 min of continuous seizure activity because the synaptic $GABA_A$ receptors targeted by benzodiazepines are internalized (Niquet, Baldwin et al. 2016).

There is a wide distribution of various nAChRs in the human body, which has triggered significant interest in identifying subunit selective antagonists to specifically target subpopulations of nAChRs. An interesting observation was that while MEC pretreatment completely blocked DFP-induced seizure behavior, pretreatment with DHβE did not prevent the initiation of seizure behavior, but seizure scores began dropping in DHβE-treated mice ~20 min after DFP. One explanation is that the dose of DHβE was too low to block DFP-induced seizures. However, a higher dose of 10 mg/kg of DHβE caused significant lethality even before injection

with DFP. In a study on nicotine-induced seizures in mice using identical doses (Damaj, Glassco et al. 1999), the α7-selective antagonist MLA was successful in blocking seizure behavior. The findings of the current study are inconsistent with this report, because MLA was not effective in preventing DFP-induced seizures. One potential explanation for this difference is that α7-containing nAChRs are not contributing to OP-induced seizure behavior, consistent with previous studies using α7 antagonism before or after DFP (Ferchmin, Andino et al. 2014). The findings of the Ferchmin study suggest that the α7 nAChR subunit is involved in DFP-induced neuropathology, because significant neuroprotection was observed with the use of an α7 nAChR antagonist even though seizure scores were unaffected.

Consistent with the α4-selective antagonist DhβE experiment, mice lacking the α4 nAChR subunit displayed significant reductions in EEG spike amplitude after DFP relative to WT controls. However, the absence of increases in EEG spike amplitude was not expected based on seizure behavior scores of DFP mice pretreated with the α4-selective antagonist DHβE. One possible explanation for the observation of seizure behavior in the absence of EEG abnormalities is that the cortical EEG electrodes are not sensitive enough to detect focal seizures in more ventral regions of the brain. Additionally, it is not yet determined whether the dose of DHβE used in this study is sufficient to block all α4-containing nAChRs, which could allow some activity to persist. Studies are currently ongoing *ex vivo* to gain a better understanding of ideal timing for future dosing strategies.

Nicotinic antagonism could be highly beneficial as a prophylactic therapy for OP intoxication, and studies are ongoing to evaluate its potential. A current prophylactic standard of care for OP intoxication is pyridostigmine bromide (Lorke and Petroianu 2019), which is a reversible AChE inhibitor taken orally (90mg/d) for a maximum of 7 days (USAMRICD 1990).

However, this therapeutic strategy suffers from concerns about side effects, and it is suspected as a possible cause of Gulf War Illness (Charatan 1999). There is also troubling evidence that pyridostigmine bromide (PB) provides no therapeutic benefit in preclinical models of DFP-induced SE (Bruun, Guignet et al. 2019), raising the question of whether a different prophylactic strategy could be more effective at preventing or reducing OP-induced SE. There is literature suggesting that the duration of SE predicts the severity of negative health outcomes (Sisó, Hobson et al. 2017, Gainza-Lein, Fernandez et al. 2019) because excessive neuronal signaling is understood to induce excitotoxicity in the brain (Dong, Wang et al. 2009). Therefore, seizure prevention should be the primary focus of prophylactic treatment strategies for OP intoxication, to block the initiation of excitatory signaling cascades leading to a cholinergic crisis and glutamatergic storm.

Another important finding of this work is that pretreatment with MEC or DHβE, but not MLA, reduced not only seizure behavior, but also clinical signs of cholinergic crisis, such as excessive salivation, lacrimation, urination, and defecation as evident by reduced weight loss at 4 and 24 h after DFP intoxication. Nicotinic antagonism with hexamethonium has been shown to cause constipation and urinary retention (Dreyer 1954), which provides a possible explanation for the reduced weight loss in DFP animals treated with MEC or DHβE. Indeed, parasympathetic blockade with nicotinic ganglionic blockers causes dry mouth, urinary retention, and increased ocular pressure (Kaushal and Tadi 2020). Because mice with reduced seizure behavior also displayed significantly less weight loss, it remains unclear whether this therapeutic benefit was a direct result of nicotinic antagonism, or due to a phenomenon associated with the prevention or termination of SE. Therefore, more mechanistic studies are needed to gain a better understanding of the role for nicotinic receptors in the symptoms of SLUD.

In conclusion, the findings of the current study support the inclusion of a nicotinic antagonist as a preventative antidote for acute OP intoxication, but more studies are needed to determine if nicotinic antagonism is more effective via intramuscular route or when combined with benzodiazepine rescue. Due to the recruitment of multiple neurotransmitter systems during SE, it is not likely that one single targeted therapy will be enough to prevent the neurologic sequelae of OP intoxication. However, identifying the temporal profile of vulnerable receptor targets can provide critical information about when to administer medical countermeasures and can better inform triage decisions to assign the appropriate line of therapy based on duration of SE.

Acknowledgements

The authors gratefully acknowledge Dr. Suzette Smiley-Jewell (UC Davis CounterACT Center of Excellence) for assistance with manuscript preparation, Dr. Danielle Harvey (UC Davis) for consultation on statistical analyses, and Dr. Henry Lester (California Institute of Technology) for providing the α4-KO mice. This research was supported by the CounterACT Program, National Institutes of Health Office of the Director, and the National Institute of Neurological Disorders and Stroke (NINDS) under Grant U54 NS079202. J.J.C. was supported by a predoctoral fellowship from the UC Davis School of Veterinary Medicine; E.A.G., by predoctoral fellowships from the National Institute of Neurological Disorders and Stroke [grant number F31 NS110522] and the National Institutes of Health Initiative for Maximizing Student Development [grant number R25 GM5676520]; This project used core facilities supported by the UC Davis MIND Institute Intellectual and Developmental Disabilities Research Center (Eunice Kennedy Shriver National Institute of Child Health and Human Development grant P50 HD103526). The sponsors were not involved in the study design, in the collection, analysis, or interpretation of data, in the writing of the report, or in the decision to submit the paper for publication.

Conflict of Interest Statement

The authors declare that they have no conflicts of interest.

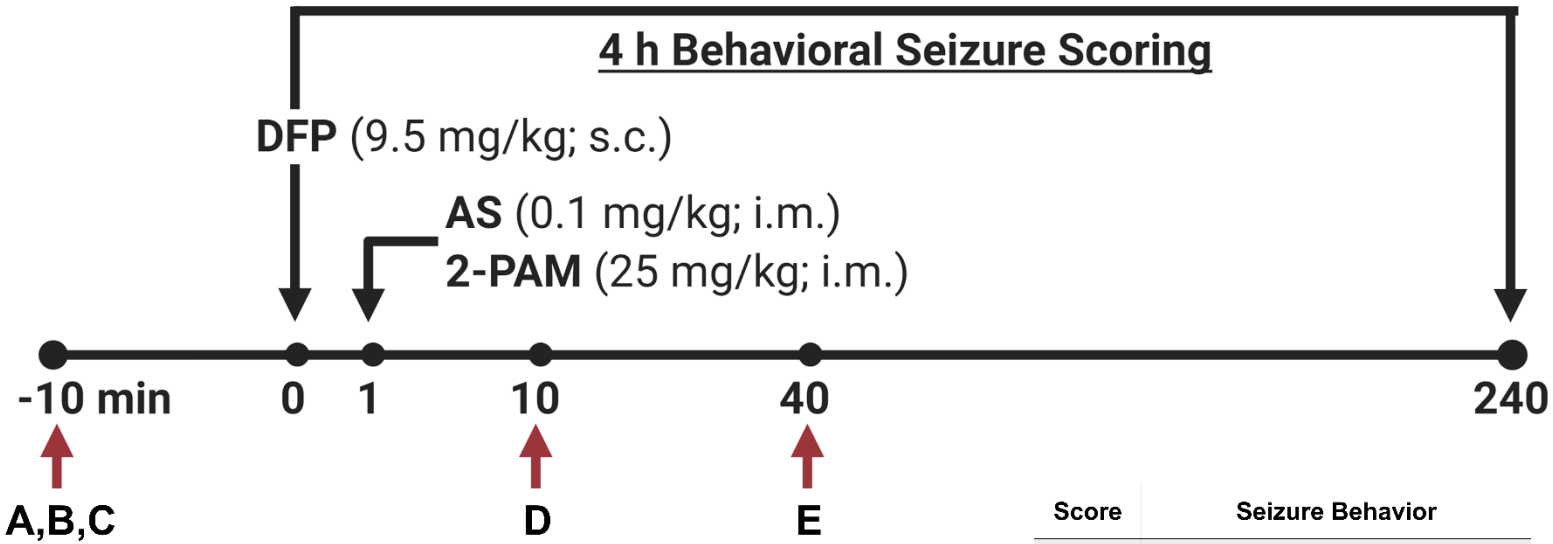

Experiment	Selectivity	Antagonist Used
A	broad nicotinic	mecamylamine (0.3-9.5 mg/kg, s.c.)
B	α4-selective	dihydro-β-erythroidine (2-5 mg/kg, s.c.)
C	α7-selective	methyllycaconitine (2-10 mg/kg, s.c.)
D	broad nicotinic	mecamylamine (9.5 mg/kg, s.c.)
E	broad nicotinic	mecamylamine (9.5 mg/kg, s.c.)

Score	Seizure Behavior
5	Falling with loss of righting reflex
4	Rearing, falling, tonic extensions
3	Forelimb or hindlimb clonus
2	Muscle tremors, head nod
1	Straub tail, SLUD
0	No abnormal symptoms

Figure 4.1. Experimental design of this study. Adult C57BL/6J mice were injected with diisopropylfluorophosphate (DFP) at time 0, followed 1 min later by atropine sulfate (AS) and 2-pralidoxime (2-PAM) to prevent peripheral cholinergic toxicity. Seizure behavior was scored for each animal during the 4 h after injection to quantify seizure severity using a scale from 0-5 ranked by severity of seizure behavior. Cohorts of wildtype (WT) mice in this study (n=4-6 per experimental group) were randomly assigned to one of three time points for therapeutic intervention with a nicotinic antagonist (red vertical arrows). Mice used in experiments to assess the effects of genetic deletion of specific nicotinic receptor subunits were not treated with nicotinic antagonists at any time point.

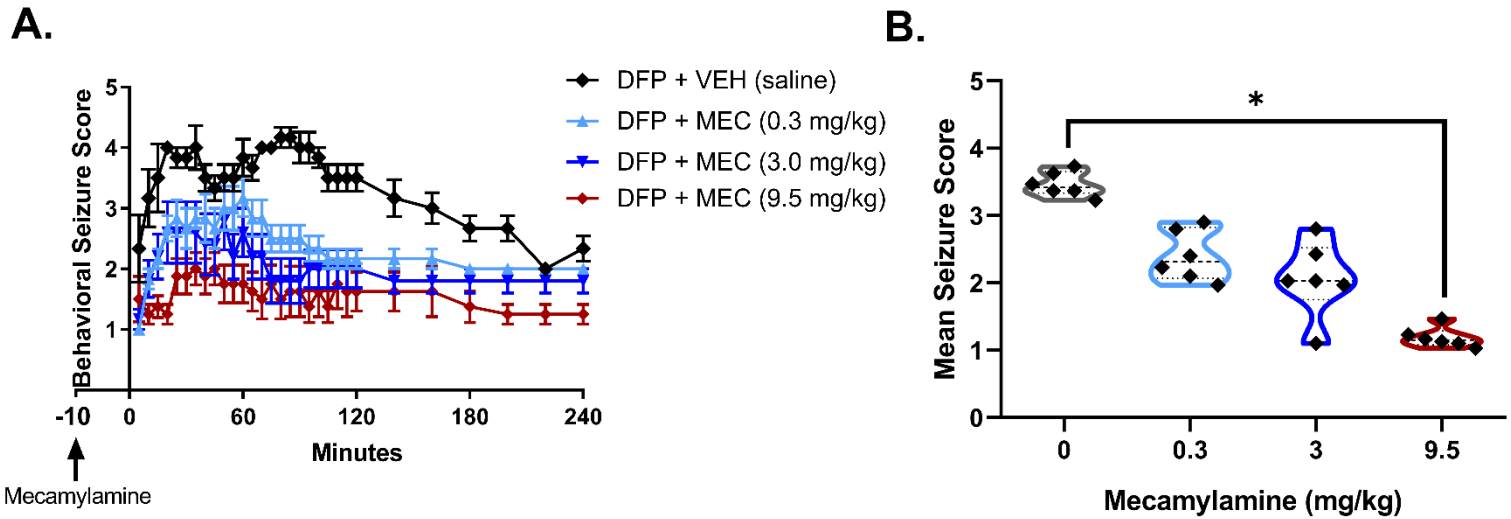
A.
Behavioral Seizure Score
5
4
3
2
1
-10
0
60
120
180
240
Minutes
Mecamylamine
DFP + VEH (saline)
DFP + MEC (0.3 mg/kg)
DFP + MEC (3.0 mg/kg)
DFP + MEC (9.5 mg/kg)
B.
Mean Seizure Score
*
5
4
3
2
1
0
0
0.3
3
9.5
Mecamylamine (mg/kg)

Figure 4.2. Pretreatment with mecamylamine 10 min prior to DFP injection dose-dependently attenuated DFP-induced seizure behavior. (A) Behavioral seizure scores after acute exposure to DFP with 10 min pretreatment with varying doses of mecamylamine (MEC) or vehicle. Data points correspond to the mean group seizure score (± S.E.M.) at each observation time (n=6 animals per experimental group). (B) Mean 4 h seizure scores for each experimental group represented by violin plots displaying the median and quartiles (horizontal dotted lines). *Significantly different from DFP with no MEC pretreatment at $p<0.0001$ as determined by one-way ANOVA with Dunnett's multiple comparisons test.

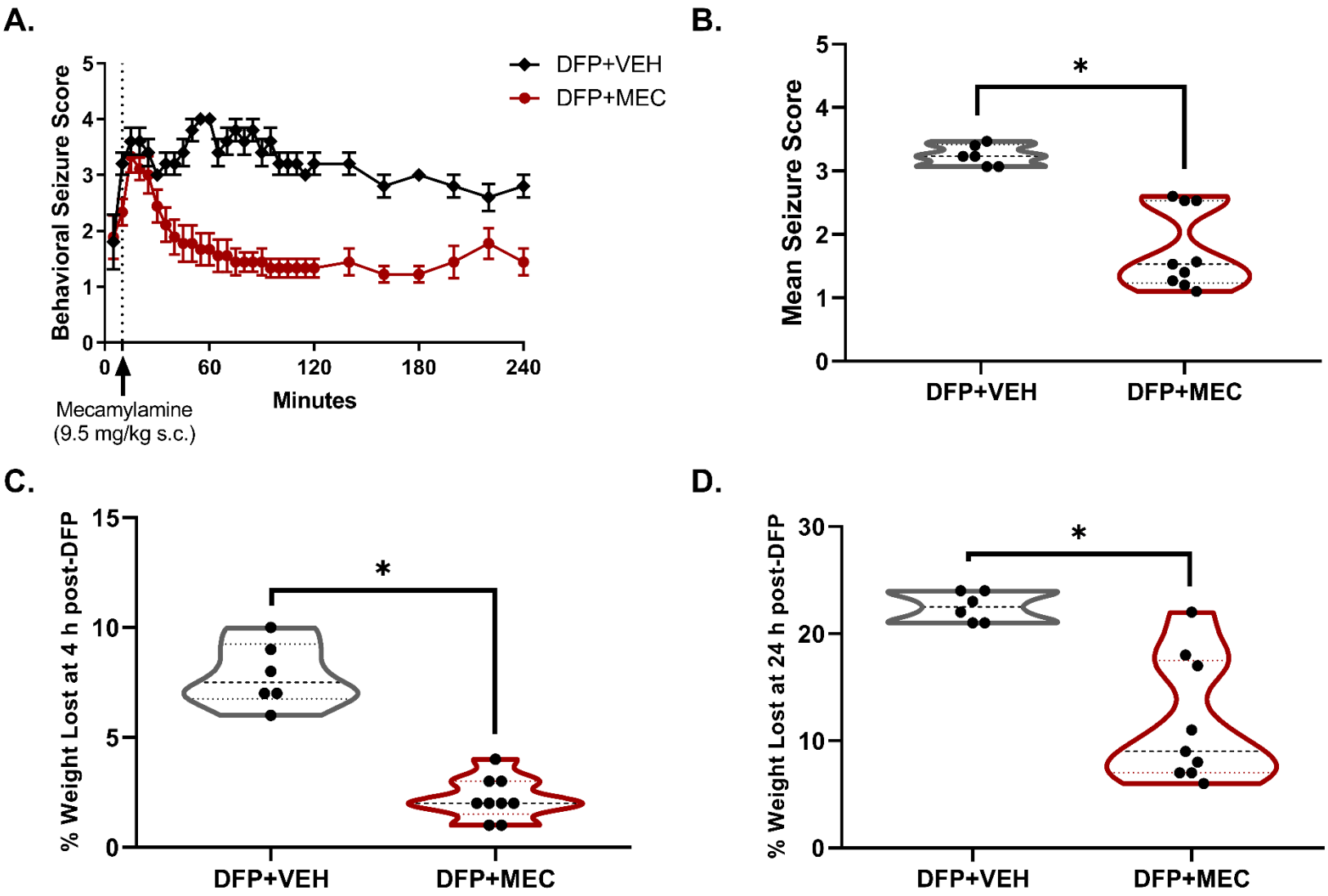
A.
Behavioral Seizure Score
DFP+VEH
DFP+MEC
Minutes
Mecamylamine
(9.5 mg/kg s.c.)
B.
Mean Seizure Score
DFP+VEH
DFP+MEC
C.
% Weight Lost at 4 h post-DFP
DFP+VEH
DFP+MEC
D.
% Weight Lost at 24 h post-DFP
DFP+VEH
DFP+MEC

Figure 4.3. Treatment with mecamylamine at 10 min post-DFP significantly reduced seizure scores and weight loss in DFP animals. (A) MEC (9.5 mg/kg, s.c.) or an equal volume of vehicle (VEH; saline) was administered 10 min after DFP administration. Data points correspond to the mean group seizure score (± S.E.M.) at each observation time (n=6-9 animals per group). (B) Mean 4 h seizure scores for each experimental group represented by violin plots displaying the median and quartiles (horizontal dotted lines). *Significantly different from DFP alone at $p<0.0005$ as determined by an unpaired two-tailed t-test with *post hoc* Mann Whitney test. (C) Body weights were recorded from mice before and 4 h after DFP injection to monitor acute effects of DFP intoxication. The mean change in body weight for each experimental group (n=6-9 per experimental group) was plotted as the percentage of body weight lost from baseline before DFP exposure using violin plots that display the median and quartiles (horizontal dotted lines). *Significantly different from controls at $p<0.0005$ as determined by an unpaired two-tailed t-test with *post hoc* Mann Whitney test. (D) Body weights were recorded at 24 h post-DFP and plotted as the percentage of body weight lost from baseline before DFP exposure (n=6-9 per experimental group) using violin plots that display the median and quartiles (horizontal dotted lines). *Significantly different from controls at $p<0.005$ as determined by an unpaired two-tailed t-test with *post hoc* Mann Whitney test.

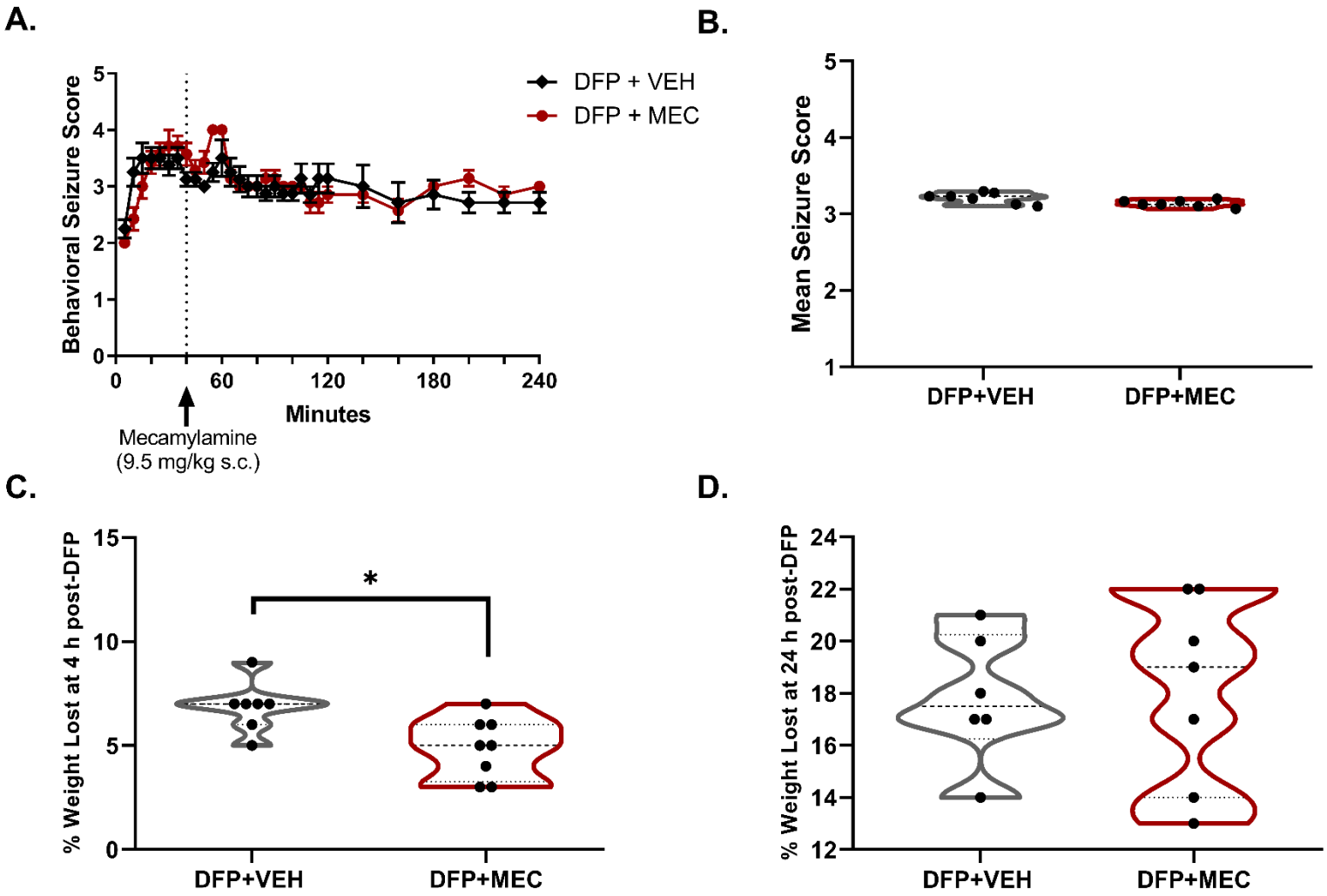
A.
Behavioral Seizure Score
DFP + VEH
DFP + MEC
Minutes
Mecamylamine
(9.5 mg/kg s.c.)
B.
Mean Seizure Score
DFP+VEH
DFP+MEC
C.
% Weight Lost at 4 h post-DFP
*
DFP+VEH
DFP+MEC
D.
% Weight Lost at 24 h post-DFP
DFP+VEH
DFP+MEC

Figure 4.4. Post-treatment with mecamylamine treatment at 40 min post-exposure did not reduce seizure scores or 24 h weight loss in DFP animals. (A) Mecamylamine (MEC, 9.5 mg/kg, s.c.) or an equal volume of vehicle (VEH; saline) was administered 40 min after DFP exposure. Data points correspond to the mean group seizure score (± S.E.M.) at each observation time (n=6-8 animals per experimental group). (B) Mean 4 h seizure scores for each experimental group (n=6-8 per group). (C, D) Body weights were recorded from mice, before and after DFP injection, to monitor the effect of DFP intoxication on body weight. The mean change in body weight, measured as % weight lost from baseline prior to DFP injection, for each experimental group (n=6-8 per group) was determined 4 h (C) and 24 h (D) after DFP intoxication. Violin plots display the median and quartiles (horizontal dotted lines) for each group. *Significantly different from controls at $p<0.05$ as determined by an unpaired two-tailed t-test with *post hoc* Mann Whitney test.

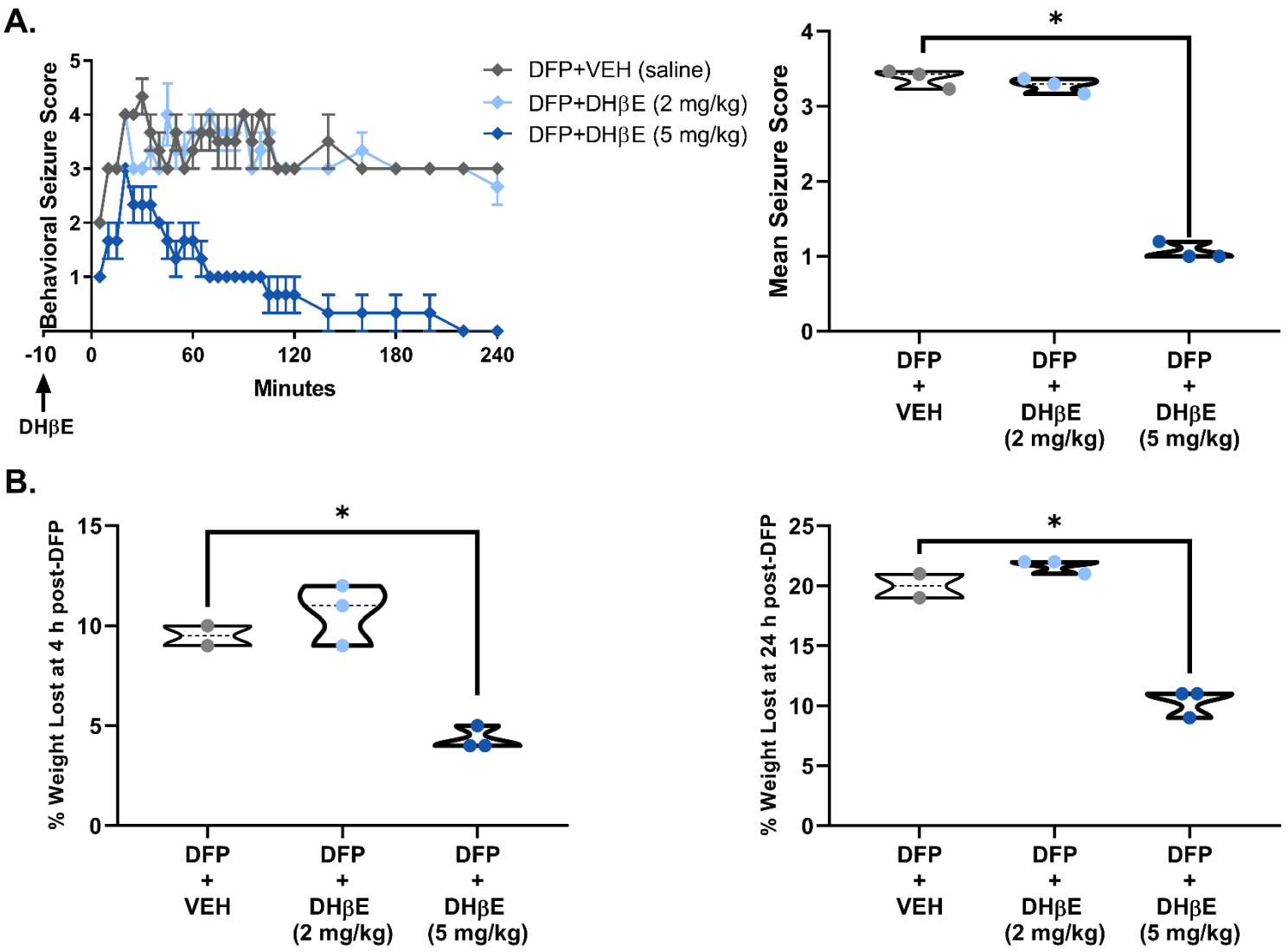
A.
Behavioral Seizure Score
Minutes
DHβE
DFP+VEH (saline)
DFP+DHβE (2 mg/kg)
DFP+DHβE (5 mg/kg)
Mean Seizure Score
DFP + VEH
DFP + DHβE (2 mg/kg)
DFP + DHβE (5 mg/kg)
B.
% Weight Lost at 4 h post-DFP
% Weight Lost at 24 h post-DFP

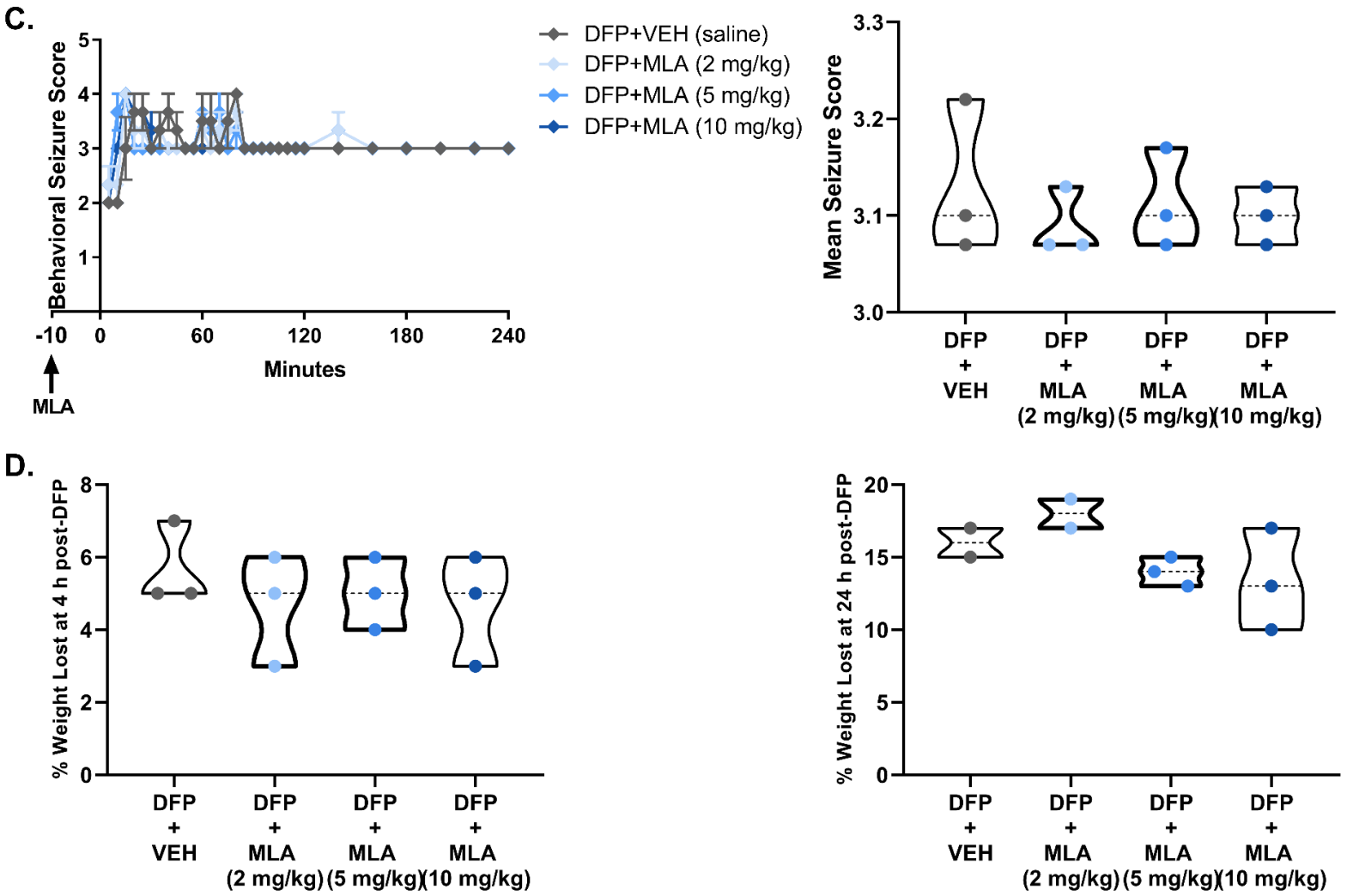
C.
Behavioral Seizure Score
Minutes
-10
0
60
120
180
240
MLA
DFP+VEH (saline)
DFP+MLA (2 mg/kg)
DFP+MLA (5 mg/kg)
DFP+MLA (10 mg/kg)
Mean Seizure Score
DFP + VEH
DFP + MLA (2 mg/kg)
DFP + MLA (5 mg/kg)
DFP + MLA (10 mg/kg)
D.
% Weight Lost at 4 h post-DFP
% Weight Lost at 24 h post-DFP

Figure 4.5. Pretreatment with an α4 but not α7 subunit-selective nAChR antagonist 10 min before DFP significantly reduced seizure scores and weight loss. The nAChR subunit selective antagonist DHβE (α4-selective), MLA (α7-selective), or an equal volume of vehicle (VEH; saline) was injected 10 min before DFP to examine the role of the α4 or α7 nAChR subunit in OP-induced SE. (A) Resulting seizure scores after acute exposure to DFP ± DHβE and 4 h seizure scores for each experimental group shown as the mean ± S.E.M. (n=4 per group). *Significantly different from controls at $p<0.05$ as determined by one-way ANOVA with Dunnett's multiple comparisons test. (B) The percent change in body weight from baseline at 4 and 24 h post-exposure presented as the mean ± S.E.M. (n=4 per group). *Significantly different from DFP control at $p<0.05$ as determined by one-way ANOVA with Dunnett's multiple comparisons test. (C) Resulting seizure scores after acute exposure to DFP (+/- MLA) and mean 4 h seizure scores for each experimental group (n=4 per group). (D) The percent change in body weight from baseline at 4 and 24 h post-exposure presented as the mean ± S.E.M. (n=4 per group).

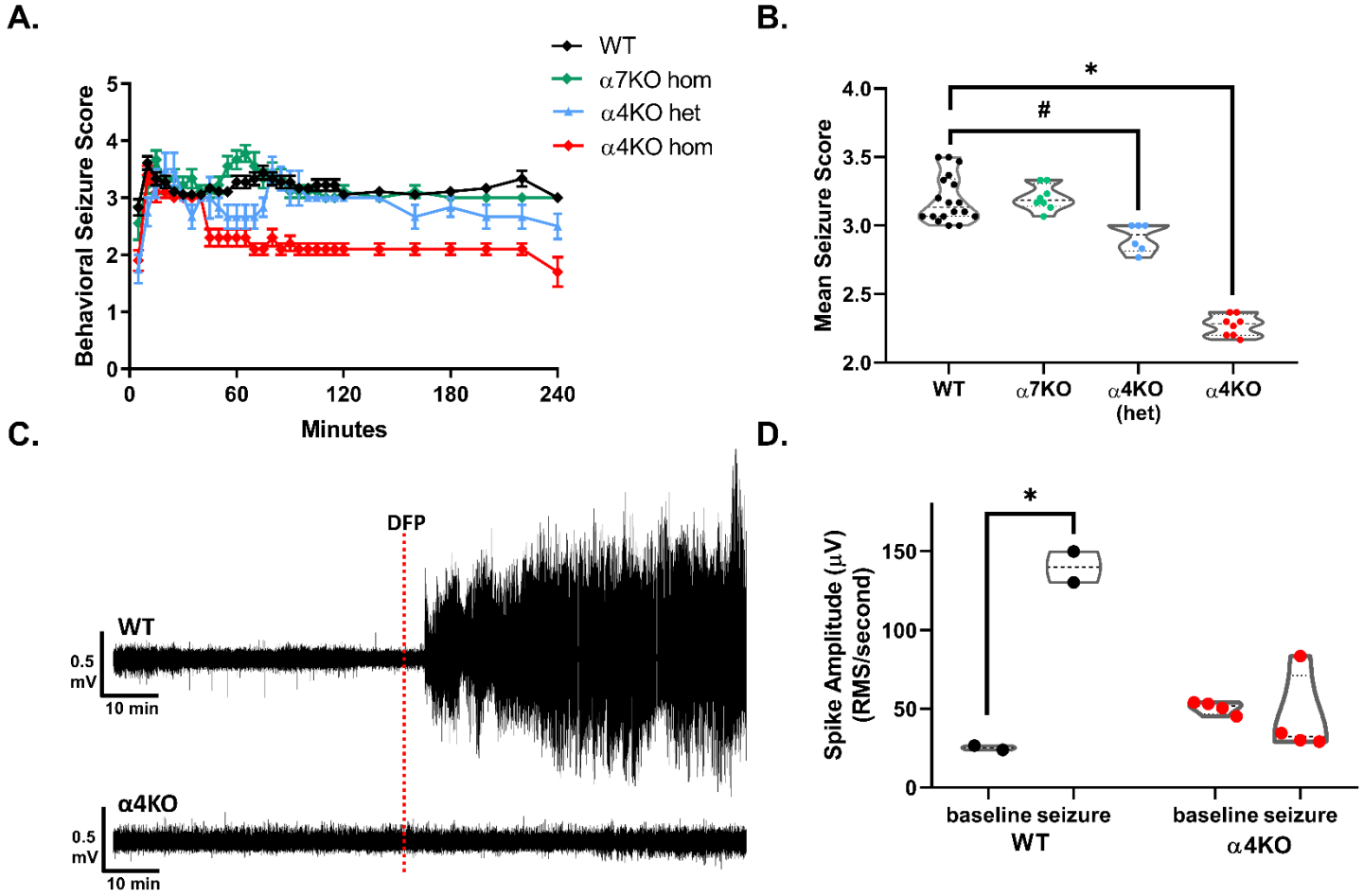
A.
WT
α7KO hom
α4KO het
α4KO hom
Behavioral Seizure Score
Minutes
B.
Mean Seizure Score
WT
α7KO
α4KO (het)
α4KO
C.
DFP
WT
0.5 mV
10 min
α4KO
D.
Spike Amplitude (μV) (RMS/second)
baseline seizure WT
baseline seizure α4KO

Figure 4.6. Mice lacking α4 nicotinic receptor subunit displayed significantly decreased severity and shorter duration of SE relative to wildtype mice. (A) Resulting seizure scores after acute exposure to DFP. Seizure scores were recorded at 5 min intervals during the first 120 min following administration of DFP (n=6-18 per experimental group), and at 20 min intervals between 120- and 240-min post-exposure. Data points correspond to the mean group seizure score (± S.E.M.) at each observation time. (B) Mean 4 h seizure scores for each experimental group. Violin plots display the median and quartiles (horizontal dotted lines) for each group. Significantly different from WT controls at *=$p<0.0001$ and #=$p<0.05$ as determined by one-way ANOVA with Dunnett's multiple comparisons test. (C) 1 hour baseline and seizure periods of EEG recordings from WT and α4KO mice (n=2-4 per group) injected with DFP (red dotted line). (D) EEG spike amplitude (RMS/sec) after DFP injection in WT and α4KO mice (n=2-4 per group). *Significantly different from baseline at $p<0.005$ as determined by two-way ANOVA with Sidak's multiple comparisons test. Violin plots display the median and quartiles (horizontal dotted lines) for each group.

References

Adeyinka, A. and N. P. Kondamudi (2019). "Cholinergic crisis." StatPearls [Internet].

Aroniadou-Anderjaska, V., T. H. Figueiredo, J. P. Apland and M. F. Braga (2020). "Targeting the glutamatergic system to counteract organophosphate poisoning: A novel therapeutic strategy." Neurobiol Dis **133**: 104406.

Bruun, D. A., M. Guignet, D. J. Harvey and P. J. Lein (2019). "Pretreatment with pyridostigmine bromide has no effect on seizure behavior or 24 hour survival in the rat model of acute diisopropylfluorophosphate intoxication." Neurotoxicology **73**: 81-84.

Calsbeek, J. J., E. A. González, D. A. Bruun, M. A. Guignet, N. A. Copping, M. E. Dawson, A. J. Yu, J. A. McMahon, D. J. Harvey, J. L. Silverman and P. J. Lein (2021). "Persistent neuropathology and behavioral deficits in a mouse model of status epilepticus induced by acute intoxication with diisopropylfluorophosphate." under review at Neurotoxicology.

Chai, P. R., B. D. Hayes, T. B. Erickson and E. W. Boyer (2018). "Novichok agents: a historical, current, and toxicological perspective." Toxicol Commun **2**(1): 45-48.

Charatan, F. (1999). "Nerve gas antidote a possible cause of Gulf war illness." BMJ: British Medical Journal **319**(7218): 1154.

Colovic, M. B., D. Z. Krstic, T. D. Lazarevic-Pasti, A. M. Bondzic and V. M. Vasic (2013). "Acetylcholinesterase inhibitors: pharmacology and toxicology." Curr Neuropharmacol **11**(3): 315-335.

Copping, N. A. and J. L. Silverman (2021). "Abnormal electrophysiological phenotypes and sleep deficits in a mouse model of Angelman Syndrome." Mol Autism **12**(1): 9.

Damaj, M. I., W. Glassco, M. Dukat and B. R. Martin (1999). "Pharmacological characterization of nicotine-induced seizures in mice." J Pharmacol Exp Ther **291**(3): 1284-1291.

Davis, T. J. and C. M. de Fiebre (2006). "Alcohol's actions on neuronal nicotinic acetylcholine receptors." Alcohol Res Health **29**(3): 179-185.

Dong, X. X., Y. Wang and Z. H. Qin (2009). "Molecular mechanisms of excitotoxicity and their relevance to pathogenesis of neurodegenerative diseases." Acta Pharmacologica Sinica **30**(4): 379-387.

Dreyer, N. (1954). "Action of Hexamethonium (C6) on Intestine, Gall Bladder and Urinary Bladder." Gastroenterology **26**(5): 765-768.

Eddleston, M. (2019). "Novel Clinical Toxicology and Pharmacology of Organophosphorus Insecticide Self-Poisoning." Annu Rev Pharmacol Toxicol **59**: 341-360.

Ferchmin, P. A., M. Andino, R. Reyes Salaman, J. Alves, J. Velez-Roman, B. Cuadrado, M. Carrasco, W. Torres-Rivera, A. Segarra, A. H. Martins, J. E. Lee and V. A. Eterovic (2014).

"4R-cembranoid protects against diisopropylfluorophosphate-mediated neurodegeneration." Neurotoxicology **44**: 80-90.

Fonck, C., R. Nashmi, P. Deshpande, M. I. Damaj, M. J. Marks, A. Riedel, J. Schwarz, A. C. Collins, C. Labarca and H. A. Lester (2003). "Increased sensitivity to agonist-induced seizures, straub tail, and hippocampal theta rhythm in knock-in mice carrying hypersensitive alpha 4 nicotinic receptors." J Neurosci **23**(7): 2582-2590.

Gainza-Lein, M., I. S. Fernandez, A. Ulate-Campos, T. Loddenkemper and A. P. Ostendorf (2019). "Timing in the treatment of status epilepticus: From basics to the clinic." Seizure **68**: 22-30.

Gao, J., S. X. Naughton, H. Wulff, V. Singh, W. D. Beck, J. Magrane, B. Thomas, N. A. Kaidery, C. M. Hernandez and A. V. Terry, Jr. (2016). "Diisopropylfluorophosphate Impairs the Transport of Membrane-Bound Organelles in Rat Cortical Axons." J Pharmacol Exp Ther **356**(3): 645-655.

Ghasemi, M. and A. Hadipour-Niktarash (2015). "Pathologic role of neuronal nicotinic acetylcholine receptors in epileptic disorders: implication for pharmacological interventions." Rev Neurosci **26**(2): 199-223.

Giniatullin, R., A. Nistri and J. L. Yakel (2005). "Desensitization of nicotinic ACh receptors: shaping cholinergic signaling." Trends Neurosci **28**(7): 371-378.

Haley, N. (2018). "Remarks at an Emergency UN Security Council Briefing on Chemical Weapons Use by Russia in the United Kingdom." United States Mission to the United Nations.

Harris, L. and D. Stitcher (1984). "Protection against diisopropylfluorophosphate intoxication by pyridostigmine and physostigmine in combination with atropine and mecamylamine." Naunyn Schmiedebergs Arch Pharmacol **327**(1): 64-69.

Hassel, B. (2006). "Nicotinic mechanisms contribute to soman-induced symptoms and lethality." Neurotoxicology **27**(4): 501-507.

HRW. (2021). "The Syrian Government's Widespread and Systematic Use of Chemical Weapons." from https://www.hrw.org/report/2017/05/01/death-chemicals/syrian-governments-widespread-and-systematic-use-chemical-weapons.

Jett, D. A. and S. M. Spriggs (2020). "Translational research on chemical nerve agents." Neurobiology of disease **133**: 104335.

Kaushal, S. and P. Tadi (2020). "Nicotinic Ganglionic Blocker."

Lorke, D. E. and G. A. Petroianu (2019). "Reversible cholinesterase inhibitors as pretreatment for exposure to organophosphates. A review." Journal of Applied Toxicology **39**(1): 101-116.

Niquet, J., R. Baldwin, L. Suchomelova, L. Lumley, D. Naylor, R. Eavey and C. G. Wasterlain (2016). "Benzodiazepine-refractory status epilepticus: pathophysiology and principles of treatment." Annals of the new york academy of sciences **1378**(1): 166.

OPCW (2018). Statement by h.e. ambassador Ahmad Nazri Yusof permanent representative of malaysia to the OPCW at the eighty-seventh session of the executive council

OPCW. (2020). "OPCW Issues Report on Technical Assistance Requested by Germany; Alexei Navalny." from https://www.opcw.org/media-centre/news/2020/10/opcw-issues-report-technical-assistance-requested-germany.

Orr-Urtreger, A., F. M. Goldner, M. Saeki, I. Lorenzo, L. Goldberg, M. De Biasi, J. A. Dani, J. W. Patrick and A. L. Beaudet (1997). "Mice deficient in the alpha7 neuronal nicotinic acetylcholine receptor lack alpha-bungarotoxin binding sites and hippocampal fast nicotinic currents." J Neurosci **17**(23): 9165-9171.

Pope, C. N. and S. Brimijoin (2018). "Cholinesterases and the fine line between poison and remedy." Biochemical Pharmacology **153**: 205-216.

Sheridan, R. D., A. P. Smith, S. R. Turner and J. E. Tattersall (2005). "Nicotinic antagonists in the treatment of nerve agent intoxication." J R Soc Med **98**(3): 114-115.

Sisó, S., B. A. Hobson, D. J. Harvey, D. A. Bruun, D. J. Rowland, J. R. Garbow and P. J. Lein (2017). "Editor's highlight: Spatiotemporal progression and remission of lesions in the rat brain following acute intoxication with diisopropylfluorophosphate." Toxicological sciences **157**(2): 330-341.

Steinlein, O. K., J. C. Mulley, P. Propping, R. H. Wallace, H. A. Phillips, G. R. Sutherland, I. E. Scheffer and S. F. Berkovic (1995). "A missense mutation in the neuronal nicotinic acetylcholine receptor alpha 4 subunit is associated with autosomal dominant nocturnal frontal lobe epilepsy." Nat Genet **11**(2): 201-203.

USAMRICD (1990). "USAMRICD Special Publication 98-01, Pyridostigmine."

Chapter 5

Conclusion

Abbreviations

ACh = acetylcholine

AChE = acetylcholinesterase

DFP = diisopropylfluorophosphate

EEG = electroencephalography

KO = knockout

MRI = magnetic resonance imaging

PET = positron emission tomography

OP = organophosphate

SE = *status epilepticus*

TETS = tetramethylenedisulfotetramine

Introduction

Based on evidence over the past 30 years of intentional and accidental human poisonings with tetramethylenedisulfotetramine (TETS) and organophosphates (OPs; Li, Gao et al. 2014, Figueiredo, Apland et al. 2018), it is clear that these chemical threats remain relevant public health risks. Current standard of care (SOC) is not sufficient to protect the brain of survivors (de Araujo Furtado, Rossetti et al. 2012, Figueiredo, Apland et al. 2018, Lauková, Velíšková et al. 2020), thus, more work is needed to identify antidotal therapies for treating individuals acutely intoxicated with these chemical threat agents. Since it may be challenging for first responders to initially determine which chemical is causing seizures in a mass casualty situation, there is an urgent need to investigate the cellular mechanisms of *status epilepticus* (SE) induced by either TETS or OPs to identify broad-spectrum, low-regret antidotes. However, this need may be challenging to meet because SE can recruit several different neurotransmitter systems, and the timing of this recruitment in the pathophysiology of TETS or OP intoxication has not been well characterized in the literature. Therefore, it is critical to gain a better mechanistic understanding of seizure initiation and the time course of neuropathology after intoxication with TETS or OPs. This knowledge will help to determine whether convergent mechanisms can be leveraged to normalize brain activity during SE to provide maximal antiseizure or neuroprotective efficacy in the absence of information about the intoxicating chemical.

Another outstanding question in the field is the relative contribution of genetic factors vs. seizure severity in determining neuropathological outcomes following chemical-induced seizures. Indeed, previous studies have established that the genetic background of rodents or non-human primates can produce unique profiles of vulnerability to seizures and neurological consequences after chemical intoxication (Löscher, Ferland et al. 2017, Matson, McCarren et al.

2018, Copping, Adhikari et al. 2019). It has also been demonstrated in preclinical OP models that the extent of brain injury is positively correlated with the duration of SE because neuropathology intensifies in severity as the duration of SE increases (McDonough Jr, Dochterman et al. 1995, McDonough Jr and Shih 1997). Furthermore, studies of OP-induced SE using outbred strains of rats have observed neuropathological outcomes that increased in severity with the occurrence of SE (Prager, Aroniadou-Anderjaska et al. 2013, González, Rindy et al. 2020), consistent with the suggestion that genetic factors and the duration of SE can influence subsequent neuropathological consequences. Addressing this question in regards to TETS-induced SE has been challenging because preclinical models of acute TETS intoxication have failed to replicate SE (Shakarjian, Veliskova et al. 2012, Zolkowska, Banks et al. 2012, Rice, Rauscher et al. 2017) that is observed in humans acutely intoxicated with high doses of TETS (Zhou, Liu et al. 1998, Barrueto, Furdyna et al. 2003). To overcome this limitation, we recently developed a mouse model of TETS-induced seizures that quickly progress to SE that continues for at least 40 min (Pessah, Rogawski et al. 2016, Zolkowska, Wu et al. 2018). This novel mouse model offers a viable platform to address whether TETS-induced SE is associated with long-term neuropathology as has been demonstrated in preclinical models of OP-induced SE (Naughton and Terry 2018, Andrew and Lein 2021, Tsai and Lein 2021). Additionally, while preclinical models of TETS-induced seizures have primarily used NIH Swiss or C57BL/6 mice, no direct comparison has been made to address strain differences in chronic responses to acute TETS intoxication. These data gaps provide the rationale to investigate the spatiotemporal patterns of neuropathology after TETS-induced SE and to determine whether these patterns vary between two mouse strains commonly used to study TETS-induced seizures.

The cellular and molecular mechanisms involved in the induction of OP-induced seizures represents another knowledge gap in the field (Tsai and Lein 2021). While it is clear that acute OP-induced acetylcholinesterase (AChE) inhibition triggers seizures (Figueiredo, Apland et al. 2018), the receptor subtypes involved in the initiation and progression of seizures to SE remain poorly characterized (Tsai and Lein 2021). Acute OP poisoning is understood to begin with a cholinergic crisis due to excessive accumulation of acetylcholine, which causes overstimulation of nicotinic and muscarinic receptors (Adeyinka and Kondamudi 2019). Although muscarinic receptors are targeted by antagonists such as atropine in the current SOC for OP intoxication (Jett and Spriggs 2020), this does not terminate OP-induced SE. This is attributed to poor penetration of atropine into the brain. However, the role of nicotinic receptors in OP-induced SE has not been rigorously investigated, which may underlie the lack of therapeutic strategies targeting the overstimulation of nicotinic receptors. The data described in this thesis address these knowledge gaps. This dissertation also described novel preclinical models of acute intoxication with chemical threat agents that provide advantages, but also have some limitations, relative to existing preclinical models. Findings of these studies extend understanding of the molecular mechanisms involved in the acute and chronic effects of acute intoxication with TETS or OPs and provide insights on therapeutic strategies for protecting against the neurotoxic effects of chemical threat agents.

Novel models of acute intoxication with chemical threat agents

Mouse model of TETS-induced SE

Previous mouse models studying the consequences of TETS intoxication faced challenges with replicating the human condition after poisoning with TETS (Barrueto, Furdyna

et al. 2003), because mice injected with TETS did not experience SE after acute exposure (Shakarjian, Veliskova et al. 2012, Zolkowska, Banks et al. 2012). The newly generated mouse model of TETS-induced SE in Chapter 2 addressed this limitation with the use of riluzole pretreatment to protect against the lethal effects of TETS, which allows TETS-induced seizures to progress to SE until termination with benzodiazepine rescue after 40 min. TETS mice in this model also displayed a subsequent spatiotemporal pattern of neuropathology via magnetic resonance imaging (MRI) and positron emission tomography (PET) imaging for up to 7 days after TETS exposure. This finding suggests this new model is more consistent with literature describing the effects of TETS in cases of human poisoning, where survivors display continuous seizures and SE with varying evidence of subsequent brain damage (Barrueto Jr, Furdyna et al. 2003, Tan 2005). Therefore, the use of mice to study SE after TETS exposure is advantageous for mechanistic studies focused on the role of various neurotransmitters in the initiation of SE and the downstream consequences. However, more research is needed to determine the long-term behavioral consequences of TETS-induced SE in mice to further establish its clinical relevance. One major disadvantage with using mice for PET imaging in Chapter 2 is that the cerebellum of the mouse is in very close proximity to the skull. Thus, this brain region is difficult to use as a reference region for PET imaging analysis because high tracer uptake in the skull confounds cerebellar values. Despite these limitations, the new mouse model of TETS-induced SE is a viable platform for studying the initiation and propagation of SE and could be leveraged for mechanistic studies to determine the best timing for antiseizure or neuroprotective therapies after TETS intoxication.

Mouse model of DFP-induced SE

Rodent models of OP-induced seizures and SE can be highly predictive of the human condition after acute intoxication (Pereira, Aracava et al. 2014), and endpoints quantified in this dissertation recapitulate some of the long-term consequences seen in human survivors such as neuropathology or cognitive/behavioral deficits (de Araujo Furtado, Rossetti et al. 2012, Jett, Sibrizzi et al. 2020). Data presented in Chapter 3 characterized long-term neuropathology and behavioral deficits in a new mouse model of SE induced by diisopropylfluorophosphate (DFP). In this model, injection with DFP caused SE in adult male mice that lasted for hours, resulting in persistent brain damage, including neurodegeneration and neuroinflammation, in multiple brain regions. This finding is consistent with what has been shown in the rat model of DFP-induced SE, where an acute dose of DFP causes seizures that progress rapidly to SE, followed by a robust spatiotemporal pattern of neuropathology (Flannery, Bruun et al. 2016, Guignet, Dhakal et al. 2020). These findings are also consistent with human cases of intoxication with OPs, where survivors have been shown to display continuous seizures preceding long-term brain damage and a range of behavioral consequences (Figueiredo, Apland et al. 2018). However, in contrast with the rat model, behavioral deficits in anxiety and hyperactivity were apparent in mice 28 days after dosing with DFP, whereas DFP rats have not been shown to develop deficits related to anxiety or locomotor activity. This finding highlights a disadvantage of using mice to study OP-induced learning and memory deficits due to hyperactivity observed in the open field. This finding confounded tests for exploratory or freezing behavior for learning and memory behavioral tests, so future studies should wait for a later time point than 28 days post-exposure to examine learning and memory behavior in mice. On the other hand, since learning and memory deficits have already been observed in rat models of OP-induced SE (Schultz, Wright et al. 2014,

Guignet, Dhakal et al. 2020), it may be ideal to use rats for modeling the OP-induced learning and memory deficits. Taken together, the DFP rat model appears to better replicate learning and memory deficits seen in human survivors of OP poisoning (Savage, Keefe et al. 1988, Jett, Sibrizzi et al. 2020), so it is important for researchers to determine the appropriate species to select for mechanistic or behavioral study. Despite these limitations, these observations suggest that the new mouse model of DFP-SE recapitulates many of the acute and chronic neurotoxic effects observed in humans following acute OP exposure such as SE with subsequent long-term neuropathology and anxiety-related behavioral deficits and is particularly advantageous to investigate the molecular mechanisms of OP intoxication.

Mechanistic implications of findings described in this thesis

Neuropathologic consequences of TETS-induced SE

It is generally believed that the duration and severity of seizures or SE influences the occurrence or severity of negative health outcomes in survivors of TETS or OP intoxication (McDonough Jr, Dochterman et al. 1995, Hobson, Siso et al. 2017, Calsbeek, Gonzalez et al. 2021). This association between brain damage and SE has been hypothesized to be due to prolonged aberrant epileptiform activity, which rapidly intensifies after 20 min of seizure activity (McDonough Jr, Dochterman et al. 1995). Findings reported in this dissertation are consistent with this relationship, because as described in Chapter 2, TETS SE mice displayed more severe neuropathology with increased duration of SE. Specifically, a mouse that failed to respond to benzodiazepine treatment experienced a prolonged duration of SE for more than 120 min and displayed evidence of severe neurodegeneration and neuroinflammation. These severe neuropathological consequences are in contrast with the subtle and transient neuropathology

observed in mice that experienced TETS-induced SE for 40 min before termination with benzodiazepines. Therefore, these findings are consistent with the suggestion that the duration of TETS-induced SE may correlate with the severity of neuropathology, but more studies with larger sample sizes are needed to confirm this association. The minimal amount of brain damage seen in TETS mice with 40 min of SE was a direct contradiction to the long-standing postulate in OP literature that seizures occurring for longer than 20 cause significant brain damage (Figueiredo, Apland et al. 2018, Guignet and Lein 2019). This contrast between chemical models of SE suggests that there could be different molecular mechanisms driving seizures between models, or that the pathogenic mechanisms linking seizures to long-term outcomes vary between TETS and OPs.

It has recently been reported that genetic background can influence the susceptibility of mice to seizure response and behavioral outcomes (Copping, Adhikari et al. 2019). Another major finding in Chapter 2 is consistent with this literature, because two different strains of TETS mice that experienced SE for 40 min after an acute dose of TETS exhibited different spatiotemporal profiles of neuropathology. Relative to vehicle controls, NIH Swiss mice displayed significant brain damage at 3 days post-TETS intoxication, whereas C57BL/6J mice exhibited significant brain damage at 3 and 7 days post-TETS as evidenced by MRI and PET. Because the dosage of TETS was increased in C57BL/6J mice to achieve comparable severity of SE between strains, there remains an open question as to whether these variations in neuropathology were strictly due to strain-specific responses to SE, or to dose-dependent toxicodynamic effects of TETS. Nevertheless, these findings indicate that the neuropathological consequences of TETS-induced SE are affected by genetic background and are, therefore, likely

to vary in a diverse human population who display comparable seizures after intoxication with TETS.

Role of nicotinic cholinergic receptors in initiation vs. propagation of OP-induced seizures

One advantage afforded by mouse models of OP-induced seizures is the ability to leverage existing knockout (KO) strains of mice to study the role of particular receptors in the initiation and progression of OP-induced SE. The data described in Chapter 4 leveraged this benefit by using KO mice lacking α4- or α7-containing nicotinic receptors to confirm the role of α4-containing receptors in OP-induced SE. These experiments showed that α4 KO mice injected with DFP exhibited significantly reduced seizure activity relative to wildtype mice; in contrast, reduced duration and/or severity of DFP-induced seizure behavior was not observed for α7 KO mice. A key role for α4 nicotinic receptors in OP-induced seizures was supported by pharmacologic experiments comparing the efficacy of α4- and α7-selective nicotinic antagonists in blocking and terminating OP-induced seizures. When selective antagonists were injected 10 min before DFP, symptoms of SE were significantly reduced in mice treated with the α4-selective antagonist, but not the α7-selective. These findings confirm the role of α4-containing nicotinic receptors in the initiation of SE, and more studies are needed to determine if this specific receptor has a role in SE propagation after DFP. Further studies using the non-selective nicotinic antagonist, mecamylamine, confirmed that pretreatment 10 min prior to DFP exposure blocked the initiation of seizures. Similarly, post-exposure administration of mecamylamine at 10, but not 40 min, after DFP injection terminated seizure activity. These observations suggest that by 40 min post-DFP, SE has progressed to a cholinergic-independent mechanism, consistent with the hypothesis that a transition occurs from the cholinergic crisis to a glutamatergic storm

sometime between 20-40 min post-exposure (McDonough Jr and Shih 1997). An alternative explanation for the lack of antinicotinic efficacy after 40 min of DFP-SE is that nicotinic receptor desensitization occurs due to overstimulation (Giniatullin, Nistri et al. 2005). A similar limitation in first-line antiseizure therapy has been observed, when survivors of SE suffer from a loss of response to delayed benzodiazepine treatment due to receptor internalization and refractoriness to therapeutic intervention (Niquet, Baldwin et al. 2016). One surprising finding from the studies using α4KO mice or the α4-selective nicotinic antagonists was in the different profiles of seizure scores observed after DFP injection between these exposure groups. While pretreatment with the nonselective or α4-selective antagonist prevented the initiation or propagation of SE, α4KO mice displayed initial symptoms of SE that appeared to terminate ~40 min post-DFP. One potential explanation for this difference could be a compensatory genetic mechanism in the KO mouse to upregulate other nicotinic receptors, to conserve normal function in the KO over the lifetime of the animal (Kreiner 2015). However, no significant differences in the expression of other nicotinic receptors has been reported in α4KO versus wildtype mice (Ross, Wong et al. 2000), suggesting this difference may not be the result of genetic compensation. Additionally, electrographic recordings from the brains of α4KO mice demonstrated an absence of electrographic abnormalities after DFP. This suggests that either the observed behavioral seizure scores were strictly due to peripheral effects of OP intoxication, or that the cortical electrographic recording electrode was not sensitive enough to detect abnormalities in deeper brain regions driving the initial seizures. Despite these remaining questions, the findings in Chapter 4 confirm a necessary role for nicotinic receptors in the initiation and propagation of OP-induced SE. However, more research is needed to determine if

subunit selective antagonists can offer protection against the propagation of OP-induced SE when injected 10 min after DFP.

Therapeutic implications of findings described in this thesis

Therapeutic window for TETS

The data described in Chapter 2 illustrated the positive correlation between seizure duration and the extent of neuropathological outcomes after acute TETS intoxication, which is consistent with other models of OP-induced SE (McDonough Jr and Shih 1997). However, another important observation from this study was that 40 min duration of TETS-induced SE only caused a subtle and transient profile of neuropathology in mice, suggesting that the therapeutic window for neuroprotection is significantly longer following TETS-induced SE vs. OP-induced SE. Specifically, it is well understood that there is a narrow therapeutic window for OP-induced SE, because benzodiazepines fail to protect against persistent, long-term consequences even when administered after 30-40 min of SE (Shrot, Ramaty et al. 2014, Supasai, Gonzalez et al. 2020). Furthermore, other preclinical rodent models of OP-induced SE have demonstrated that a duration of SE for 20-40 min can cause a robust spatiotemporal profile of neuropathology that persists for days to months (reviewed by de Araujo Furtado, Rossetti et al. 2012, Guignet and Lein 2019). Therefore, the data presented in Chapter 2 suggest that the therapeutic window for mitigating brain damage following TETS-induced SE may be longer than that reported for OP-induced SE, but more studies are needed to confirm the efficacy of benzodiazepines administered at time points beyond 40 min post-TETS.

Nicotinic antagonists as prophylactic treatment for acute OP intoxication

The cholinergic crisis that is induced by acute OP intoxication results from the excessive accumulation of acetylcholine, causing overstimulation at muscarinic and nicotinic receptors (Adeyinka and Kondamudi 2019). However, the current SOC for OP intoxication, which includes an oxime to reactivate AChE and a muscarinic antagonist, lacks a nicotinic antagonist, raising important questions about this exclusion (Smythies and Golomb 2004, Sheridan, Smith et al. 2005). The findings of Chapter 4 confirmed that non-selective or α4-selective nicotinic antagonists are effective at blocking seizures when injected 10 min before DFP. Another important finding in Chapter 4 was that pretreatment with the broad or α4-selective antagonist protected against symptoms of the cholinergic crisis such as salivation, lacrimation, urination, and defecation. While post-exposure treatment at 10 min after DFP also exhibited anti-seizure efficacy, treatment at 40 min post-exposure had no effect on DFP-induced seizures. However, this therapeutic benefit was no longer afforded when the nonselective nicotinic antagonist was injected 40 min after DFP. One explanation for this could be that nicotinic receptors are no longer involved in the propagation of SE at 40 min post-DFP, due to a shift in neurotransmission from cholinergic to glutamatergic (McDonough Jr and Shih 1997). This would suggest that although these receptors are still functional, they are no longer required for maintenance of OP-induced SE by 40 min post-DFP. These observations suggest that the delayed administration of nicotinic antagonists after OP intoxication is not of therapeutic value; however, they do suggest that nicotinic antagonism may be useful as a prophylactic or immediate post-exposure therapeutic. The current prophylactic SOC for OP exposure is pyridostigmine bromide (PB), which is suspected to cause Gulf War Illness in humans (Charatan 1999), and has not offered protection against SE in preclinical rat models of OP intoxication (Bruun, Guignet et al. 2019).

Given that the duration of seizure seems to predict negative health outcomes, it is likely that neuroprotection could be afforded using nicotinic antagonists, although neuropathology and behavioral deficits were not inspected in the work presented here. Taken together, the primary focus for first responders and the SOC should be to stop seizure behavior as quickly as possible, because delayed therapy may be ineffective to terminate SE and to reduce subsequent neuropathology.

Outstanding Research Questions and Concluding Remarks

While the research described in this dissertation addresses the question of the role of seizure duration and genetic background on neuropathological outcomes following acute TETS-induced SE, several data gaps remain to be investigated. First, it remains an open question as to whether the TETS-SE mouse model is truly representative of TETS-induced SE in humans, due to the subtle and transient nature of neuroinflammation and brain pathology detected in TETS mice that experienced SE for 40 min. However, the mouse that experienced TETS-SE for 120 min displayed severe neuropathology, which suggests that mice with prolonged SE after TETS could better recapitulate the human condition after intoxication (Zhou, Liu et al. 1998). Therefore, it may be beneficial to develop a mouse model of TETS-induced SE that either does not require benzodiazepine rescue or survives with delayed administration of antiseizure medication at later time points to evaluate therapies for survivors who do not receive or respond to a first-line therapy in the field. Second, it would be useful to determine if the transient neuroinflammation observed in TETS SE (40 min) mice is sufficient to cause behavioral deficits. If so, this would strengthen the conclusion that this new model of TETS-induced SE reasonably represents the human condition after TETS intoxication.

Another data gap not addressed in the studies of the DFP mouse model described in Chapter 3 is the lack of treatment with benzodiazepines to terminate DFP-induced SE. Since first-line benzodiazepines like midazolam can be effective in reducing OP-induced SE in rats when given at delayed time points up to 120 min post-DFP (Spampanato, Pouliot et al. 2019), it is of great interest to know if this approach can terminate SE in DFP-intoxicated mice and to characterize the optimal therapeutic windows for such therapies. Rat models of OP intoxication have displayed a vulnerability to benzodiazepine refractory SE, which mimics the human condition, where delayed administration of benzodiazepine therapy is not effective because of the internalization of GABAergic receptors (Niquet, Baldwin et al. 2016). Therefore, it will also be important to determine if DFP mice are similarly vulnerable to this phenomenon. Additionally, it is still unknown if DFP mice will develop spontaneous recurrent seizures (SRS) like rats, who experience them in the weeks and months following acute OP intoxication (Figueiredo, Apland et al. 2018, Dhir, Bruun et al. 2020, Guignet, Dhakal et al. 2020). Long-term electrographic studies could be designed to instrument mice with wireless telemetry devices and record brain activity over the weeks and months following acute DFP exposure. These studies could determine if mice are also vulnerable to the development of SRS after DFP-induced SE like rats or humans, which would allow for mechanistic studies into the progression of this adverse neurologic outcome.

Chapter 4 was a mechanistic study using pharmacologic and genetic tools to assess the role of nicotinic receptors in SE induced by DFP in the mouse model. While the finding of their role in DFP-SE is important to the field at large, several questions and data gaps remain to be investigated. First, it will be important to evaluate the efficacy of selective versus nonselective nicotinic antagonism in preventing long-term neuropathology and behavioral deficits. This

research could enhance knowledge of the role of SE in the neuropathological outcomes of DFP intoxication and determine if the potential neuroprotective efficacy of this strategy can be improved using selective antagonists to avoid the ganglionic block caused by broad nicotinic antagonism (Sheridan, Smith et al. 2005). Second, the experiments in Chapter 4 did not evaluate intramuscular delivery of nicotinic antagonists to delay absorption, metabolism, and elimination, or compare them to the current prophylactic SOC, pyridostigmine bromide. This is an important consideration for the field because of the current use of autoinjectors to administer the SOC and improving the prophylactic therapy with this strategy could mitigate long-term consequences of acute OP exposure. If SE duration predicts the extent or severity of neuropathology, then it is logical that successful termination of SE using nicotinic antagonists could protect the brain from severe neuropathology. Third, there is literature suggesting the α7 nicotinic subunit plays a role in epileptic disorders (Ghasemi and Hadipour-Niktarash 2015), neurodegeneration (Ferchmin, Andino et al. 2014) and neuroinflammation (Mizrachi, Marsha et al. 2021), so it is important to know how the use of selective agonists or antagonists can protect against the neuropathological response seen after DFP in mice. While α7-selective antagonism was not effective in mitigating the induction of SE, it is of great interest to know what role these receptors might have in the progression of neuropathology after DFP intoxication.

Concluding remarks

The data presented in this dissertation suggest that recently developed mouse models of SE induced by TETS or DFP recapitulate many of the hallmark symptoms of human intoxication with these chemicals. Because SE itself is understood to recruit multiple neurotransmitter systems in the brain, it is likely that successful antiseizure treatment strategies will need to

employ combination therapies to effectively terminate SE and prevent the long-term sequelae of neurological consequences. For example, after acute exposure to an OP, the early delivery of nicotinic, muscarinic, and glutamatergic antagonists followed by a GABAergic positive allosteric modulator could provide maximum efficacy to stop SE. However, it is critical to first gain a deeper understanding of the timing for the optimal therapeutic windows for each mechanistic drug class. Therefore, more studies are needed to gain insight on cellular mechanisms of intoxication with chemical threat agents. The development of mouse models of SE induced by TETS or DFP in this dissertation provide a rigorous platform to leverage knockout or transgenic mice to address outstanding gaps in the field.

References

Adeyinka, A. and N. P. Kondamudi (2019). "Cholinergic crisis." StatPearls [Internet].

Andrew, P. M. and P. J. Lein (2021). "Neuroinflammation as a Therapeutic Target for Mitigating the Long-Term Consequences of Acute Organophosphate Intoxication." Frontiers in Pharmacology **12**: 1184.

Barrueto, F., Jr., P. M. Furdyna, R. S. Hoffman, R. J. Hoffman and L. S. Nelson (2003). "Status epilepticus from an illegally imported Chinese rodenticide: "tetramine"." J Toxicol Clin Toxicol **41**(7): 991-994.

Barrueto Jr, F., P. M. Furdyna, R. S. Hoffman, R. J. Hoffman and L. S. Nelson (2003). "Status epilepticus from an illegally imported Chinese rodenticide:“tetramine”." Journal of Toxicology: Clinical Toxicology **41**(7): 991-994.

Bruun, D. A., M. Guignet, D. J. Harvey and P. J. Lein (2019). "Pretreatment with pyridostigmine bromide has no effect on seizure behavior or 24 hour survival in the rat model of acute diisopropylfluorophosphate intoxication." Neurotoxicology **73**: 81-84.

Calsbeek, J. J., E. A. Gonzalez, C. A. Boosalis, D. Zolkowska, D. A. Bruun, D. J. Rowland, D. J. Harvey, N. H. Saito, M. A. Rogawski and P. J. Lein (2021). "Strain and seizure duration influence the extent of brain injury in mice after tetramethylenedisulfotetramine-induced status epilepticus." In prep for submission to Neurotoxicology.

Charatan, F. (1999). "Nerve gas antidote a possible cause of Gulf war illness." BMJ: British Medical Journal **319**(7218): 1154.

Copping, N. A., A. Adhikari, S. P. Petkova and J. L. Silverman (2019). "Genetic backgrounds have unique seizure response profiles and behavioral outcomes following convulsant administration." Epilepsy Behav **101**(Pt A): 106547.

de Araujo Furtado, M., F. Rossetti, S. Chanda and D. Yourick (2012). "Exposure to nerve agents: from status epilepticus to neuroinflammation, brain damage, neurogenesis and epilepsy." Neurotoxicology **33**(6): 1476-1490.

Dhir, A., D. A. Bruun, M. Guignet, Y. H. Tsai, E. Gonzalez, J. Calsbeek, J. Vu, N. Saito, D. J. Tancredi, D. J. Harvey, P. J. Lein and M. A. Rogawski (2020). "Allopregnanolone and perampanel as adjuncts to midazolam for treating diisopropylfluorophosphate-induced status epilepticus in rats." Ann N Y Acad Sci **1480**(1): 183-206.

Ferchmin, P. A., M. Andino, R. Reyes Salaman, J. Alves, J. Velez-Roman, B. Cuadrado, M. Carrasco, W. Torres-Rivera, A. Segarra, A. H. Martins, J. E. Lee and V. A. Eterovic (2014). "4R-cembranoid protects against diisopropylfluorophosphate-mediated neurodegeneration." Neurotoxicology **44**: 80-90.

Figueiredo, T. H., J. P. Apland, M. F. Braga and A. M. Marini (2018). "Acute and long-term consequences of exposure to organophosphate nerve agents in humans." Epilepsia **59**: 92-99.

Flannery, B. M., D. A. Bruun, D. J. Rowland, C. N. Banks, A. T. Austin, D. L. Kukis, Y. Li, B. D. Ford, D. J. Tancredi, J. L. Silverman, S. R. Cherry and P. J. Lein (2016). "Persistent neuroinflammation and cognitive impairment in a rat model of acute diisopropylfluorophosphate intoxication." J Neuroinflammation **13**(1): 267.

Ghasemi, M. and A. Hadipour-Niktarash (2015). "Pathologic role of neuronal nicotinic acetylcholine receptors in epileptic disorders: implication for pharmacological interventions." Reviews in the Neurosciences **26**(2): 199-223.

Giniatullin, R., A. Nistri and J. L. Yakel (2005). "Desensitization of nicotinic ACh receptors: shaping cholinergic signaling." Trends Neurosci **28**(7): 371-378.

González, E. A., A. C. Rindy, M. A. Guignet, J. J. Calsbeek, D. A. Bruun, A. Dhir, P. Andrew, N. Saito, D. J. Rowland and D. J. Harvey (2020). "The chemical convulsant diisopropylfluorophosphate (DFP) causes persistent neuropathology in adult male rats independent of seizure activity." Archives of toxicology **94**(6): 2149-2162.

Guignet, M., K. Dhakal, B. M. Flannery, B. A. Hobson, D. Zolkowska, A. Dhir, D. A. Bruun, S. Li, A. Wahab, D. J. Harvey, J. L. Silverman, M. A. Rogawski and P. J. Lein (2020). "Persistent behavior deficits, neuroinflammation, and oxidative stress in a rat model of acute organophosphate intoxication." Neurobiol Dis **133**: 104431.

Guignet, M. and P. J. Lein (2019). Organophosphates. Advances in Neurotoxicology: Role of Inflammation in Environmental Neurotoxicity. M. Aschner and L. G. Costa. Cambridge, MA, Academic Press**:** 35-79.

Hobson, B. A., S. Siso, D. J. Rowland, D. J. Harvey, D. A. Bruun, J. R. Garbow and P. J. Lein (2017). "From the Cover: MagneticResonance Imaging Reveals Progressive Brain Injury in Rats Acutely Intoxicated With Diisopropylfluorophosphate." Toxicol Sci **157**(2): 342-353.

Jett, D. A., C. A. Sibrizzi, R. B. Blain, P. A. Hartman, P. J. Lein, K. W. Taylor and A. A. Rooney (2020). "A national toxicology program systematic review of the evidence for long-term effects after acute exposure to sarin nerve agent." Crit Rev Toxicol **50**(6): 474-490.

Jett, D. A. and S. M. Spriggs (2020). "Translational research on chemical nerve agents." Neurobiol Dis **133**: 104335.

Kreiner, G. (2015). "Compensatory mechanisms in genetic models of neurodegeneration: are the mice better than humans?" Frontiers in cellular neuroscience **9**: 56.

Lauková, M., J. Velíšková, L. Velíšek and M. P. Shakarjian (2020). "Tetramethylenedisulfotetramine neurotoxicity: What have we learned in the past 70 years?" Neurobiology of disease **133**: 104491.

Li, Y., Y. Gao, X. Yu, J. Peng, F. Ma and L. Nelson (2014). "Tetramine poisoning in China: changes over a decade viewed through the media's eye." BMC Public Health **14**(1): 1-6.

Löscher, W., R. J. Ferland and T. N. Ferraro (2017). "The relevance of inter-and intrastrain differences in mice and rats and their implications for models of seizures and epilepsy." Epilepsy & Behavior **73**: 214-235.

Matson, L. M., H. S. McCarren, C. L. Cadieux, D. M. Cerasoli and J. H. McDonough (2018). "The role of genetic background in susceptibility to chemical warfare nerve agents across rodent and non-human primate models." Toxicology **393**: 51-61.

McDonough Jr, J. H., L. W. Dochterman, C. D. Smith and T.-M. Shih (1995). "Protection against nerve agent-induced neuropathology, but not cardiac pathology, is associated with the anticonvulsant action of drug treatment." Neurotoxicology **16**(1): 123-132.

McDonough Jr, J. H. and T.-M. Shih (1997). "Neuropharmacological mechanisms of nerve agent-induced seizure and neuropathology." Neuroscience & biobehavioral reviews **21**(5): 559-579.

Mizrachi, T., O. Marsha, K. Brusin, Y. Ben-David, G. A. Thakur, A. Vaknin-Dembinsky, M. Treinin and T. Brenner (2021). "Suppression of neuroinflammation by an allosteric agonist and positive allosteric modulator of the α7 nicotinic acetylcholine receptor GAT107." Journal of Neuroinflammation **18**(1): 1-14.

Naughton, S. X. and A. V. Terry, Jr. (2018). "Neurotoxicity in acute and repeated organophosphate exposure." Toxicology **408**: 101-112.

Niquet, J., R. Baldwin, L. Suchomelova, L. Lumley, D. Naylor, R. Eavey and C. G. Wasterlain (2016). "Benzodiazepine-refractory status epilepticus: pathophysiology and principles of treatment." Annals of the new york academy of sciences **1378**(1): 166.

Pereira, E. F., Y. Aracava, L. J. DeTolla, E. J. Beecham, G. W. Basinger, E. J. Wakayama and E. X. Albuquerque (2014). "Animal models that best reproduce the clinical manifestations of human intoxication with organophosphorus compounds." Journal of Pharmacology and Experimental Therapeutics **350**(2): 313-321.

Pessah, I. N., M. A. Rogawski, D. J. Tancredi, H. Wulff, D. Zolkowska, D. A. Bruun, B. D. Hammock and P. J. Lein (2016). "Models to identify treatments for the acute and persistent effects of seizure-inducing chemical threat agents." Ann N Y Acad Sci **1378**(1): 124-136.

Prager, E. M., V. Aroniadou-Anderjaska, C. P. Almeida-Suhett, T. H. Figueiredo, J. P. Apland and M. F. Braga (2013). "Acetylcholinesterase inhibition in the basolateral amygdala plays a key role in the induction of status epilepticus after soman exposure." Neurotoxicology **38**: 84-90.

Rice, N. C., N. A. Rauscher, J. L. Langston and T. M. Myers (2017). "Behavioral intoxication following voluntary oral ingestion of tetramethylenedisulfotetramine: Dose-dependent onset, severity, survival, and recovery." Neurotoxicology **63**: 21-32.

Ross, S. A., J. Y. Wong, J. J. Clifford, A. Kinsella, J. S. Massalas, M. K. Horne, I. E. Scheffer, I. Kola, J. L. Waddington and S. F. Berkovic (2000). "Phenotypic characterization of an α4 neuronal nicotinic acetylcholine receptor subunit knock-out mouse." Journal of Neuroscience **20**(17): 6431-6441.

Savage, E. P., T. J. Keefe, L. M. Mounce, R. K. Heaton, J. A. Lewis and P. J. Burcar (1988). "Chronic neurological sequelae of acute organophosphate pesticide poisoning." Archives of Environmental Health: An International Journal **43**(1): 38-45.

Schultz, M., L. Wright, M. de Araujo Furtado, M. Stone, M. Moffett, N. Kelley, A. Bourne, W. Lumeh, C. Schultz and J. Schwartz (2014). "Caramiphen edisylate as adjunct to standard therapy attenuates soman-induced seizures and cognitive deficits in rats." Neurotoxicology and teratology **44**: 89-104.

Shakarjian, M. P., J. Veliskova, P. K. Stanton and L. Velisek (2012). "Differential antagonism of tetramethylenedisulfotetramine-induced seizures by agents acting at NMDA and GABA(A) receptors." Toxicol Appl Pharmacol **265**(1): 113-121.

Sheridan, R. D., A. P. Smith, S. R. Turner and J. E. Tattersall (2005). "Nicotinic antagonists in the treatment of nerve agent intoxication." Journal of the Royal Society of Medicine **98**(3): 114-115.

Shrot, S., E. Ramaty, Y. Biala, G. Bar-Klein, M. Daninos, L. Kamintsky, I. Makarovsky, L. Statlender, Y. Rosman and A. Krivoy (2014). "Prevention of organophosphate-induced chronic epilepsy by early benzodiazepine treatment." Toxicology **323**: 19-25.

Smythies, J. and B. Golomb (2004). "Nerve gas antidotes." J R Soc Med **97**(1): 32.

Spampanato, J., W. Pouliot, S. L. Bealer, B. Roach and F. E. Dudek (2019). "Antiseizure and neuroprotective effects of delayed treatment with midazolam in a rodent model of organophosphate exposure." Epilepsia **60**(7): 1387-1398.

Supasai, S., E. A. Gonzalez, D. J. Rowland, B. Hobson, D. A. Bruun, M. A. Guignet, S. Soares, V. Singh, H. Wulff, N. Saito, D. J. Harvey and P. J. Lein (2020). "Acute administration of diazepam or midazolam minimally alters long-term neuropathological effects in the rat brain following acute intoxication with diisopropylfluorophosphate." Eur J Pharmacol **886**: 173538.

Tan, I. (2005). "Tetramine poisoning." Hong Kong Med J **11**(6): 511-514.

Tsai, Y. H. and P. J. Lein (2021). "Mechanisms of organophosphate neurotoxicity." Current Opinion in Toxicology **26**: 49-60.

Zhou, Y., L. Liu and L. Tang (1998). "[An autopsy analysis on 5 cases of poisoning death with tetramethylenedisulfotertramine]." Fa Yi Xue Za Zhi **14**(4): 214-215, 217, 252.

Zolkowska, D., C. N. Banks, A. Dhir, B. Inceoglu, J. R. Sanborn, M. R. McCoy, D. A. Bruun, B. D. Hammock, P. J. Lein and M. A. Rogawski (2012). "Characterization of seizures induced by acute and repeated exposure to tetramethylenedisulfotetramine." J Pharmacol Exp Ther **341**(2): 435-446.

Zolkowska, D., C. Y. Wu and M. A. Rogawski (2018). "Intramuscular allopregnanolone and ganaxolone in a mouse model of treatment-resistant status epilepticus." Epilepsia.